ISJET

INTERNATIONAL SCIENTIFIC JOURNAL OF ENGINEERING AND TECHNOLOGY

Volume 7 No. 1 January-June 2023

ISSN 2586-8527 (Online)

Panyapiwat Institute of Management

Indexed in the Thai-Journal Citation Index (TCI 2)

INTERNATIONAL SCIENTIFIC JOURNAL OF ENGINEERING AND TECHNOLOGY (ISJET)

Volume 7 No. 1 January-June 2023

ISSN 2586-8527 (Online)
PANYAPIWAT INSTITUTE OF MANAGEMENT

INTERNATIONAL SCIENTIFIC JOURNAL OF ENGINEERING AND THCHNOLOGY (ISJET)
Volume 7 No. 1 January-June 2023
ISSN 2586-8527 (Online)

Copyright
Panyapiwat Institute of Management
85/1 Moo 2, Chaengwattana Rd.,
Bang Talat, Pakkred,
Nonthaburi, 11120, Thailand
Tel. +66 2855 1560
E-mail: isjet@pim.ac.th
Website: https://ph02.tci-thaijo.org/index.php/isjet/index

Copyright©2017, Panyapiwat Institute of Management

INTERNATIONAL SCIENTIFIC JOURNAL OF ENGINEERING AND THCHNOLOGY (ISJET)

Volume 7 No. 1 January-June 2023 ISSN 2586-8527 (Online)

Objective:
International Scientific Journal of Engineering and Technology will be dedicated to serving as a forum to share knowledge on research advances in all fields of sciences: Engineering, Technology, Innovation, Information Technology, Management Information Systems, Logistics and Transportation, Agricultural Science and Technology, Animal Science and Aquaculture, Food Science, and other areas in Sciences and Technology. Submissions are welcomed from both PIM as well as other Thai and foreign institutions.

Scope:
Engineering, Technology, Innovation, Information Technology, Management Information Systems, Logistics and Transportation, Agricultural Science and Technology, Animal Science and Aquaculture, Food Science, and other areas of Sciences and Technology.

Type of Article:
• Research article
• Academic article
• Book review
• Review article

Languages of academic works:
An article written in either English language is accepted for publication.

Reviewing Policy:
1. Any manuscript to be accepted for publication must have been reviewed and approved by at least three peer reviewers in that particular field or related fields. The Journal has a double-blind peer review policy which means that neither the peer reviewer nor the author knows the identity of each other.
2. The submitted manuscript must have never been published in any other periodical, and must not be in the approving process for publication by any other periodical. Also, the author must not plagiarize the work of other people.
3. The article, expression, illustrations, and tables that are published in the Journal are the sole responsibility of the author, and definitely not that of Panyapiwat Institute of Management.
4. The Editorial Board of International Scientific Journal of Engineering and Technology reserves the right to change or revise the name(s) and unit(s) of the author(s) in all cases after the issuance of the letter.
5. The Editorial Board of International Scientific Journal of Engineering and Technology reserves the right to cancel the publication that has been issued a certification of publication in the Journal.
6. The Editorial Board of International Scientific Journal of Engineering and Technology reserves the right for decision making on publishing any article in the Journal.

Frequency of Publication:
Twice a year
• The first issue: January-June
• The second issue: July-December

Publication and Access Charges:
There are no charges to submit and publish all types of articles. Full articles in pdf format can be downloaded free from the journal website at https://ph02.tci-thaijo.org/index.php/isjet/index

ISJET Journal Editorial Board
The office of Research and Development
Panyapiwat Institute of Management
85/1 Moo 2, Chaengwattana Rd.,
Bang Talat, Pakkred, Nonthaburi, 11120, Thailand
Tel. +66 2855 1560
E-mail: isjet@pim.ac.th
Website: https://ph02.tci-thaijo.org/index.php/isjet/index

INTERNATIONAL SCIENTIFIC JOURNAL OF ENGINEERING AND TECHNOLOGY (ISJET)
Volume 7 No. 1 January-June 2023
ISSN 2586-8527 (Online)

Advisors Board

Assoc. Prof. Dr. Somrote Komolavanij	Panyapiwat Institute of Management, Thailand
Assoc. Prof. Dr. Pisit Charnkeitkong	Panyapiwat Institute of Management, Thailand
Assoc. Prof. Dr. Paritud Bhandhubanyong	Panyapiwat Institute of Management, Thailand
Assoc. Prof. Dr. Chom Kimpan	Panyapiwat Institute of Management, Thailand
Prof. Dr. Rattikorn Yimnirun	Vidyasirimedhi Institute of Science and Technology, Thailand

Editor-in-chief

Assoc. Prof. Dr. Parinya Sanguansat	Panyapiwat Institute of Management, Thailand

Associate Editor of Engineering and Technology

Asst. Prof. Dr. Phannachet Na Lamphun	Panyapiwat Institute of Management, Thailand

Associate Editor of Information Technology

Asst. Prof. Dr. Nivet Chirawichitchai	Panyapiwat Institute of Management, Thailand

Associate Editor of Science

Dr. Wirin Sonsrettee	Panyapiwat Institute of Management, Thailand

Associate Editor of Logistics and Transportation

Dr. Tantikorn Pichpibul	Panyapiwat Institute of Management, Thailand

Associate Editor of Agriculture Science and Food Technology

Asst. Prof. Dr. Korawit Chaisu	Panyapiwat Institute of Management, Thailand

Editorial Board

Prof. Dr. Chidchanok Lursinsap	Chulalongkorn University, Thailand
Prof. Dr. Parames Chutima	Chulalongkorn University, Thailand
Prof. Dr. Phadungsak Rattanadecho	Thammasat University, Thailand
Prof. Dr. Prabhas Chongstitvatana	Chulalongkorn University, Thailand
Prof. Dr. Prasanta Kumar Dey	Aston Business School, Aston University, UK
Prof. Dr. Rosemary R. Seva.	De La Salle University, Philippines
Prof. Dr. Sandhya Babel	Sirindhorn International Institute of Technology, Thammasat University, Thailand
Prof. Dr. Takashi Yukawa	Nagaoka University of Technology, Japan
Prof. Dr. Thanaruk Theeramunkong	Sirindhon International Institute of Technology, Thammasat University, Thailand
Prof. Duane P. Bartholomew	University of Hawaii at Manoa Honolulu, USA
Assoc. Prof. Dr. Chawalit Jeenanunta	Sirindhon International Institute of Technology, Thammasat University, Thailand
Assoc. Prof. Dr. Nattapon Chantarapanich	Kasetsart University, Sriracha Campus, Thailand
Assoc. Prof. Dr. Panich Intra	Rajamangala University of Technology Lanna, Thailand
Assoc. Prof. Dr. Ruengsak Kawtummachai	Panyapiwat Institute of Management, Thailand
Assoc. Prof. Dr. Wilaiporn Lee	King Mongkut's University of Technology North Bangkok, Thailand
Asst. Prof. Dr. Adisak Joomwong	Maejo University, Thailand
Asst. Prof. Dr. Anan Boonpan	Panyapiwat Institute of Management, Thailand
Asst. Prof. Dr. Rangsima Chanphana	Chulalongkorn University, Thailand
Asst. Prof. Dr. Thongchai Kaewkiriya	Independent Scholar
Dr. Anand Mary	Faculty of Dentistry, University of Puthisastra, Cambodia
Dr. Jochen Hermann Josef Amrehn	Nanjing Tech University Pujiang Institute, China
Dr. Nattakarn Phaphoom	TD Tawandang Company Limited, Thailand
Dr. Nattaporn Chotyakul	Panyapiwat Institute of Management, Thailand

Journal Secretary

Ms. Suchinda Chaluai	Panyapiwat Institute of Management, Thailand

INTERNATIONAL SCIENTIFIC JOURNAL OF ENGINEERING AND TECHNOLOGY (ISJET)
Volume 7 No. 1 January-June 2023
ISSN 2586-8527 (Online)

Peer Reviewers

Prof. Dr. Parames Chutima	Chulalongkorn University, Thailand
Assoc. Prof. Dr. Arsa Tangjitsomkit	Thammasat University, Thailand
Assoc. Prof. Dr. Koonlaya Kanokjaruvijit	Naresuan University, Thailand
Assoc. Prof. Dr. Mathanee Sanguansermsri	Naresuan University, Thailand
Assoc. Prof. Dr. Nattapon Chantarapanich	Kasetsart University, Sriracha Campus, Thailand
Assoc. Prof. Dr. Piyanun Charoensawan	Naresuan University, Thailand
Assoc. Prof. Dr. Sangsuree Vasuponggayya	Prince of Songkla University, Hatyai Campus, Thailand
Assoc. Prof. Dr. Wilaiporn Lee	King Mongkut's University of Technology North Bangkok, Thailand
Asst. Prof. Dr. Chatchawin Namman	Ubonratchathani University, Thailand
Asst. Prof. Dr. Chorkaew Jaturanonda	King Mongkut's University of Technology Thonburi, Thailand
Asst. Prof. Dr. Chutima Beokhaimook	Rangsit University, Thailand
Asst. Prof. Dr. Nipat Jongsawat	Rajamangala University of Technology Thanyaburi, Thailand
Asst. Prof. Dr. Panomkhawn Riyamongkol	Naresuan University, Thailand
Asst. Prof. Dr. Pornthip Keangin	Mahidol University, Thailand
Asst. Prof. Dr. Teerapot Wessapan	King Mongkut's University of Technology Thonburi, Thailand
Dr. Kwankamon Dittakan	Prince of Songkla University, Thailand

INTERNATIONAL SCIENTIFIC JOURNAL OF ENGINEERING AND TECHNOLOGY (ISJET)
Volume 7 No. 1 January-June 2023
ISSN 2586-8527 (Online)

PANYAPIWAT INSTITUTE OF MANAGEMENT
85/1 Moo 2, Chaengwattana Rd.,
Bang Talat, Pakkred, Nanthaburi,11120 Thailand

Dear Colleagues,

The importance of information and artificial intelligence in contemporary society is indisputable. The timely utilization of information can provide organizations with a competitive advantage. However, the process of extracting meaningful insights from data can be challenging and may require a significant investment of time. Artificial intelligence, specifically neural networks, possesses the ability to adjust to various inputs and generate optimal outcomes that accomplish the required informational requirements.

The potential outcome of increased effectiveness and efficiency in the work process has been demonstrated in various research articles: Autonomous Driving Smart Car Based on Deep Learning, Comparison of Backbones for Microscopic Object Detection Algorithms, Comparison of Keywords Extraction Techniques in Kickstarter and Indiegogo Projects, Design and Development of a Carry-On Bag to Support Women in Work-and-Travel Activities, Study of Effects of Inlet Wind Velocity and Direction on Airflow around the Buildings Using CFD Turbulence Models: A Case Study of the Rajamangala University of Technology Rattanakosin (Salaya Campus), Thailand, and Sentiment Analysis on Thai Social Media Using Convolutional Neural Networks and Long Short-Term Memory.

All authors and readers from around the world are invited to visit the website https://ph02.tci-thaijo.org/index.php/isjet/index. This link will grant you to submit your research to publish in our journal or will access electronic versions of all issues of our journal. On behalf of the Editorial Board, I would like to take this opportunity to thank everyone who has complimented our goal by contributing to the ISJET.

With Kind regards,

Asst. Prof. Dr. Nivet Chiravichitchai
Associate Editor of Information Technology
isjet@pim.ac.th

INTERANTIONAL SCIETIFIC JOURNAL OF ENGINEERIN AND TECHNOLOGY (ISJET)
Volume 7 No. 1 January-June 2023
ISSN 2586-8527 (Online)

CONTENTS

Autonomous Driving Smart Car Based on Deep Learning

Zihao Nie[1] and Jian Qu[2]

[1,2]Faculty of Engineering and Technology, Panyapiwat Institute of Management, Nonthaburi, Thailand
E-mail: 6372100151@stu.pim.ac.th, jianqu@pim.ac.th

Received: December 17, 2021/ Revised: May 26, 2022 / Accepted: June 17, 2022

***Abstract*—Road tracking as an essential task in autonomous driving is crucial for artificial intelligence. Most research is conducted in virtual environments, but it is vital to conduct practical experiments on real cars. The current researchers use toy cars for road track, but the toy cars can only drive at a fixed speed and a fixed angle for steering, which leads to reproduction errors during the experiment. We built a smart car based on a scale model using Jetson Nano as a mainboard, which can adjust the speed and steering gain to improve road tracking performance and reduce reproduction errors. To analyze the impact of hyperparameters, we conducted experiments on 48 autonomous driving models and proposed optimal hyperparameter configuration schemes, and trained the optimal autonomous driving model BH-ResNet. In addition, we also research the effect of the speed and steering gain on the performance of the smart car and propose an optimal gain value. Moreover, we compare BH-ResNet with other existing models, and BH-ResNet outperforms other models, scoring the highest in both tracks, with 94 and 90. Furthermore, the BH-ResNet model can also achieve road tracks with superior performance in unseen scenes, and our proposed model has excellent applicability and practicality.**

***Index Terms*—Autonomous Driving, Convolutional Neural Networks, Deep learning, Deep residual network, Jetson Nano**

I. Introduction

Deep learning is one of the current breakthroughs in artificial intelligence, and the application of deep learning methods to autonomous driving research has solid practical and theoretical significance [1], [2].

Road tracking is the primary task of autonomous driving. In the existing autonomous driving research, most of the research remains in the virtual stage to save costs and ensure the safety of the experiment. Lin et al. chose a software simulator as the experimental environment platform to obtain the relative positions of the car and the road using deep neural networks as the computational framework. Finally, they achieved road track on the simulator track [3]. Although it is convenient and safe to conduct experiments in a virtual environment, this approach is not as accurate as training autonomous cars directly in the real world. Therefore, we propose to make a self-made car and an autonomous driving track in the real world, where the steps of data collection and model testing are done in the world.

Although more and more research is being done to achieve experiments in the real world using self-made cars, most research usually uses toy cars as research cars. Hossain et al. and Karni et al. conducted autonomous driving research by modifying abandoned toy cars, but toy cars are different from real cars [4], [5]. For example, a toy car cannot adjust the speed gain and steering gain like a real car. The toy car can only drive at a fixed speed and a fixed range for steering during the experiment, so the toy car often has reproduction errors, which affects the experimental results. We propose to achieve the autonomous driving experiment by building an autonomous driving smart car, which can replicate the driving situation of the actual car to the greatest extent. In addition, by fine-tuning the speed and steering gain, the autonomous driving performance of the smart car can be improved. For example, it can drive with low steering gain when there are many curves. The second is the use of sensors. Most of the existing research uses sensors to assist the smart car in achieving the autonomous driving experiment, but this makes the smart car not intelligent enough and independent. Banerjee et al. installed radar sensors on the smart car [6], and Yilmaz et al. installed many sensors such as infrared sensors and ultrasonic sensors [7]. However, humans do not use sensors when driving a car and only make judgments through hearing and vision. Therefore, the research needs to achieve the autonomous driving task of the smart car using fewer sensors. This article proposes that the smart car uses only one camera as a sensor for environmental perception to achieve the task of road tracking. As the brain of the smart car, the choice of the mainboard of the smart car is critical. The mainboard with powerful computing power can increase the performance of intelligent agents. Most of the research often uses

Arduino, and Raspberry Pi, as the mainboard of the intelligent agent. Yuenyong et al. used Arduino as the computing platform for reinforcement learning training in the research, but the computing power of Arduino is low, and a computer needs to be used as a backend for computing [8]. Do et al. used the Raspberry Pi for autonomous driving research, which was also limited by the low computing speed and performance of the Raspberry [9]. In order to solve the above problems, this article proposes to use Jetson Nano with superior computing power as the mainboard, which can make the smart car not attached to any back-end and can independently calculate and load the autonomous driving model, and the performance of the smart car is outstanding.

In addition, the construction of the track is also a critical step in achieving the road-tracking task. Both Zhang et al. and Li et al. built a circular track [10, 11], but these tracks are simple, which is not conducive to the test of the steering ability of the smart car. Therefore, we need a more complex track. This article makes two different tracks to meet the track diversity required for autonomous driving.

In achieving road tracking experiments, training deep neural networks and the optimal selection of structural parameters (different networks, batch size, epoch) is a challenging task. Do et al. constructed a new Convolutional Neural Network (CNN) to achieve the road tracking task by mapping the raw input image to a predicted steering angle through the CNN [9]. Rausch V et al. proposed an end-to-end control system based on Convolutional Neural Networks (CNN) for steering autonomous driving cars [12]. In the above research, the difference in the neural network will directly affect the accuracy of the smart car in achieving the automatic driving task. Therefore, this article proposes to use two popular neural networks, ResNet-18 and ResNet-50, to conduct experiments to research the impact of different neural networks on autonomous driving and select the optimal neural network to achieve the road tracking task.

In addition to the neural network, two hyper-parameters, batch size, and epoch, also affect model training results. Radiuk et al. explored the approach of improving the performance of convolutional neural networks and researched the effect of batch size on the network also researched the batch size and found the optimal batch size for training the Deep Q network on the shopping cart system [14]. However, they did not extend their research to autonomous driving. Similar to batch size, the choice of epoch will vary for different research. Chowdhuri et al. and Kocić et al. obtained the minimum error values in different epoch intervals, respectively [15], [16], so selecting different epoch intervals for different experiments is essential. We propose using different batch sizes and epochs to train the autonomous driving model to get the optimal batch size and epoch and their relationship with autonomous driving performance.

In summary, this article proposes to use a scale model to build an autonomous driving car in the real world that uses only one camera as an environment perception sensor, which can drive at an adjustable speed and steering range just like a real car. Furthermore, we choose Jetson Nano as the computing platform, which makes the autonomous driving smart car in this article an independent agent. Since hyperparameters play a vital role in the success of the model training stage, this article discusses and conducts a series of experiments on the effects of different hyperparameters on autonomous driving. Finally, we propose the optimal hyperparameter configuration scheme. In addition, we also discussed the influence of speed gain and steering gain on the smart car and proposed a set of optimal gain values, which further improved the performance of the smart car to achieve road tracks. Finally, we put the smart car in an unseen scene for experiments to verify the applicability of the optimal hyperparameter configuration scheme proposed in this article. In total, we compared 48 sets of hyperparameter configuration schemes, found possible optimal combinations, and trained the optimal model. In addition, we also compared five sets of speed gain values and five sets of steering gain values and found the optimal gain value. In addition, we also compared the optimal autonomous driving model with three groups of other models and achieved road-tracking experiments in unseen scenarios.

II. Literature Review

In recent years, autonomous driving technology has developed rapidly, and there has been much research on the hardware and hyperparameters of autonomous driving smart cars.

A. Hardware Improvement of Autonomous Driving Smart Cars

Research on autonomous driving is usually divided into virtual and real experiments. Most researchers use virtual platforms to ensure the safety and convenience of experiments. Lin et al. achieved road tracking in a virtual environment. After the trained virtual car obtains its position relative to the track, it can use this information as the basis for feedback control and eventually achieve road track in the simulator [3]. However, the results obtained in the virtual environment are usually affected by sunlight, shadows, chromatic aberrations, and noise when migrated to the real world, resulting in poor autonomous driving performance in the real world. Therefore, researchers have gradually used self-made cars to achieve autonomous driving research in the real world.

In this article, autonomous driving smart cars are roughly divided into two categories: toy cars and smart cars. Most research is based on toy cars and modified to build autonomous driving cars. As shown in Fig. 1(a), Hossain et al. aimed to build autonomous driving cars using very low-cost and readily available hardware, so they developed a low-cost mini rover using a toy car that could roam around the area it wanted to observe [4]. As shown in Fig. 1(b), Karni et al. also researched autonomous driving cars based on toy cars, aiming to achieve the task of road tracking [5]. However, the disadvantage of the toy car is that the experiment can only be carried out at a fixed speed and a fixed angle for steering. In the experiment, the actual operation effect of the toy car is often affected because the speed and steering gain cannot be adjusted. Therefore, we improved on this in our research. We propose to build an autonomous driving smart car that can adjust the speed and steering gain to ensure the improvement of the autonomous driving performance of the smart car.

Fig. 1. (a) Autonomous driving toy car by Hossain et al., (b) Autonomous driving toy car by Karni et al.

With the improvement of technology, most research often installs many sensors on the autonomous car to make the car easy to achieve the experimental task. The environmental perception part of the autonomous driving car is divided into two types: a combination of multiple sensors, either only using a camera as a sensor. Iqbal et al. to enable the car to achieve road tracking, infrared and ultrasonic sensors are installed on the autonomous driving car [17]. Banerjee et al. install radar sensors on the autonomous car, and radar sensors detect the safe distance between the vehicle and obstacles [6]. This article proposes to use only a camera as a sensor for environmental perception and the road tracking task, which can make the car imitate human behavior to the greatest extent.

Choosing an excellent mainboard is also an approach to improving autonomous driving performance. Many mainboards cannot achieve deep learning or reinforcement learning tasks independently due to their lack of computational power. A computer is needed as a back-end to assist in achieving the tasks. Yuenyong et al. chose Arduino as the mainboard of a small RC car to achieve reinforcement learning tasks, but the disadvantage is that Arduino is only a specific purpose microcontroller and cannot handle research that requires large-scale computing. They need to use a computer with a GTX 980Ti GPU as the back-end for data calculation and connect the computer to the car using Bluetooth [8]. Do et al. although the use of Raspberry Pi solves the problem that Arduino cannot handle large-scale computing, the performance of Raspberry Pi is also limited due to the lack of a powerful GPU [9]. Therefore, this article proposes to use Jetson Nano as a smart car computing platform, which supports most of the current deep learning frameworks and contains a powerful GPU, which allows the autonomous driving car to achieve all research independently.

As the test link of autonomous driving, the design of the autonomous driving track is critical. As shown in Fig. 2, Zhang et al. and Li et al. only test the road track by building a simple circular track task [10], [11], which is far from enough because the performance of the smart car when passing through the curve can better test the autonomous driving ability of the smart car. Therefore, this article designs two different complex tracks to increase the diversity of autonomous driving tracks and restore the authenticity of racing tracks in real life as much as possible.

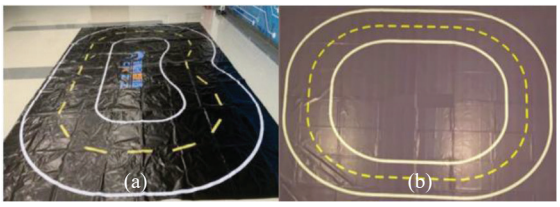

Fig. 2. (a) The track of Zhang et al., (b) The track of Li et al.

B. Research on Hyperparameters in Autonomous Driving

In addition to building an autonomous driving smart car, achieving the task of road tracking also requires setting the optimal hyperparameter configuration scheme before starting the training phase of the neural network. These hyperparameters include the neural network, batch size, epoch, and different datasets. These hyperparameters have a significant impact on the training of the model and the performance of autonomous driving.

1) Deep Neural Network

Autonomous driving technology requires many deep-learning algorithms to process complex data. Deep learning is a multi-layer perceptron that includes an input layer, multiple hidden layers, and an output layer, which can be composed of numerous processing layers. It is very good at finding complex structures in high-dimensional data. Deep learning uses backpropagation algorithms to instruct machines to change their internal parameters to find complex systems in large datasets [18]. Fig. 3 is a multi-layer neural network described by the backpropagation algorithm, which is a three-layer neural network consisting of an input layer with two input units, two hidden layers, and an output layer [19].

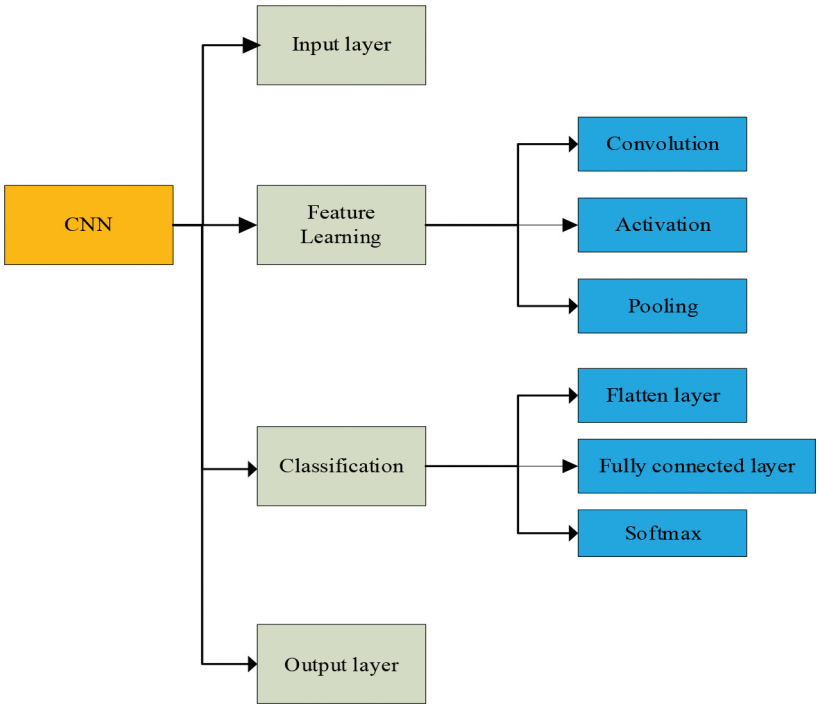

Fig. 3. Convolutional neural network architecture diagram

In deep learning, many deep neural networks are commonly used, among which convolutional neural networks are now more popular.

Convolutional Neural Network (CNN) is a deep learning neural network for image recognition and classification [20]. Each input image in the CNN model goes through a series of convolution layers, pooling layers, and fully connected layers and applies the softmax function to classify the objects. The steps of CNN are roughly divided into four steps: input, feature learning, classification, and output [21]. The feature learning step consists of the convolution layer, excitation layer, and pooling layer. The classification consists of the flattening layer, fully connected layer, and softmax classification layer. The specific steps of CNN are shown in Fig. 4.

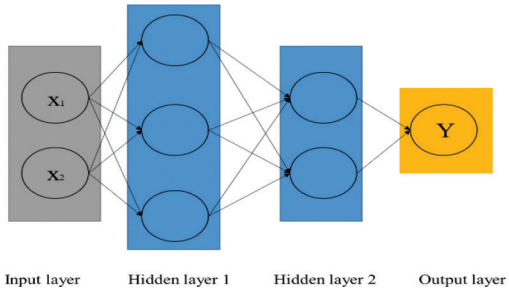

Fig. 4. Neural network architecture diagram

Convolution is the first layer and extracts features from the input image. Convolution uses small squares of input data to learn image features to preserve the relationship between pixels. The purpose of convolution operations is to extract high-level features from the input image, which has profound implications for image processing. For example, Fig. 5(a) is an image matrix with an input image of 7*7, and its image pixel values are 0 and 1. Fig. 5(b) is a 5*5 filter matrix called a convolution kernel.

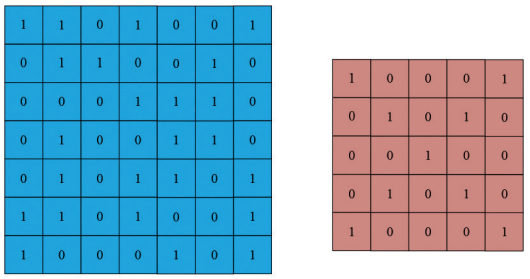

(a) 7*7 image matrix (b) 5*5 filter matrix

Fig. 5. (a) The input image is an image matrix of 7*7, (b) The filter matrix of 5*5

As shown in Fig. 6(a), multiplying the convolution of the 7*7 image matrix by the 5*5 filter matrix becomes a “feature map”. The value in Fig. 6(b) is 4, which is obtained after one convolution. Convolving the image with different filters (convolution kernels) can perform edge detection and blurring operations. The filter will move to the right by a particular “step value” until the entire image is walked, completing the convolution process.

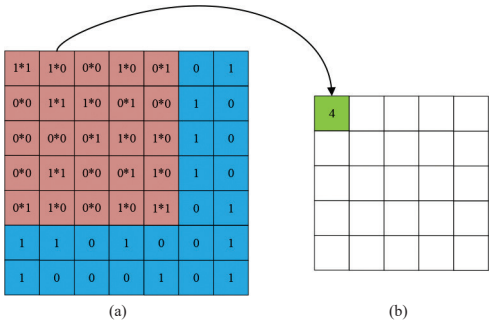

Fig. 6. (a) Process of convolution operation, (b) Results of the convolution operation

After the convolutional layer completes the convolution and extracts the information in the input image, it will perform a nonlinear mapping on the output of the convolutional layer through the excitation layer because the calculation of the convolutional layer is still linear, and the data in the real-world hope what is learned by CNN is a non-negative linear value.

Pooling is also known as spatial pooling. The pooling layer has two functions. First, by reducing the dimension of the feature map, the space size of the convolutional feature is reduced, and the computing power required to process the data is reduced. Second, maintain the process of effectively training the model, extracting essential features invariant to rotation and position. Its most common pooling methods are max pooling and average pooling [22]. The method of the max pooling layer is to use the maximum value of each region of the input part to perform max pooling and generate the max pooling layer, as shown (a) in Fig. 7. The method of the average pooling layer is to use the average value of each region of the input part to perform average pooling (b). Fig. 7 is an example of the average pooling layer.

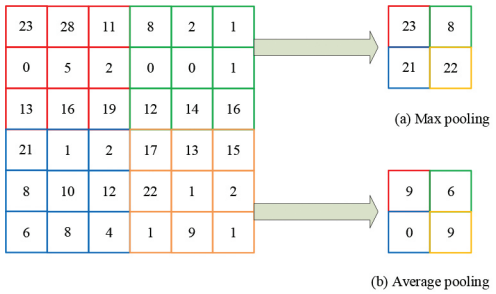

Fig. 7. Example of the calculation process of max pooling and average pooling

The last layer of the CNN starts classification. First, the matrix is converted into a vector by a flattening layer, then sent to a fully connected layer. Adding a fully connected layer is a common way to learn non-linear high-level features, represented by the output of a convolutional layer. The combined method finally classifies the output with a softmax or sigmoid and a classification function.

We summarize the processing steps of convolutional neural networks. First, the input image is provided to the convolutional layer. Second, the parameters are chosen, and filters with stride and padding are applied if necessary. Next, convolve the image and apply an activation function to the matrix. Then merge and reduce the dimensionality. Add as many convolutional layers as possible. Finally, flatten the output and send it to a fully connected layer, use the activation function to output the class, and merge the classified images.

Much research also uses different networks based on CNN for experiments in the current research. Do et al. proposed a 9-layer structure, including five convolutional layers, and four fully connected layers to form a new deep neural network, and build a monocular vision autonomous car with Raspberry Pi as the mainboard, using the end-to-end method to directly map the input image to the predicted steering angle as the output, and finally achieved the road tracking task [9]. Rausch et al. proposed a convolutional neural network consisting of three convolutional layers, two pooling layers, and one fully connected layer for end-to-end driving of the autonomous driving car. The trained terminal controller of the network directly transmits instructions through the mapping relationship between pixel data and steering commands, enabling the smart car to achieve the task of autonomous driving [12]. In the above research, the experimental results are directly related to deep neural networks. Therefore, we propose to use ResNet as the basic model, train different ResNet networks, explore the impact of different neural networks on autonomous driving, and select the optimal neural network to achieve the road tracking experiment.

2) Batch Size and Epoch

Batch size and epoch play an essential role in the model training process. Radiuk et al. researched a parameter of the training set: batch size. The goal was to find out the effect of the batch size on the performance of the neural network. They used the MNIST dataset and CIFAR-10 datasets to obtain consistent results and concluded that batch size affects experimental accuracy [13]. In the research of Choi , he fixed other hyperparameter values, and the neural network was trained for ten different batch sizes and obtained the logarithm of the quadratic relationship between the total training time and batch size [14]. However, they did not extend the results to other research. The research on epoch is also gradually increasing. In training the neural network of autonomous driving, Chowdhuri et al. neneedso choose the epoch that minimizes the average error of the network, which occurs at the 23rd epoch [15]. Kocić et al. proposed

an end-to-end deep neural network, J-Net, for autonomous driving, where J-Net provided the best driving performance when trained for sixth epochs [16]. We found that the epoch interval of the best training model is different, and the choice of epoch affects the fitting degree of the neural network. Therefore, this article will research batch size and epoch and propose their optimal hyperparameters for road-tracking experiments.

To sum up, this article will explore the influence of hyperparameters on model training and the actual operation effect of autonomous driving and propose an optimal configuration scheme of hyperparameters, which will ultimately enable the autonomous driving smart car to achieve the road tracking task. We will elaborate on the construction of the smart car and the autonomous driving track.

III. Our Approach

This article proposes a set of optimal hyperparameter configuration schemes and independently builds an autonomous driving smart car and achieves road tracking in the real world. In addition, we also conducted experiments to adjust the speed and steering gain and proposed a set of optimal gain values, which can further improve the performance of the smart car. We trained the optimal autonomous driving model using the optimal hyperparameter configuration and compared it with existing research and other neural network models. Finally, to verify the applicability of our model, we also test in unseen scenarios. The detailed flow chart of this research is shown in Fig. 8.

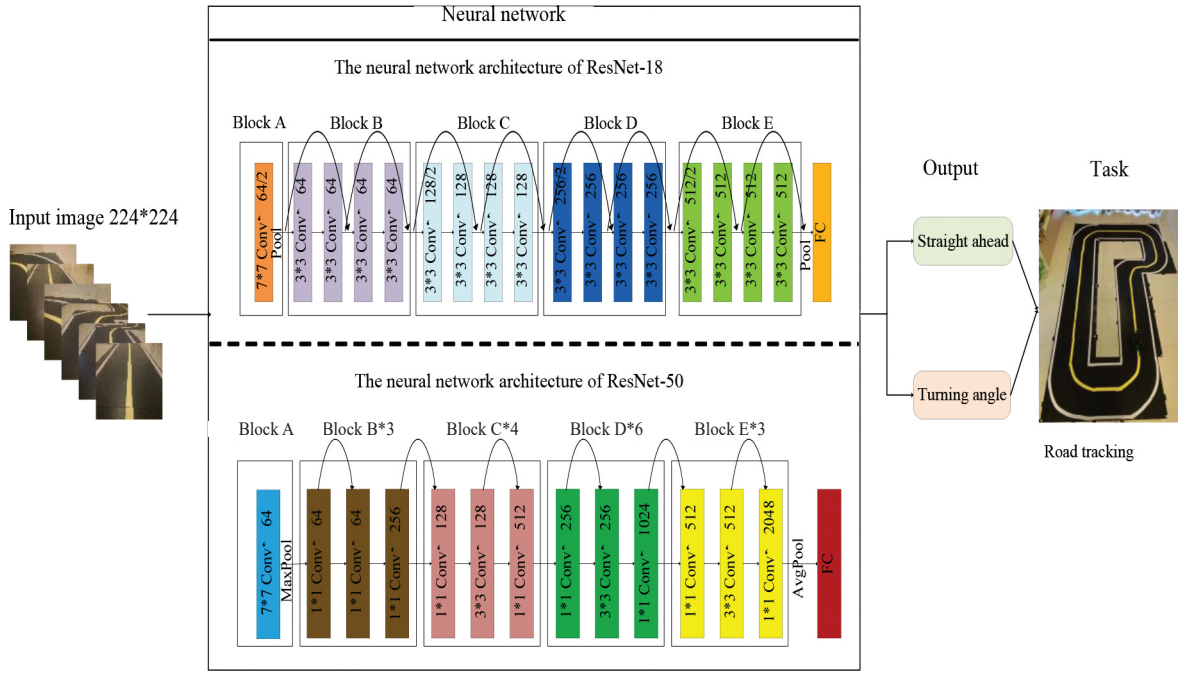

Fig. 8. Overview of the detailed process for achieving road tracking

A. Hardware settings of the Jetson Nano Autonomous Driving Smart Car

The hardware connection diagram of the Jetson Nano autonomous driving smart car is shown in Fig. 9. We chose Jetson Nano as the mainboard of the smart car, and the Jetson Nano is the center to send control signals to various components of the smart car so that the smart car can achieve the road tracking task.

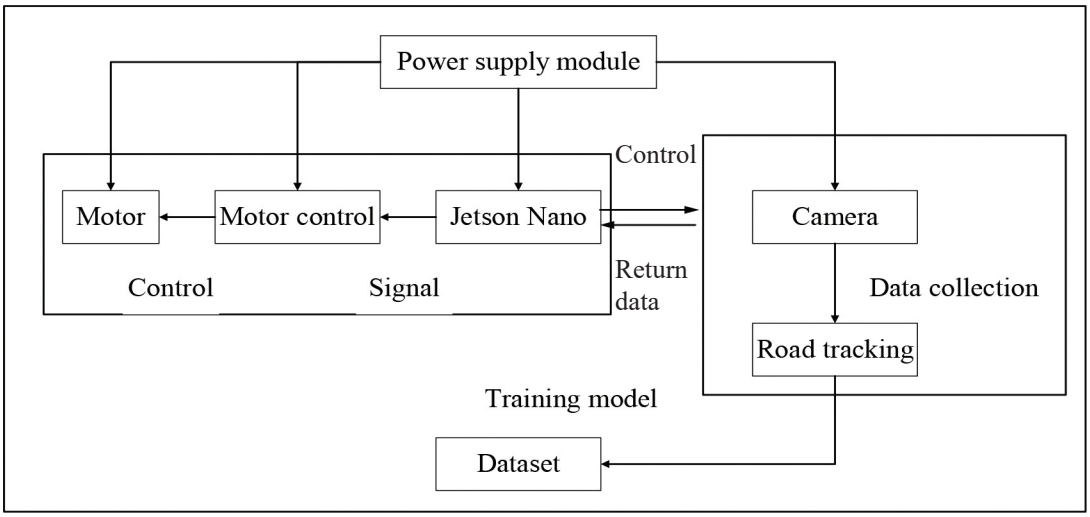

Fig. 9. The hardware framework of Jetson Nano smart car

1) Jetson Nano Mainboard

This article uses a smart car with only one camera as a sensor for research and collects data on the real track through the camera of the smart car for model training. Also, most of the research uses Raspberry Pi or Arduino as the mainboard for intelligent agents, but Arduino alone cannot do deep learning. The computing power and efficiency of the Raspberry Pi are low, and it cannot carry complex deep learning networks. We propose to use Jetson Nano as the mainboard of the smart car, which has a powerful GPU. The CPU of the Jetson Nano is a quad-core Cortex-A57, and the GPU is a graphics card of the NVIDIA Maxwell architecture. It has 128 CUDA units. We train the model using a ResNet network based on the Pytorch framework to recognize lane lines and output driving instructions [23], [24]. A picture of the Jetson Nano is shown in Fig. 10.

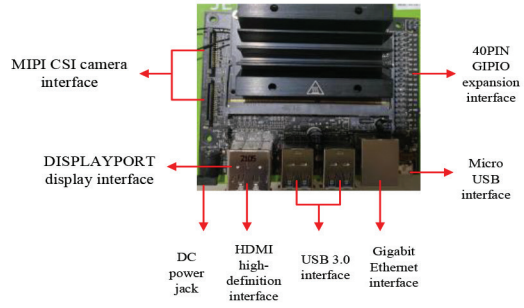

Fig. 10. Jetson Nano mainboard

The difference between the Raspberry Pi and the Jetson Nano is that the Jetson Nano has a higher performance and a more powerful GPU. As shown in Table I, Jetson Nano supports many deep learning frameworks, enabling us to use more complex deep learning models, obtain faster computing speeds, and reduce development time by 70%.

TABLE I
MAINBOARD INFORMATION TABLE

List	Raspberry Pi 4B	NVIDIA Jetson Nano
CPU	Quad-core ARM Cortex-A72 64-bit @ 1.5 GHz	Quad-core ARM Cortex-A57 64-bit @ 1.42 GHz
GPU	Broadcom VideoCore VI (32-bit)	NVIDIA Maxwell w/128 CUDA cores @ 921 Mhz
Memory	4 GB LPDDR4	4 GB LPDDR4
Net working	Gigabit Ethernt/ Wifi 802.1 1ac	Gigabit Ethernt/ M.2 Key E
Display	2x micro-HDMI (up to 4Kp60)	HDMI 2.0 and eDP 1.1
USB	2x USB 3.0,2x USB 2.0	4x USB 3.0, USB 2.0 Micro-B
Other	40-pin GPIO	40-pin GPIO
Video Encode	H264(1080P30)	H.264/H.265 (4Kp30)
Video Decode	H.265(4Kp60), H.264(1080P60)	H.264/H.265 (4Kp60,2x 4Kp30)
Camera	MIPI CSI port*1	MIPI CSI port*2

2) Materials Used in Jetson Nano Smart Car

Using the Jetson Nano mainboard as the core is an excellent choice for building an autonomous driving smart car. The smart car has the ability of independent computing. The smart car perceives the environment through high-definition cameras and uses the trained neural network to achieve the road tracking task. The hardware required to assemble the smart car is shown in Table II.

TABLE II
JETSON NANO SMART CAR MATERIAL TABLE

Serial Number	Part	Specifications/Remarks	Quantity
1	Jetson Nano	-	1
2	IC Expansion Board	-	1
3	Motor	370P	2
4	Servo	-	2
5	Smart Car Chassis	Including Servo and Camera Mount	1
6	Camera	Sony 8 Million HD Camera	1
7	Wireless Network Card	-	1
8	Track	-	1
9	Battery	-	1
10	Smart Car Crawler Gear	-	4

3) Jetson Nano Autonomous Driving Smart Car Achieved

The Jetson Nano autonomous driving smart car we built using the scale model is shown in Fig.11. The toy cars in the existing research have simple structures and can only drive with a fixed speed gain and a fixed steering gain. Therefore, toy cars often have reproduction errors during experiments, and toy cars have poor autonomous driving performance. The smart car in this article can improve the automatic driving performance of the smart car by adjusting the speed and steering gain. In addition, the experimental effects brought by different speeds and steering gains will also be different. For example, if the steering gain is large, the turning range of the smart car will be large when it is in a curve, and sometimes it will drive out of the track. Therefore, we will also research the speed and steering gain of the smart car and strive to propose an optimal gain value to improve the nomous driving performance.

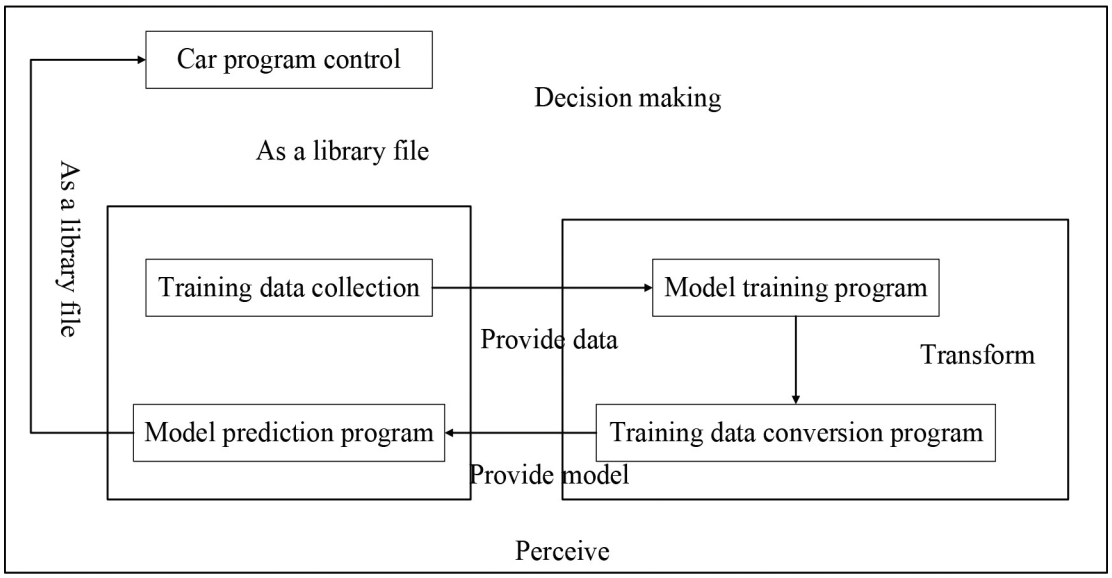

Fig. 11. Flowchart for achieving the road tracking of the Jetson Nano smart car

The achievement of the road tracking task of the Jetson Nano smart car is shown in Fig.12. It can be divided into four parts: the car control program, the training data acquisition program, the model training program, and the model prediction program.

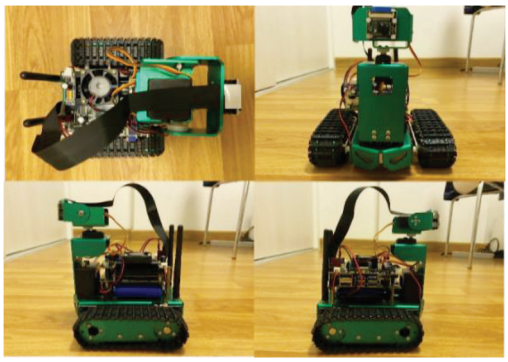

Fig. 12. Overview of the Jetson Nano autonomous driving smart car

B. Simulation Site Construction

We build a simulation site to simulate the driving of an autonomous driving car on the road. We added four corners and an S-curve to a standard circular road to restore the actual route and facilitate testing the steering of the Jetson Nano smart car when turning. The white line is the boundary line of the track, and the yellow line is the lane line of the track. The width of the entire track is 44 cm, and the distance between the yellow and white lines is 22 cm. Using two-lane lines in two colors can give the smart car better results in the road tracking experiment. Finally, we collect data and test the final model in the self-made racing track to determine the performance of road tracking under different neural networks, batch sizes, and different amounts of datasets and epochs. Fig.13 and Fig.14 are schematic diagrams of the smart car simulation site.

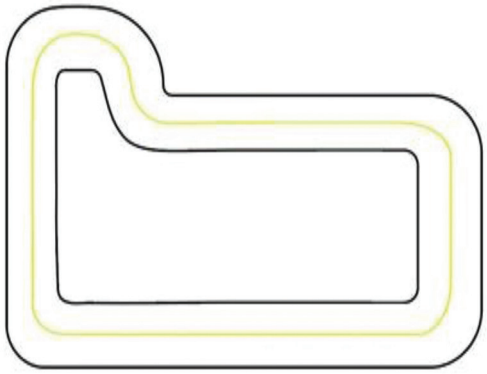

Fig.13. Simulation site model diagram

Fig.14. Actual map of the simulation site

C. Use of Neural Networks

The road tracking of the smart car is to collect a large amount of data and divides it into a training set and a test set. After deep neural network training, a model is formed, and the road tracking experiment is achieved. In this experiment, the lane lines taken by the camera of the smart car on the self-made track will be used as training data. The selected deep neural network is ResNet, and different ResNet neural networks are used to train under different epochs and batch sizes. Finally, the quality of the training results is compared. However, different ResNet neural networks achieve different effects. To improve the accuracy and impact of the model as much as possible while the smart car can be within the limits of Jetson Nano memory and computing power, we must rationally use different ResNet neural networks and choose an appropriate number of datasets, epochs, and batch sizes. This research compares the verification loss value of the ResNet-18 neural network and the ResNet-50 neural network with a certain number of datasets, epochs, and batch sizes and analyzes the impact of these hyperparameters on the verification loss value. Moreover, we will also load the trained model into the smart car for actual operation and analyze the real operation effect.

IV. Experimental Setup

The experimental process is divided into data collection, model training, and model testing. Finally, an autonomous driving model is trained to enable the Jetson Nano smart car to achieve road tracks.

In the data collection stage, we placed the smart car at different positions on the track and used the real-time camera as input for data collection. We collected six sets of datasets, respectively, and this is to compare the autonomous driving performance of the smart car with different numbers of datasets.

During the model training stage, different hyperparameters have a significant impact on the performance of the autonomous driving model. Therefore, we train the autonomous driving model using different deep neural networks, batch sizes, epochs, and different datasets and finally propose a set of optimal hyperparameter configuration schemes. Finally, we load the trained model on the smart car to achieve road tracks. We also analyzed the number of datasets and the impact of different hyperparameters on autonomous driving according to the actual operation effect and verification loss value. The experimental procedure diagram is shown in Fig.15.

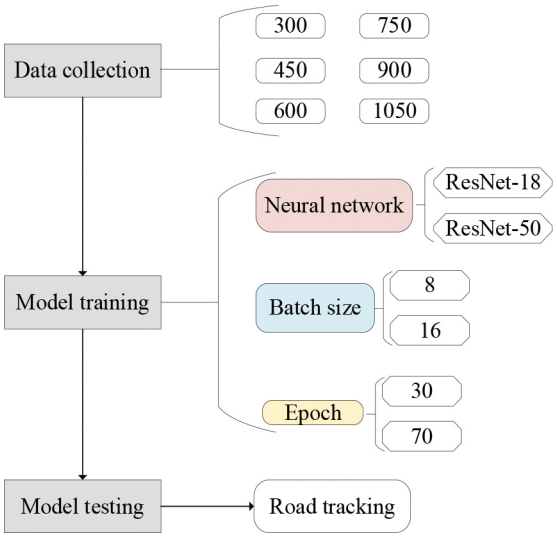

Fig. 15. Experimental procedure diagram

In addition, we also research the effect of different speed and steering gains on the performance of road tracking and propose a set of optimal gain values. Finally, to verify the applicability of our optimal autonomous driving model, we will achieve the road tracking task in unseen and untrained scenarios.

A. Data collection

The first step in this experiment is data collection. The quality of the training dataset will directly affect the performance of the autonomous driving model. The steps of data collection are shown in Fig.16.

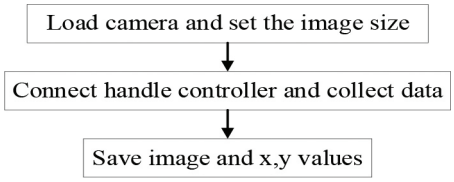

Fig. 16. Diagram of data collection steps

We initialize and display our camera. We choose to use a 224x224 pixel image as input. We set the photo to this size to minimize the memory of the dataset and speed up the training of the model.

Then the approach we take photos with is handle shooting. We create an instance of the PlayStation controller and collect images through the buttons on the controller.

We will place the smart car on different positions of the track according to the lane line and move the "x" and "y" sliders to mark the "green dot" in the center of the lane line during the road tracking experiment. The position marked by the green dot is the target position to be reached when the smart car drives. After the action is completed, press the "L1" button on the handle to save. At the same time, we will create a component to display the real-time image feed, the number of collected images, and the value of the storage target. It can be seen in Fig. 17 that the number of collected data is 1050 photos, and the method of moving the green dots can be seen in Fig. 18.

Fig. 17. Live preview of data collection (1050 represents the number of photos collected as 1050)

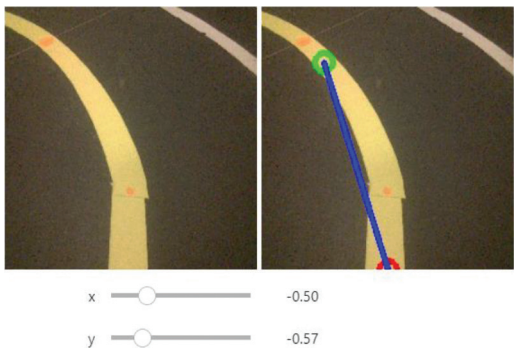

Fig. 18. The method of collecting points (drag X can change the left and right position of the green dot, and drag Y can change the distance of the green dot)

Finally, the collected data set is automatically saved to the corresponding new folder after collecting the corresponding data. When we train, we will transfer the data to the PC to load the image and parse the x and y values in the filename. Fig.19 is an example of the contents of the data folder. Each photo in the dataset folder is named with its x and y coordinates.

Fig. 19. Example of the contents of the data folder

B. Model Training

We can train the optimal autonomous driving model through model training, and this step is essential. The model training part aims to use the trained artificial neural network to reproduce the values when collecting the data: the x and y values. The steps of model training are shown in Fig. 20.

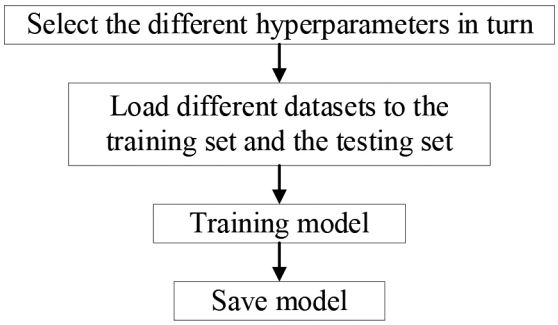

Fig. 20. The steps of model training

In training the model, the dataset will be divided into the training set and testing set. This research split the data into 90% as the training set and 10% as the testing set. The training set is used to train the autonomous driving model, and the testing set will be used to verify the accuracy of our trained model. Then we load the data in batches and shuffle the data. Most of the current research usually sets batch size=8, epoch=30 for training. Therefore, our initial batch size is set to 8, and the initial epoch is set to 30. we increase the batch size and epoch to 16 and 70, respectively, depending on the GPUs available in memory. This allows us to research the effect of different batch sizes and epochs on the autonomous driving model.

Next, we use the now popular ResNet-18 and ResNet-50 neural networks to train the model and transfer it to the GPU to run the model training through "CUDA". Once the model is trained, it will generate a model file that we will use for road tracking.

Table III shows the 48 hyperparameter settings in this experiment. They are trained with different neural networks, different numbers of datasets, different batch sizes, and epochs.

TABLE III
HYPERPARAMETER SETTINGS for ROAD TRACKING MODELS

Neural Network	Dataset	Batch Size	Epoch
ResNet-18	300	8	30
	450		
	600		
ResNet-50	750	16	70
	900		
	1050		

Through model training, we can get the validation loss value of each model. The validation loss value can reflect the performance of the model. We also load the trained autonomous driving model on the smart car for experiments, which can more accurately judge the impact of different hyperparameters on autonomous driving. We can get accurate results by combining the verification loss value with the actual operation effect of the smart car.

C. Model Testing

Through the training of the models, we were able to obtain the validation loss values for each model separately. The validation loss values can show the performance of the models on the data, and in order to get more accurate results, we also need to combine the real effects of the smart car operation, so we started the final step of the experiment by loading the trained models on the smart car and testing the models on a real track.

We can reduce the reproduction errors of toy cars often by setting the speed and steering gain. We drive the smart car with an initial speed and initial steering angle of 0.65 and 0.21, according to the design of the smart car. After obtaining the influence of hyperparameters on the autonomous driving model and proposing the optimal hyperparameter configuration scheme, we conduct research on the influence of the gain value on the autonomous driving model by adjusting the speed and steering gains and propose an optimal gain value to improve the road tracking performance.

When the smart car is driving in a straight line, no matter what dataset, neural network, batch size, or epoch, the smart car can achieve excellent performance. However, when the smart car is driving on a curve, the performance of different autonomous driving models can be demonstrated.

Therefore, to accurately compare the actual performance of autonomous driving models trained with different hyperparameter configuration schemes, we selected three points as measurement points at the S-turn of the self-made racing track.

We will judge the performance of the smart car according to two judgment criteria. 1) The distance between the center of the smart car and the measurement point when the smart car is driving. The smaller the distance between the centerline of the smart car and the measurement point, the better road tracking performance. 2) When the smart car is driving, the angle between the center of the smart car and the measurement point. The smaller the angle that the centerline of the smart car deviates from the measurement point, the better the performance of road tracks. The autonomous driving model it loaded will be better. In addition, we also marked a standard block on the map, and we can scale the standard block to the actual distance to get the accurate distance and angle. As shown in Fig. 21, P1, P2, and P3 are three measurement points, respectively. The white squares marked with green fonts are the standard blocks we reserved. Fig. 21(a) is the actual track map with the measurement points and the standard block marked. Fig. 21(b) is the track model diagram with marked measurement points and the standard block. Moreover, we also marked the detailed dimensions of the track in the track model diagram.

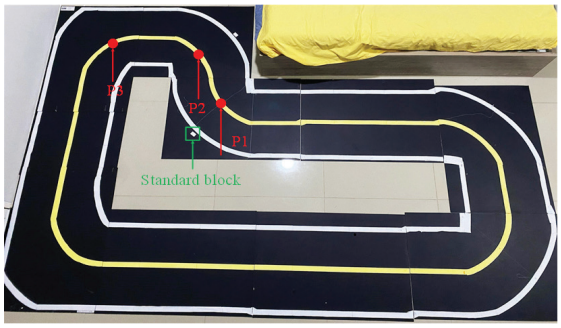

Fig. 21(a). The actual track map with the measurement points and standard blocks marked

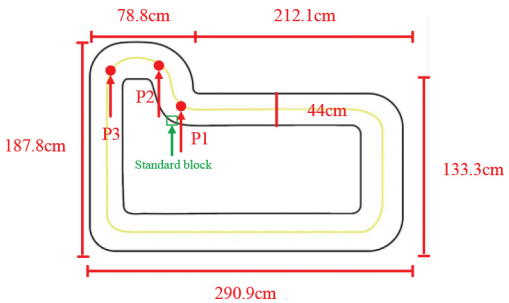

Fig. 21(b). The track model diagram with marked measurement points and the standard block, and detailed dimensions of the track

We shot the video with a camera and tripod during the experiment, took screenshots when the center of the smart car passed the measurement point, and measured. During the experiment, we will keep the light consistent and the measurement height and position unchanged to ensure the accuracy of the experiment. The specific experimental situation is shown in Fig. 22.

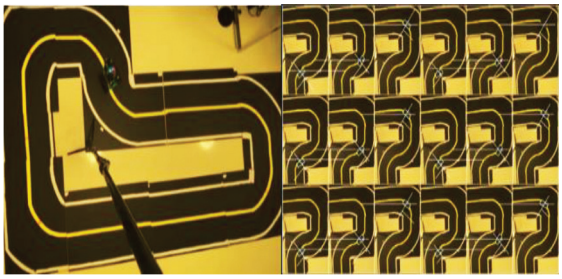

Fig. 22. Specific experimental situation diagram

We will obtain the performance of 48 models trained by different hyperparameter configuration schemes in actual operation through the above experiments. The next chapter will discuss obtained validation loss values and actual measurements.

V. Experimental Results and Analysis

This chapter will describe and analyze the impact of different neural networks, datasets, batch sizes, and epochs on the validation loss and the actual operation effect of smart cars. Finally, we propose an optimal hyperparameter configuration scheme and train an optimal autonomous driving model.

A. The Impact of Different Neural Networks, Different Datasets, Batch Sizes, and Epochs on the Verification Loss Value

The validation loss value can reflect the performance of the model. Table IV shows the validation loss values of our 48 sets of autonomous driving models trained with different hyperparameter configuration schemes to analyze the effect of different hyperparameters on the validation loss values.

TABLE IV
THE VALIDATION LOSS VALUES OF 48 SETS OF AUTONOMOUS DRIVING MODELS TRAINED WITH DIFFERENT HYPERPARAMETER CONFIGURATION SCHEMES

Neural Network	Dataset	Batch Size	Epoch	Loss	Neural Network	Dataset	Batch Size	Epoch	Loss
ResNet-18	300	8	30	0.011001	ResNet-50	300	8	30	0.013148
			70	0.010553				70	0.005804
		16	30	0.011973			16	30	0.011661
			70	0.007873				70	0.006367
	450	8	30	0.006913		450	8	30	0.01226
			70	0.008783				70	0.009035
		16	30	0.012878			16	30	0.01102
			70	0.006626				70	0.011696
	600	8	30	0.011351		600	8	30	0.008344
			70	0.008674				70	0.008863
		16	30	0.011769			16	30	0.011322
			70	0.011649				70	0.008776
	750	8	30	0.008598		750	8	30	0.007925
			70	0.011314				70	0.009001
		16	30	0.01077			16	30	0.011043
			70	0.009004				70	0.009863
	900	8	30	0.011724		900	8	30	0.018298
			70	0.014531				70	0.015377
		16	30	0.019155			16	30	0.018096
			70	0.012837				70	0.011401
	1050	8	30	0.0214		1050	8	30	0.018373
			70	0.015585				70	0.019586
		16	30	0.01889			16	30	0.015242
			70	0.021052				70	0.019499

1) The Impact of Different Neural Networks on Verification Loss Value

Based on the experimental results of 48 sets of autonomous driving models, we judge the influence of different neural networks on the validation loss value. Fig. 23 is a plot of validation loss results trained with ResNet-18 and ResNet-50. The horizontal ordinate is a different setting. For example, "P300_B8_E30" means that the dataset is 300 photos, batch size=8, epoch=30, the blue line represents the model trained with the ResNet-18 neural network, and the red line represents the model trained with the ResNet-50 neural network.

As shown in Fig. 23, when the model is trained with ResNet-50, the validation loss value is generally lower than the model trained with ResNet-18. As the depth of the network deepens, the degree of abstraction of features is higher. The accuracy of the trained model will increase, and the validation loss will decrease,

The maximum value appears in "ResNet-18_P1050_B80_E30", the validation loss value is 0.0214, and the minimum value appears in "ResNet-50_P300_B8_E70", and the validation loss value is 0.005804.

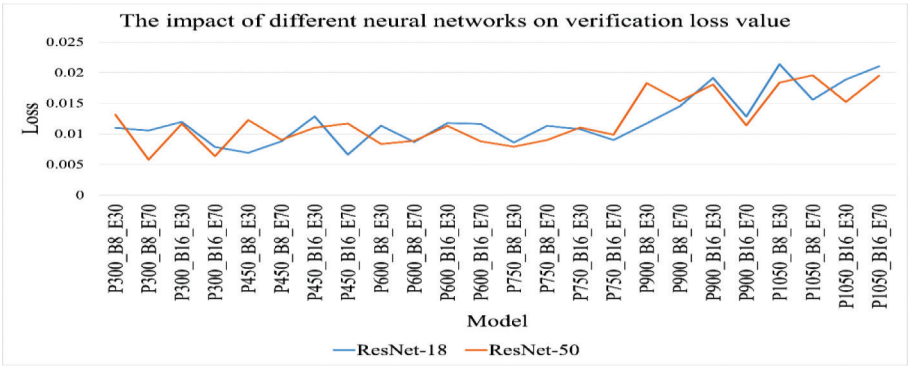

Fig. 23. The results of verification loss for different neural networks

2) The impact of different numbers of datasets on verification loss value

The amount of data in the dataset also affects model training. In this research, six datasets with different numbers of data were selected for training, and the impact of dataset on the model was explored. Fig. 24 shows the validation loss results when training with six datasets.

As shown in Fig. 24, when the dataset is 300 photos, 450 photos or 900 photos, 1050 photos, the validation loss value will fluctuate wildly. Furthermore, the validation loss is significantly reduced when using the ResNet-50 neural network. Through experiments, the number of datasets for the ResNet-18 neural network is not inversely proportional to the validation loss value, but for the ResNet-50 neural network, the larger the number of datasets, the smaller the validation loss value. Therefore, the size of the dataset has a more significant impact on the deep network. As the network depth deepens, the amount of data required to train the model also needs to increase.

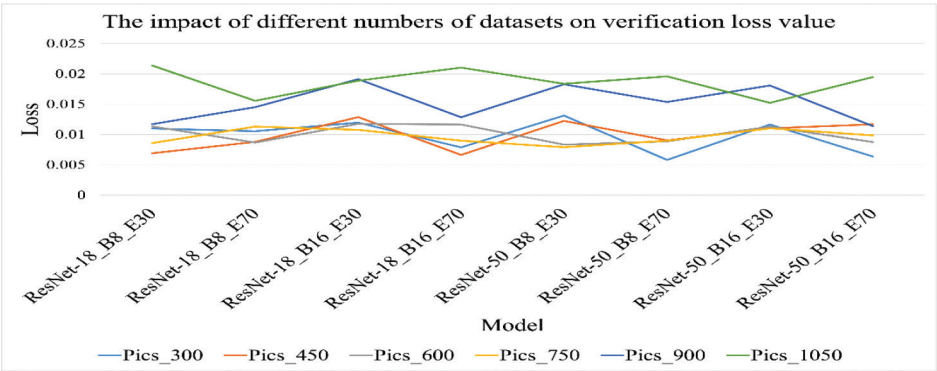

Fig. 24. The results of verification loss for different numbers of datasets

3) The impact of Different Batch Sizes on Verification Loss Value

Batch size is a crucial hyperparameter in deep learning. Batch size will affect memory utilization, processing speed, and model accuracy. Therefore, the choice of batch size also affects the quality of the model.

Most research usually sets the batch size to 8. We increase the batch size during training to 16 according to the available GPU in memory, set batch size=8 and 16 for model training, respectively, and then judge the impact of batch size for model training and validation loss.

Fig. 25 shows the validation loss results for batch size=8 and 16 training. It can be seen that the small batch size has little effect on the model validation loss.

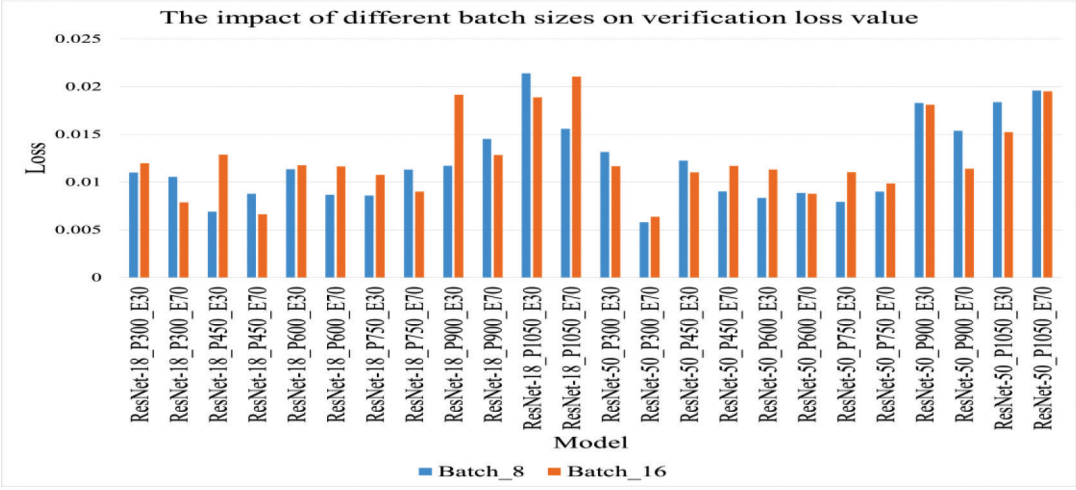

Fig. 25. The results of verification loss for different batch sizes

4) The Impact of Different Epochs on Verification Loss Value

Epoch refers to the number of times to train all data. Most research usually sets the epoch to 30 for model training. We also increased the epoch value to 70 according to the available GPU conditions and analyzed the impact of different epochs on the model validation loss value.

Fig. 26 is a plot of the validation loss results for training with epoch=30 and 70. As shown in Fig. 26, the validation loss value of the model with epoch=70 is smaller than epoch=30. Therefore, on the premise that the model does not enter the overfitting state, the more iterations of weight update, the more epoch, the smaller the validation loss of the model, and the better the effect of training the model.

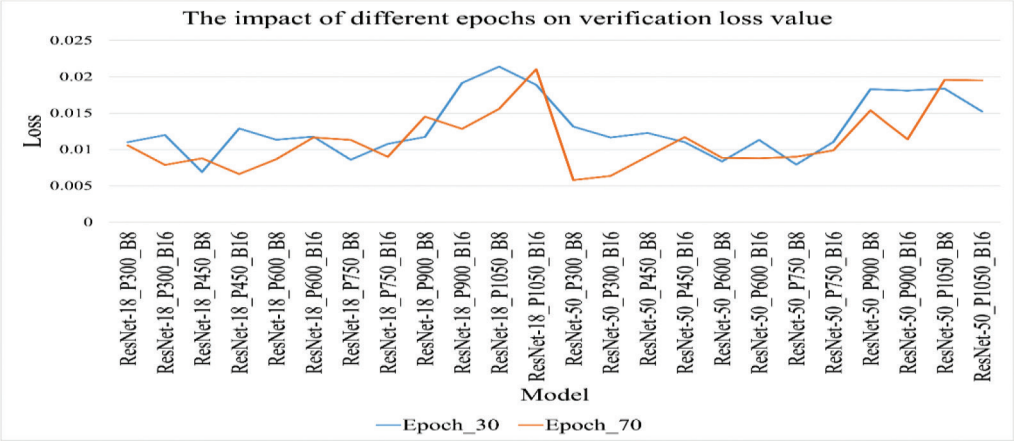

Fig. 26. The results of verification loss for different epochs

5) Summary of Validation Loss Values of Models Trained Under Different Hyperparameter Configuration Schemes

This experiment trains 48 autonomous driving models according to different hyperparameter configuration schemes. Fig. 27 shows the validation loss values for 48 autonomous driving models. From Fig. 27, it can be seen that the validation loss values of the autonomous driving model trained with ResNet-50 are smaller than those of the model using ResNet-18. Among them, when the dataset is 300 photos, batch size=8, epoch=70, the validation loss is the smallest, 0.005804.

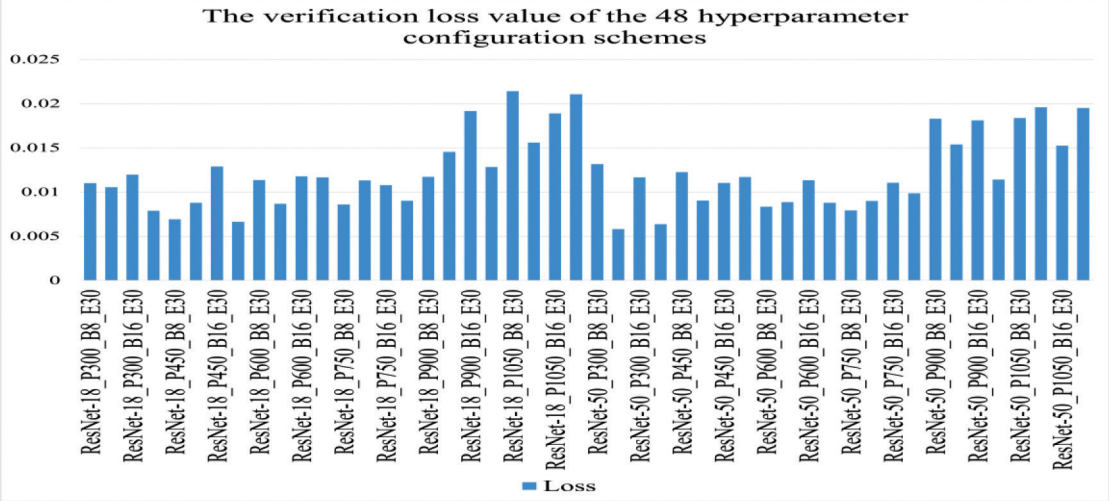

Fig. 27. The validation loss values for 48 autonomous driving models

Although the validation loss value can reflect the performance of the model, when the models are trained with ResNet-18, the difference in the validation loss value of each model is very small.

Therefore, to get accurate results, we need to evaluate further the quality of the autonomous driving model based on the actual road tracking performance after loading the model into the smart car. Finally, an optimal hyperparameter configuration scheme is proposed.

B. The Impact of Different Neural Networks, Different Datasets, Batch Sizes, and Epochs on the Actual Performance of the Smart Car

We load the trained model on the autonomous driving smart car. We analyze the performance of autonomous driving models trained by different hyperparameter configuration schemes by comparing the average offset distance and average offset angle of the smart car when passing through 3 measurement points and analyze different neural networks, different datasets, batch sizes, and epochs on the actual performance of the smart car.

Table V shows the actual operating results of the smart car after loading different autonomous driving models. The neural network used in Table V (A) is ResNet-18, and the neural network used in Table V (B) is ResNet-50.

TABLE V (A)
THE ACTUAL OPERATION RESULTS OF THE SMART CAR (RESNET-18)

Neural Network	Dataset	Batch Size	Epoch	Distance (P1 P2 P3) cm			Average Distance	Angle (P1 P2 P3)°			Average Angle
ResNet-18	300	8	30	5.19	2.61	2.24	3.35	16	6	1	7.67
			70	6.2	2.5	0.72	3.14	3	8	5	5.33
		16	30	5.4	1.94	0.88	2.74	10	1	4	5
			70	4.56	0.47	4.36	3.13	7	7	5	6.33
	450	8	30	5.66	1.16	2.66	3.16	1	11	5	5.67
			70	7.51	1.06	0.75	3.11	10	26	19	18.33
		16	30	7.38	1.1	2.8	3.76	3	1	7	3.67
			70	5.86	0.64	4.35	3.62	1	0	11	4
	600	8	30	4.42	0.91	0.77	2.03	4	2	6	4
			70	3.99	1.66	2.4	2.68	9	4	0	4.33
		16	30	8.46	3.77	1.86	4.7	1	6	2	3
			70	3.91	1.88	1.05	2.28	5	3	3	3.67
	750	8	30	5.24	2.09	3.04	3.46	4	2	6	4
			70	5.99	1.81	1.3	3.03	5	0	4	3
		16	30	6.84	2.65	0.66	3.38	8	2	5	5
			70	6.39	1.13	0.62	2.71	9	0	11	6.67
	900	8	30	6.59	2.75	0.44	3.26	6	3	5	4.67
			70	5.6	1.34	1.44	2.79	7	7	2	5.33
		16	30	5.11	2.47	1.4	2.99	17	1	11	9.67
			70	5.6	3.18	1.25	3.34	6	5	4	5
	1050	8	30	7.66	1.92	1.09	3.56	3	11	3	5.67
			70	6.37	1.99	1.48	3.28	11	5	3	6.33
		16	30	6.28	1.6	0.9	2.93	8	2	6	5.33
			70	5.68	1.83	0.66	2.72	9	8	12	9.67

TABLE V (B)
THE ACTUAL OPERATION RESULTS OF THE SMART CAR (RESNET-50)

Neural Network	Dataset	Batch Size	Epoch	Distance (P1 P2 P3) cm			Average Distance	Angle (P1 P2 P3)°			Average Angle
ResNet-50	300	8	30	4.98	36.45	95.36	45.6	15	96	3	38
			70	7.32	33.9	65.65	35.62	3	79	25	35.67
		16	30	5.63	22.34	32.22	20.06	10	18	7	11.67
			70	3.3	26.41	51.6	27.1	61	44	41	48.67
	450	8	30	7.59	18.09	24.76	16.81	0	10	17	9
			70	2.16	23.52	88.96	38.21	22	76	153	83.67
		16	30	2.17	5.89	10.07	6.04	9	1	33	14.33
			70	4.52	6.32	13.45	8.1	43	4	74	40.33
	600	8	30	4.39	2.16	42.72	16.42	14	11	139	54.67
			70	3.61	4.35	45.93	17.96	25	28	145	66
		16	30	2.59	4.31	15.88	7.59	5	19	14	12.67
			70	2.07	22.42	10.36	11.62	21	27	118	55.33
	750	8	30	0.92	19.66	23.54	14.71	27	30	44	33.67
			70	1.72	12.71	7.76	7.4	1	115	39	51.67
		16	30	3.01	27.93	17.05	16	19	14	61	31.33
			70	3.46	33.76	96.78	44.67	86	1.3	53	46.77
	900	8	30	7.19	23.37	57.02	29.19	39	67	15	40.33
			70	5.78	23.76	60.94	30.16	54	131	114	99.67
		16	30	8.89	11.37	13.4	11.22	13	39	14	22
			70	5.75	4.79	24.67	11.74	71	13	38	40.67
	1050	8	30	4.54	5.13	20.14	9.94	27	16	62	35
			70	3.25	14.77	3.11	7.04	7	4	34	15
		16	30	7.12	6.39	4.43	5.98	19	19	23	20.33
			70	1.36	23.61	6.01	10.33	33	0	74	35.67

1) The Impact of Different Neural Networks on the Actual Operation Effect of the Model

We judge the impact of different neural networks on model quality by analyzing the actual effect of smart car operation. Fig. 28 is the actual operation of the model trained with ResNet-18 and ResNet-50. The horizontal ordinate is the autonomous driving model trained with different hyperparameter configuration schemes, the ordinate is the average offset distance when the smart car is driving, and the second coordinate is the average offset angle.

According to Fig. 28, we can see that although the validation loss value of ResNet-50 is generally smaller than that of ResNet-18, the actual performance of the model trained with ResNet-18 is significantly better than that of ResNet-50. Moreover, as the number of photos in the dataset increases, the actual performance of ResNet-50 gradually improves. Therefore, in experiments with small datasets, even if a deeper network can bring better nonlinear expression capabilities, the actual effect of the ResNet-50 neural network is still far worse than that of the ResNet-18 neural network.

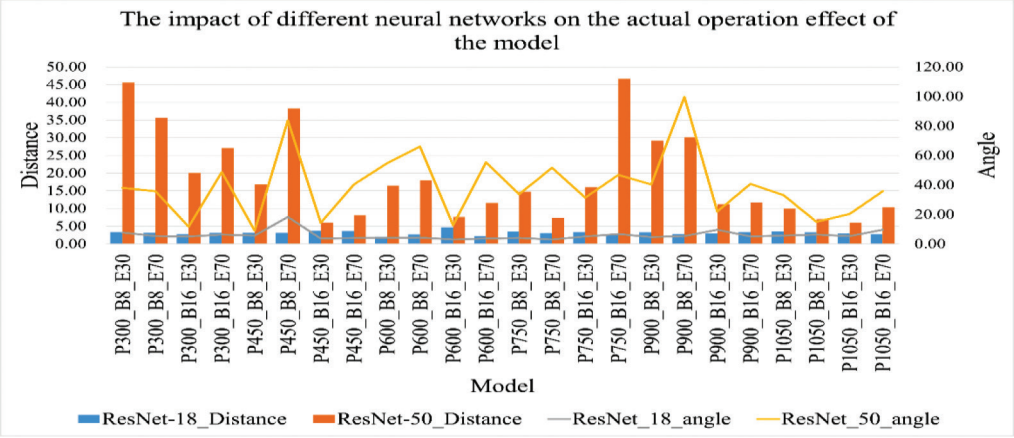

Fig. 28. Actual operation effect diagram of different neural network

The neural network in the hyperparameter configuration scheme of this article will choose ResNet-18 as the neural network.

2) The Impact of Different Numbers of Datasets on the Actual Operation Effect of the Model

Fig. 29 shows the impact of different numbers of datasets on the actual operation. From Fig. 29, we can see that when using ResNet-18 as the neural network, regardless of the number of photos in the dataset, the average offset distance and average offset angle are small, and the fluctuations are flat. However, when the neural network training is changed to ResNet-50, the average offset distance and offset angle increase sharply, and the road tracking experiments do not perform excellently. As the number of photos increases, the average distance and angle gradually decrease, and the actual operating effect gradually improves. This is due to the small number of our datasets, and ResNet-50 requires large-scale data to train a model with excellent performance. This article chooses to use the dataset of 600 photos with the best overall performance as the training dataset for the optimal hyperparameter configuration scheme.

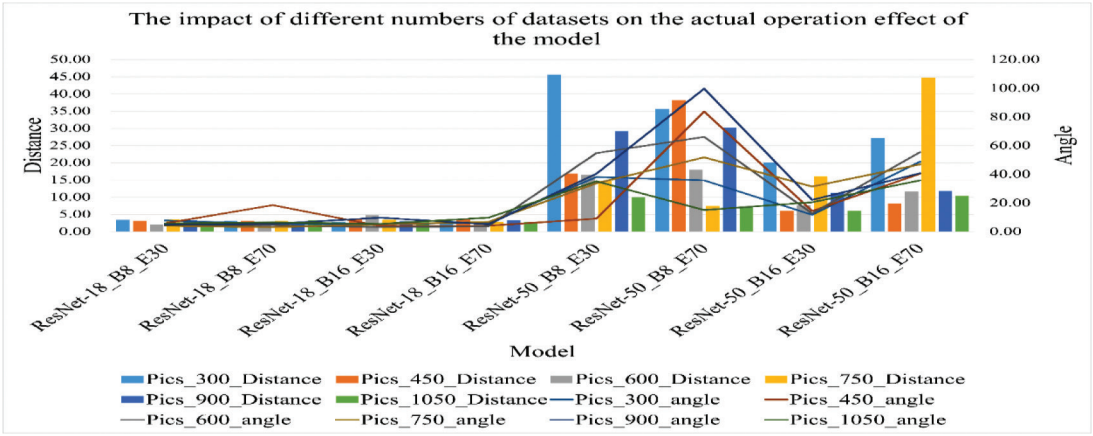

Fig. 29. Actual operation effect diagram of different numbers of datasets

3) The Impact of Different Batch Sizes on the Actual Operation Effect of the Model

From the analysis of batch size in the previous section, we can conclude that the small batch size has little effect on the model validation loss value. In order to further verify the conclusion, we analyzed the effect of different batch sizes on the actual operation of the smart car. Fig. 30 shows the actual driving effect of the model under different batch sizes. The histograms and curves also represent the actual average offset distance and angle of the model under different batch sizes.

As shown in Fig. 30, when the neural network is ResNet-18, the batch size has little effect on the average offset distance and offset angle. However, when the neural network is ResNet-50, the model trained with batch size=16 performs better than the model trained with batch size=8. Moreover, as the number of datasets increases, the actual effect of the model using batch size=16 becomes more and more stable.

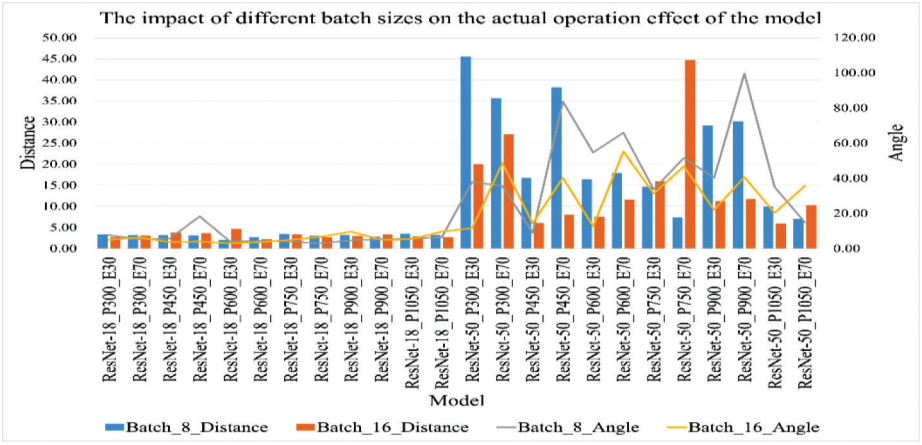

Fig. 30. Actual operation effect diagram of different batch sizes

Therefore, combined with the analysis of the verification loss value and the actual performance, the batch size=8 in the hyperparameter configuration scheme of this article is used for training with the ResNet-18 neural network. Under the condition of ensuring the training accuracy and actual performance, the training time and GPU consumption are reduced.

1) The Impact of Different Epochs on the Actual Operation Effect of the Model

Fig. 31 shows the effect of different epochs on the actual performance of the smart car. As shown in Fig. 31, the actual performance of the model trained with the ResNet-18 neural network is less affected by the epoch. However, when the model was trained with ResNet-50, the average offset distance and angle of the smart car gradually decreased with increasing epoch. Furthermore, as the number of photos increases, the impact of epochs on how well the model runs is slowly decreasing.

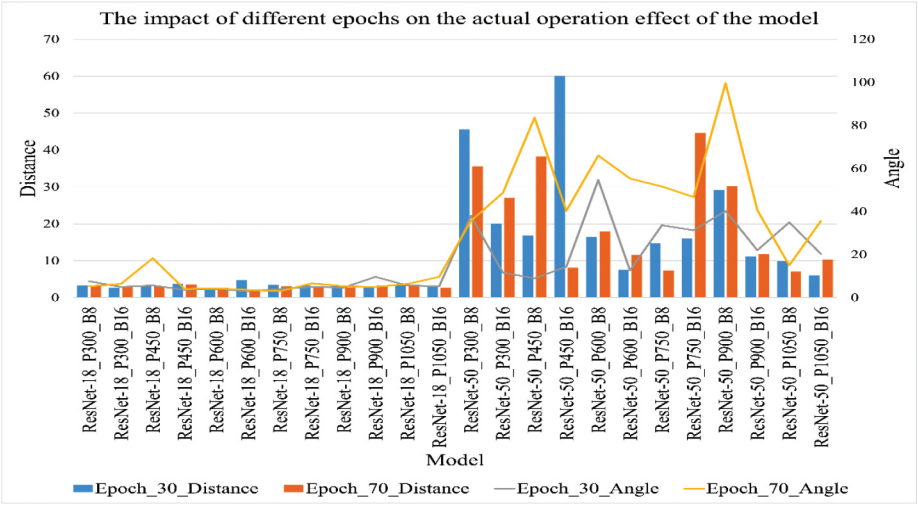

Fig. 31. Actual operation effect diagram of different epochs

Therefore, combined with the selection of neural network, dataset, and batch size, we set the epoch in the hyperparameter configuration scheme of this article to 8, which can effectively reduce the model training time and memory loss while ensuring the model accuracy and road tracking performance.

2) Summary of the Actual Operation Effects of Models Trained Under Different Hyperparameter Configuration Schemes

Fig. 32 shows the average offset distances and angles for 48 autonomous driving models trained according to the different hyperparameter configuration schemes. As shown in Fig. 32, the model trained using ResNet-18 as a neural network performs excellent, but the actual operation effect drops significantly after using ResNet-50 to train the model. In addition, with the increase in the number of photos and the increase in batch size, the performance of the model with ResNet-50 as the neural network is gradually getting better. It can be seen that the ResNet-18 neural network can be trained using small-batch datasets, and the number of datasets, batch size, and epoch have little effect on its autonomous driving performance.

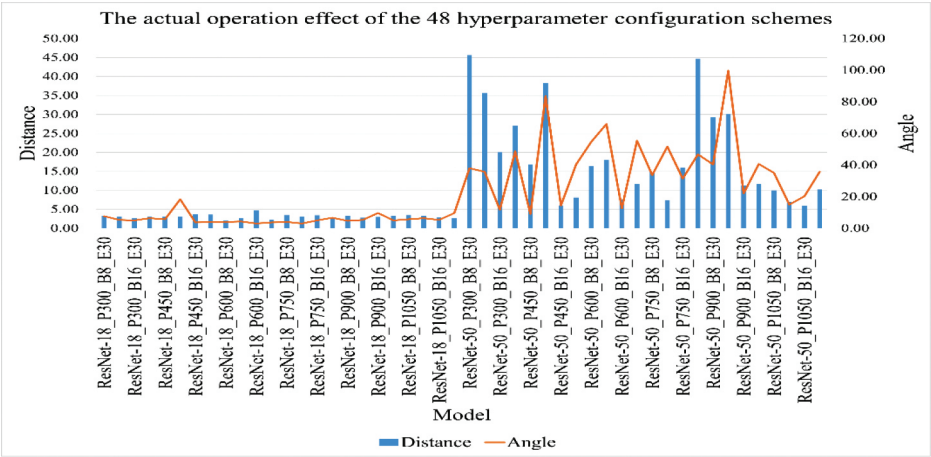

Fig. 32. The Actual operation effect for 48 autonomous driving models

Combining the influence of different hyper-parameters on the verification loss value and the actual operation effect of the smart car, we propose a set of optimal hyperparameter configuration schemes in which the neural network is ResNet-18, the batch size is 8, the epoch is 30. The dataset of 600 photos for training and the optimal autonomous driving model is obtained. The validation loss value of the optimal autonomous driving model is 0.011351. When the road tracking experiment was achieved, the average offset angle from the measurement point was 2.03cm, and the average offset angle was 4°.

3) Correlation Analysis of Verification Loss Value and Actual Operation Effect of Smart Car

In this section, we will focus on analyzing the relationships between the validation loss value and the actual performance of the model. Fig. 33 and Fig. 34 are the relationships between the verification loss value and the actual operation of the smart car when the neural network is ResNet-18 and ResNet-50, respectively.

As shown in Fig. 33 and Fig. 34, when the validation loss value is extreme (such as the minimum or maximum value), the change of the actual operating effect fluctuates wildly, and the performance is not excellent. When the verification loss value tends to the median, the variation and fluctuation of the actual operation effect are small, and the performance is excellent. Furthermore, the choice of neural network has a significant impact on the performance of the model.

The verification loss value can reflect the model training results, but it cannot directly determine the actual performance of the model. We need to make a comprehensive judgment on the performance of the model combined with the verification loss value and the actual operation effect.

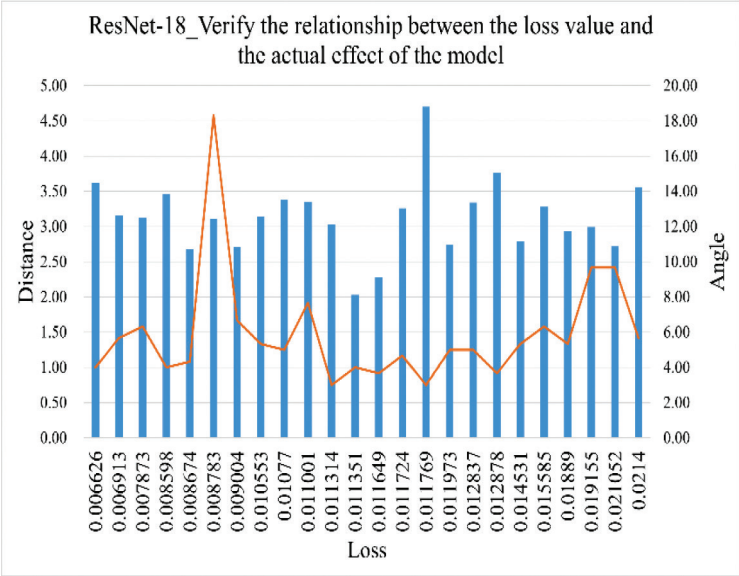

Fig. 33. ResNet-18_Verify the relationship between the loss value and the actual operation effect of the model

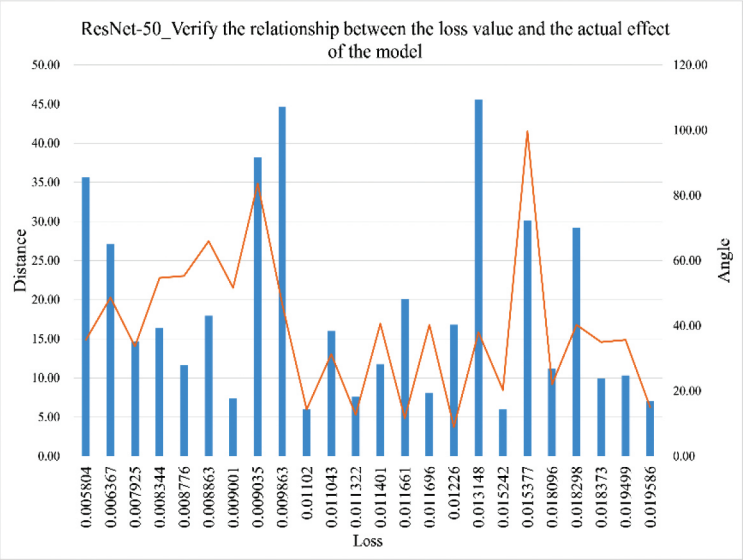

Fig. 34. ResNet-50_Verify the relationship between the loss value and the actual operation effect of the model

C. The Impact of Different Speed Gain and Steering Gain on Road Tracking

The main difference between an autonomous driving smart car and a toy car is that the smart car can reduce reproduction errors and improve the performance of autonomous driving by adjusting the speed gain and steering gain. Therefore, we will research the effect of gain value on autonomous driving performance by adjusting the speed and steering gain values and find the optimal gain value in the experimental results. The model used in the experiment is the optimal autonomous driving model trained with our proposed optimal hyperparameter configuration scheme. The neural network is ResNet-18, the batch size is 8, the epoch is 6, and the dataset is 600 photos.

Since speed gain and steering gain significantly impact autonomous driving, excessive speed or steering cause the smart car to drive off the track. Therefore, we propose a new evaluation criterion that can more intuitively represent the performance of autonomous driving models. We set the road tracking task as a 100-point scoring system. If the smart car touches the white line, 1 point will be deducted from the total score. 5 points will be deducted from the total score if the smart car drives off the track. We achieved three laps of road tracking experiments on the track and finally calculated the total score. The higher the final total score, the better the performance of the model, and we call this criterion the TO criterion. (touch the white line and off-track)

When the speed gain is below 0.35, the smart car cannot start the motor at this speed. When the speed exceeds 0.95, the smart car will drive out of the track and cannot achieve road tracks. Therefore, we choose six groups of speed gains for research in the range of speed gain from 0.35 to 0.95. The steering gain is set to the default value of 0.21. Table VI (A) shows the road tracking performance of different speed gains.

TABLE VI (A)
ROAD TRACKING PERFORMANCE FOR DIFFERENT SPEED GAINS

Speed Gain	Touch White Line	Off Track	Total Score
0.35	11	1	84
0.5	8	0	92
0.65	6	0	94
0.8	10	1	85
0.95	13	2	77

As shown in Table VI (A), with the increase of the speed gain, the driving state of the smart car changes from bad to good and then from good to bad. When the speed gain is 0.65, the performance of the smart car to achieve road tracking is the best. Therefore, 0.65 is the optimal speed gain value for the smart car.

When the steering gain is below 0.11, the smart car loses the ability to turn. When the steering gain is above 0.31, the smart car is very sensitive to steering and spins in place. Therefore, we select six groups of steering gains in the range of 0.11 to 0.31 for the research. The speed gain was set to the optimal speed gain value we obtained, 0.65. Table VI (B) shows the road tracking performance with different steering gains.

TABLE VI (B)
ROAD TRACKING PERFORMANCE WITH DIFFERENT STEERING GAINS

Steering Gain	Touch White Line	Off Track	Total Score
0.11	12	1	83
0.16	10	0	90
0.21	6	0	94
0.26	8	2	82
0.31	7	3	78

As shown in Table VI (B), when the steering gain is 0.21, the smart car has the highest performance score. 0.21 is the optimal steering gain value for the smart car. When the steering gain is 0.31, the smart car will many times drive out of the track.

In summary, we found the optimal gain values, where the speed gain is 0.65, and the steering gain is 0.21. Our optimal autonomous driving model performs best at this gain value.

D. Validation Experiment of the Optimal Hyper-parameter Configuration Scheme

This article proposes a set of optimal hyper-pa-rameter configuration schemes and trains the optimal autonomous driving model, which we call BH-ResNet. We compare this model with the excellent model proposed by Gupta P et al., which we call the GP-VGG model [25]. In addition, we also compare BH-ResNet with popular neural networks, DenseNet-121 proposed by Huang et al. [26], and AlexNet proposed by Krizhevsky et al. [27]. The performance of our BH-ResNet is validated by comparison with these existing models. Among them, the optimal speed gain and the optimal steering gain are applied in the existing method, and the evaluation standard we use is the TO criterion.

TABLE VII
COMPARISON TABLE OF BH-RESNET AND EXCELLENT MODELS

Model	Verification Loss Value	Touch White Line	Off Track	Total Score
BH-ResNet	0.011351	6	0	94
GP-VGG	0.121545	14	4	66
DenseNet-121	0.011744	12	1	83
AlexNet	0.011654	8	2	82

The comparison table of BH-ResNet and the excellent model is shown in Table VII. In the road tracking experiment, the validation loss value of BH-ResNet was lower than that of other models, and the validation loss of the GP-VGG model was the highest. In addition, according to the score of the TO scoring standard, we can see that BH-ResNet has the highest score of 94 points. Combining the validation loss value and the TO scoring criteria, the BH-ResNet model performs best.

E. Road Tracking Experiment in Unseen Scenes

Autonomous driving cars are challenging to train in all possible environments, so an excellent autonomous driving model can perform road-tracking tasks even in unfamiliar environments. Therefore, we designed a new track, which is a new environment that the smart car has not seen or trained. Fig. 35 is an unseen scene environment.

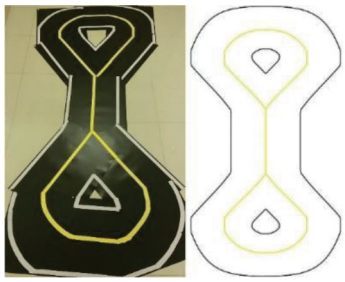

Fig. 35. An unseen scene environment

We conduct road tracking experiments in this unseen scene to verify the applicability of BH-ResNet. In addition, the three excellent models in the previous section are also involved in the experiments, which can accurately verify the performance of our BH-ResNet. The judging standard we use is the TO criterion. Table VIII shows the experimental results under the unseen scenario.

TABLE VIII
EXPERIMENTAL RESULTS IN THE UNSEEN SCENARIO

Model	Touch White Line	Off Track	Total Score
BH-ResNet	10	0	90
GP-VGG	17	6	53
DenseNet-121	15	3	70
AlexNet	12	5	63

Table VIII shows that the BH-ResNet model can also achieve the road tracking task even though the number of times touching the white line increases in unseen scenes. This means that our proposed BH-ResNet model can handle unseen environments, and the model has broad applicability and utility. Furthermore, the effects of the remaining three models are inferior, which shows that the BH-ResNe model has more ability to predict unfamiliar environments and a stronger ability to adapt to the external environment and resist external noise. After being trained in a limited environment, the smart car can be achieved road tracking in more unseen scenarios.

F. Summarize of Discussion

1) Using Jetson Nano as the mainboard of the smart car can allow the car to load more complex and efficient deep network models, and the calculation speed is excellent. The smart car can achieve all tasks independently without needing a computer as a back-end for processing operations. If the Jetson Nano is mounted on the toy car, it still cannot get superior performance, which is caused by the reproduction error brought by the hardware defect of the toy car. Therefore, we built an autonomous driving smart car based on a scale model in the real world, which can adjust the speed gain and steering gain, improves the performance of autonomous driving, and effectively reduces the problem of reproduction error of toy cars, which improves the accuracy of the experiment.

2) The hyperparameter setting is a crucial factor affecting the performance of smart cars. For different neural networks, we found that the validation loss values for models trained with ResNet-50 were generally lower than those trained with ResNet-18. The validation loss value fluctuates wildly for different datasets when the dataset is 300 or 1050 photos. When the dataset is 600 photos, the validation loss value is small and stable, and we need to choose the right amount of data according to the neural network used. The small batch size has little effect on the model validation loss for different batch sizes. For different epochs, on the premise that the model does not enter the overfitting state, the more iterations of weight update, the smaller the model validation loss.

3) The verification loss value can reflect the performance of the model. In order to make the experimental results more reliable, we need to make judgments based on the actual operation effect of the smart car. Therefore, we loaded 48 autonomous driving models into smart cars for actual measurements. The model trained by ResNet-18 performs significantly better for different neural networks than the model trained by ResNet-50. For different numbers of datasets, the size of the dataset has less impact on the model with ResNet-18 as the neural network but has a more significant impact on the model with ResNet-50 as the neural network, and the larger the number of datasets, the better the effect. For different batch sizes, when the neural network is ResNet-50, the batch size has a more significant impact on the results. For different epochs. The increase in epochs did not substantially improve the performance of the model.

4) Choosing the correct hyperparameters is very important. Based on the research on the verification

loss value and the actual operation effect of the smart car, we propose a set of optimal hyperparameter configuration schemes. The neural network is ResNet-18, the batch size is 8, and the epoch is 30. The optimal autonomous driving model BH-ResNet is obtained by training with a dataset of 600 photos.

5) Our smart car can adjust the speed gain and steering gain like a real car, so we researched the influence of the gain value on the smart car and finally proposed a set of optimal gain values. The optimal speed gain value is 0.65, and the optimal steering gain value is 0.21. The optimal gain value can significantly improve the performance of the smart car.

6) We compare BH-ResNet with three existing groups of excellent models, and we find that the BH-ResNet model outperforms other models in both validation loss value and actual operating effect, which also verifies the superiority of our model. In addition, the BH-ResNet model can achieve road-tracking experiments in unseen scenes. This demonstrates the practical utility of the model.

VI. Conclusion

Road tracking is a critical task in autonomous driving research. In the research, we use a scale model to build an autonomous driving smart car with adjustable speed gain and steering gain, equipped with a Jetson Nano which includes a high-performance GPU to achieve the road tracking task. Furthermore, we propose a set of optimal hyperparameter configuration schemes and train the optimal autonomous driving model BH-ResNet, which is proven to achieve road tracking tasks with excellent performance.

In the model training part, we tested the effect of different hyperparameters on the model validation loss value. We found that batch size has less effect on validation loss, and the different neural networks and datasets have more effect on validation loss. When the neural network is ResNet-50, the batch size is 8, the epoch is 70, and the dataset is 300, the validation loss is the smallest value of 0.005804. In the actual experiment part, we found that although the validation loss of ResNet-50 is lower than that of ResNet-18, the actual performance is far worse than that of ResNet-18. In addition, batch size and epoch have less impact on the model.

Integrating the research of validation loss values and actual operation effects, we proposed a set of optimal hyperparameter configuration schemes with the neural network of ResNet-18, a batch size of 8, an epoch of 30, and a set of 600. We trained the optimal autonomous driving model BH-ResNet.

In addition, we found that when the speed gain and steering gain increase, the number of times the smart car drives out of the track increases, and when the speed gain and steering gain decrease, the number of times the smart car touches the white line increases. When the speed gain is 0.65 and the steering gain is 0.21, the performance of the smart car to achieve the road tracking task is the best.

We compared BH-ResNet with DenseNet-121, Alexnet, and GP-VGG and found that all models can achieve road track, but DenseNet-121, Alexnet, and GP-VGG all have problems with touching the line or driving off the track when turning, with a total score of 83, 82, and 66, respectively. BH-ResNet has the highest score of 94. Compared with GP-VGG, the performance of the BH-ResNet model is improved by 42.4%.

A good model should have the ability to handle the unseen environment. Therefore, we designed a new track and proved that BH-ResNet could still achieve road tracking with high performance in an unseen environment. The existing models all showed many touchlines and driving off the track, with DenseNet-121 scoring 70, AlexNet scoring 63, and GP-VGG scoring 53. Our BH-ResNet has the highest score of 90. Compared with GP-VGG, the BH-ResNet model outperforms 69.8% in unseen environments.

Acknowledgement

The first author conducted the experiment and drafted the manuscript. The last author guided and advised the experiment and co-drafted the manuscript. The first and last authors each contributed 50% equally to this work.

References

[1] H. Fujiyoshi, T. Hirakawa, and T. J. I. R. Yamashita, "Deep Learning-Based Image Recognition for Autonomous Driving," *IATSS Research*, vol. 43, no. 4, pp. 244-252, Dec. 2019.

[2] S. Grigorescu, B. Trasnea, T. Cocias et al., "A Survey of Deep Learning Techniques for Autonomous Driving," *Journal of Field Robotics*, vol. 37, no. 3, pp. 362-386, Apr. 2020.

[3] W. Y. Lin, W. H. Hsu, and Y. Y. Chiang, "A Combination of Feedback Control and Vision-Based Deep Learning Mechanism for Guiding Self-Driving Cars," in *Proc. 2018 IEEE International Conference on Artificial Intelligence and Virtual Reality (AIVR)*, 2018, pp. 262-266.

[4] N. Hossain, M. T. Kabir, T. R. Rahman et al., "A Real-Time Surveillance Mini-Rover Based on Opencv-Python-JAVA Using Raspberry Pi 2," in *Proc. 2015 IEEE International Conference on Control System, Computing and Engineering (ICCSCE)*, 2015, pp. 476-481.

[5] U. Karni, S. S. Ramachandran, K. Sivaraman et al., "Development of Autonomous Downscaled Model Car Using Neural Networks and Machine Learning," in *Proc. 2019 3rd International Conference on Computing Methodologies and Communication (ICCMC)*, 2019, pp. 1089-1094.

[6] A. Banerjee, V. Bolar, A. Chaurasia et al., "Autonomous Driving Vehicle," *International Research Journal of Engineering and Technology*, vol. 7, no. 4, pp. 6048-6050, Apr. 2020.

[7] E. Yılmaz and S. T. Özyer. (2019, Jan.). Remote and Autonomous Controlled Robotic Car Based on Arduino with Real-Time Obstacle Detection and Avoidance. *Universal Journal of Engineering Science*. [Online]. *7(1)*, pp. 1-7. Available: http://earsiv.cankaya.edu.tr:8080/handle/handle/20.500.12416/4265

[8] S. Yuenyong and Q. Jian, "Generating Synthetic Training Images for Deep Reinforcement Learning of a Mobile Robot," *Journal of Intelligent Informatics and Smart Technology*, vol. 2, pp. 16-20, Mar. 2017.
[9] T. D. Do, M. T. Duong, Q. V. Dang et al., "Real-Time Self-Driving Car Navigation Using Deep Neural Network," in *Proc. 2018 4th International Conference on Green Technology and Sustainable Development*, 2018, pp. 7-12.
[10] Q. Zhang, T. Du, and C. Tian. (2019, Dec. 20). *Self-Driving Scale Car Trained by Deep Reinforcement Learning*. [Online]. Available: https://arxiv.org2abs/1909.03467
[11] Y. Li, J. Qu, and Technology, "Intelligent Road Tracking and Real-time Acceleration-deceleration for Autonomous Driving Using Modified Convolutional Neural Networks," *Current Applied Science and Technology*, vol. 22, no. 6, p. 26, Mar. 2022.
[12] V. Rausch, A. Hansen, E. Solowjow et al., "Learning a Deep Neural Net Policy for End-to-End Control of Autonomous Vehicles," in *Proc. 2017 American Control Conference*, Seattle, WA, USA, 2017, pp. 4914-4919.
[13] P. M. Radiuk, "Impact of Training Set Batch Size on the Performance of Convolutional Neural Networks for Diverse Datasets," *Information Technology and Management Science*, vol. 20, no. 1, pp. 20-24, Dec. 2017.
[14] M. Choi, "An Empirical Study on the Optimal Batch Size for the Deep Q-Network," in *Proc. International Conference on Robot Intelligence Technology and Applications*, 2017, pp. 73-81.
[15] S. Chowdhuri, T. Pankaj, and K. Zipser, "Multinet: Multi-Modal Multi-Task Learning for Autonomous Driving," in *Proc. 2019 IEEE Winter Conference on Applications of Computer Vision*, 2019, pp. 1496-1504.
[16] J. Kocić, N. Jovičić, and V. J. S. Drndarević, "An End-to-End Deep Neural Network for Autonomous Driving Designed for Embedded Automotive Platforms," *MDPI*, vol. 19, no. 9, p. 2064, Apr. 2019.
[17] A. Iqbal, S. S. Ahmed, M. D. Tauqeer et al., "Design of Multifunctional Autonomous Car Using Ultrasonic and Infrared Sensors," in *Proc. 2017 International Symposium on Wireless Systems and Networks (ISWSN)*, 2017, pp. 1-5.
[18] K. Yu, L. Jia, Y. Chen et al., "Deep Learning: Yesterday, Today, and Tomorrow," *Journal of Computer Research and Development*, vol. 50, no. 9, pp. 1799-1804, Sep. 2013.
[19] Y. LeCun, Y. Bengio, and G. J. N. Hinton, "Deep Learning," *Nature*, vol. 521, no. 7553, pp. 436-444, May. 2015.
[20] J. Gu, Z. Wang, J. Kuen et al., "Recent Advances in Convolutional Neural Networks," *Pattern Recognition*, vol. 77, pp. 354-377, May. 2018.
[21] A. Karpathy, G. Toderici, S. Shetty et al., "Large-Scale Video Classification with Convolutional Neural Networks," in *Proc. IEEE Conference on Computer Vision and Pattern Recognition*, 2014, pp. 1725-1732.
[22] S. Albawi, T. A. Mohammed, and S. Al-Zawi, "Understanding of a Convolutional Neural Network," in *Proc. 2017 International Conference on Engineering and Technology*, 2017, pp. 1-6.
[23] S. J. I. S. Cass, "Nvidia Makes it Easy to Embed AI: The Jetson Nano Packs a Lot of Machine-Learning Power into DIY Projects," *IEEE Spectrum*, vol. 57, no. 7, pp. 14-16, Jul. 2020.
[24] R. Febbo, B. Flood, J. Halloy et al., (2020, Jul. 26). *Autonomous Vehicle Control Using a Deep Neural Network and Jetson Nano*. [Online]. Available: https://dl.acm.org/doi/abs/10.1145/3311790.3396669
[25] P. Gupta, V. Singh, A. J. J. Parashar et al., "Smart Autonomous Vehicle Using End to End Learning," *Journal of Innovation in Computer Science and Engineering*, vol. 9, no. 2, pp. 7-11, Jan. 2020.
[26] G. Huang, Z. Liu, L. Van Der Maaten et al., "Densely Connected Convolutional Networks," in *Proc. IEEE Conference on Computer Vision and Pattern Recognition*, Honolulu, HI, USA, July 21-26, 2017, pp. 4700-4708.
[27] A. Krizhevsky, I. Sutskever, and G. E. Hinton, "Imagenet Classification with Deep Convolutional Neural Networks," *Advances in Neural Information Processing Systems*, vol. 60, no. 6, pp. 84-90, Jun. 2017.

Zihao Nie is currently studying for the Master of Engineering (Engineering and Technology), at Panyapiwat Institute of Management, Thailand. His research interests are Research direction is artificial intelligence, autonomous driving

Jian Qu is a full-time lecturer at the Faculty of Engineering and Technology, Panyapiwat Institute of Management. He received Ph.D. with Outstanding Performance award from Japan Advanced Institute of Science and Technology, Japan, in 2013. He received B.B.A with Summa Cum Laude honors from the Institute of International Studies of Ramkhamhaeng University, Thailand, in 2006, and M.S.I.T from Sirindhorn International Institute of Technology, Thammast University, Thailand, in 2010. His research interests are natural language processing, intelligent algorithms, machine learning, machine translation, information retrieval, and image processing.

Comparison of Backbones for Microscopic Object Detection Algorithms

Natthaphon Hongcharoen[1], Parinya Sanguansat[2], and Sanparith Marukatat[3]
[1,2]Faculty of Engineering and Technology, Panyapiwat Institute of Management, Nonthaburi, Thailand
[3]NECTEC, AI Research Group, Pathumthani, Thailand
E-mail: 627210108@stu.pim.ac.th, parinyasan@pim.ac.th, sanparith.marukatat@nectec.or.th

Received: April 4, 22, 2021 / Revised: April 21, 2023/ Accepted: April 22, 2022

***Abstract*—Modern object detection methods are mostly comprised of feature extractor parts and detection parts. With the rise of Vision Transformers and more advanced variants of Convolutional Neural Networks, we present the comparative experimental results of using different feature extractors on the Cascade Faster R-CNN object detection technique. We also prove the significance of using the complete pre-trained weight for the entire object detection model over the slight increase in feature extractor performance but need to randomly initialize all detection layers. The trained models were evaluated using the mean Average Precision (mAP) metric on the unseen laboratory-generated data and also visual evaluation of real-world data from medical diagnoses. The modern Vision Transformer techniques such as PVT and Swin significantly outperformed the traditional Convolutional Neural Network model such as ResNet or ResNeXt with PVT V2 achieved 78% mAP at IOU 0.7 with only the feature extractor pre-trained on ImageNet dataset compared to 60.5% of ResNet 101 and 59.2% of ResNeXt 101-64x4 with similar weight initialization. The results also show a significant increase in the accuracy of using the pre-trained model entirely as a weight initializer in every layer but the final output. ResNet 50 and ResNet 101 achieved 75.6% and 77.2% mAP respectively. A significant improvement over 59.5% and 60.5%. ResNeXt with a pre-trained detector also achieved 78.8% and 79.2% on 64 and 32 cardinality sizes respectively, actually better than PVT V2 with only random weight initialized on the detector part.**

***Index Terms*—Deep Learning, Microscopic Images, Object Detection, Vision Transformer**

I. Introduction

Liver cancer is one of the leading causes of cancer death [1]. Opisthorchis Vivertini or OV (also known as liver fluke) is one of the causes of liver cancer. Liver fluke infection is generally caused by raw fish consumption which is very common in the northeastern region of Thailand. The accumulation of liver fluke will eventually lead to liver cancer if not properly treated.

While it is possible to detect parasite infection by analyzing fecal slides, liver fluke is not the only parasite detectable by this method. Other parasites such as Minute Intestinal Flukes (MIF) has very similar eggs compared to liver fluke as shown in Fig. 1. However, they, infect different organs and cause different health problems.

With the similarity of different parasites detectable by the same method, visually differentiating them would be time-consuming even for experts. With the advances in computer vision research, it is possible to automatically detect and classify the parasite eggs in the digital images of fecal slides.

II. Literature Review

Many modern object detection techniques such as RetinaNet [2], Cascade R-CNN [3], DETR [4], and Yolact [5] rely on the use of large convolutional neural networks as feature extraction part of the detector (also known as backbones). Several convolutional neural networks of various depths such as ResNet or ResNeXt that has been trained on image classification task can be used. The results from several works showed that more accurate backbones made higher accuracy detectors at the cost of the lowered speed.

Recently, new techniques such as Vision Transformer [6] surpassed both ResNet and ResNeXt in the image classification task. Therefore Transformer-based backbones seem to be an interesting approach for object detection as well.

This paper aims to explore the difference in the performance of an object detection technique with different backbone configurations when used in microscopic images of parasite eggs.

III. Data

The dataset was divided into 2 parts, the laboratory-generated images with bounding box annotations for training and comparative evaluation and the real-world images from medical diagnoses but without annotations for visual testing.

There were 3,237 annotated images in total, with 1,684 being MIF and 1,553 being OV. They were split into 2,465 training images and 772 evaluation images.

The real-world image data consist of 1,320 images with some of them duplicated. We test all the images and select a sample of them that showed distinctions between each model.

The examples of the data are shown in Fig. 1 the real-world images are shown in Fig. 2.

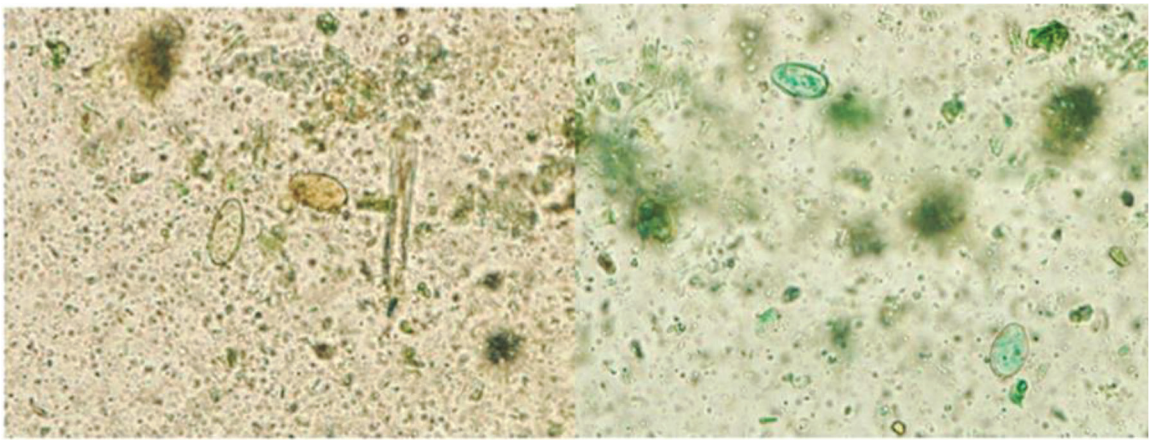

Fig. 1. Example images from the laboratory-generated data, the left image contains only MIF eggs and the right image contains OV eggs.

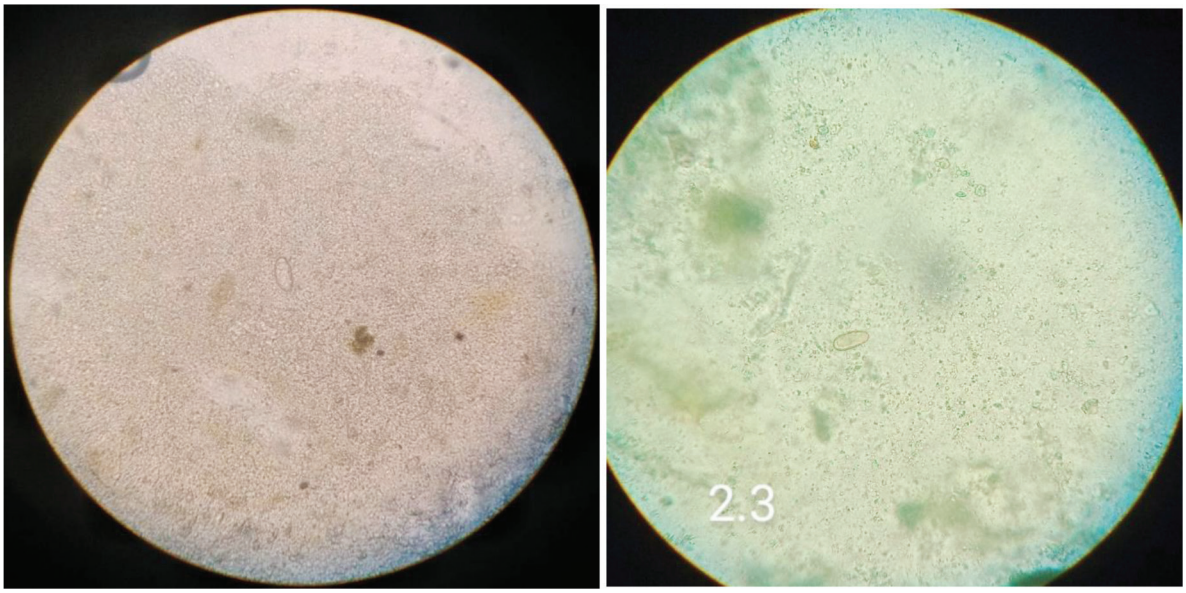

Fig. 2. Example images from the real medical diagnosis data. The left image is MIF while the right image is OV.

IV. Experiment

We selected a set of Convolutional Neural Networks and Vision Transformers that perform well in the object classification task. Then use each of them as the feature extraction part of an object detection model and compare the results using object detection metrics.

We used the modular object detection framework MMDetection [7] to train and test all models for consistency. We chose the Cascade Faster R-CNN [3] as the base object detection technique and ResNet 50 as the baseline backbone. The comparisons of Cascade Faster R-CNN and other detectors are shown in Fig. 4 to Fig. 5 and Table I

The other configurable parameters for each backbone such as the type of optimizer and initial learning rate are based on the backbone's original paper while batch size, number of epochs, input image size, learning rate schedule, and data augmentation are the same for all experiments.

We used Google's Colaboratory for training. The weights of the last epoch of the trained models were then used for further testing and evaluations.

Each model was trained for 20 epochs, with the learning rate divided by 10 at epochs 16 and 19. We also used a learning rate warm-up by using the initial learning rate of 1/1000 of the base learning rate and gradually increased to the base learning rate at 500 iterations.

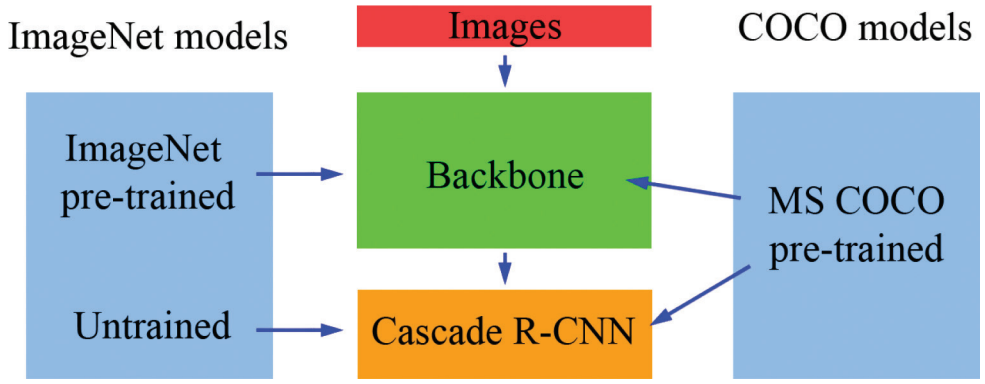

Fig. 3. The diagram of the Cascade R-CNN detector and its backbone, also shows the differences between the COCO models and ImageNet model.

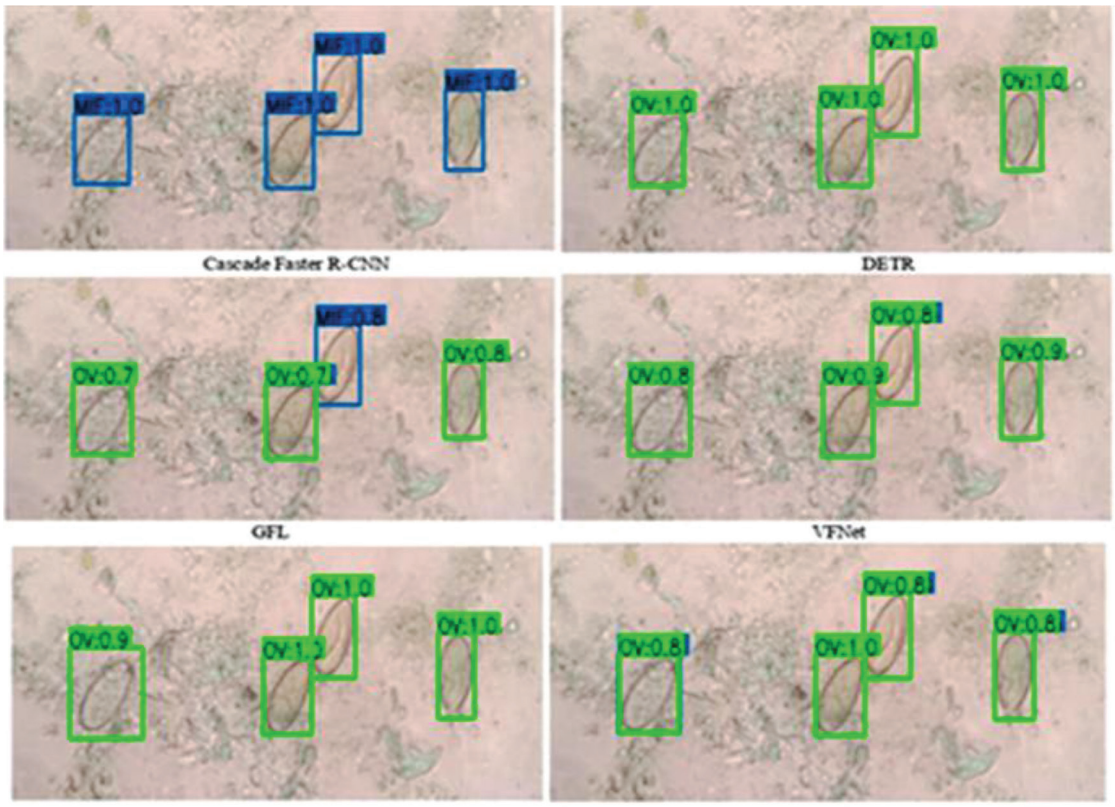

Fig. 4. The comparison of object detection techniques on MIF eggs

TABLE I
MEAN AVERAGE PRECISION AND COMPUTATION TIME OF EACH TECHNIQUE

Technique	Backbone	Mean Average Precision (mAP)				Speed (Frames/ Sec)
		0.3	0.5	0.7	0.9	
Deformable DETR	ResNet 50	0.847	0.814	0.517	0.001	4.519
YoloV3	DarkNet 53	0.845	0.835	0.723	0.097	8.364
RetinaNet	ResNet 101	0.875	0.838	0.737	0.402	4.898
Faster R-CNN	ResNet 101	0.873	0.853	0.751	0.426	4.666
Cascade Faster R-CNN	**ResNet 101**	**0.860**	**0.830**	**0.752**	**0.462**	**4.040**
RetinaNet	ResNet 50	0.888	0.857	0.755	0.433	5.660
Cascade Faster R-CNN	**ResNet 50**	**0.870**	**0.836**	**0.765**	**0.482**	**4.681**
GFL	ResNeXt 101 DCN	0.919	0.880	0.773	0.366	3.858
DETR	ResNet 50	0.916	0.898	0.800	0.096	5.996
Faster R-CNN	ResNet 50	0.912	0.885	0.807	0.457	5.474
VFNet	ResNet 50	0.944	0.927	0.840	0.565	5.313
GFL	ResNet 101 DCN	0.941	0.935	0.875	0.533	4.409
VFNET	ResNeXt 101 DCN	0.945	0.937	0.878	0.611	2.506
GFL	ResNet 50	0.945	0.941	0.882	0.518	5.770
VFNet	ResNet 50 DCN	0.953	0.944	0.897	0.597	4.729

The table is sorted by mAP at IOU 0.7.

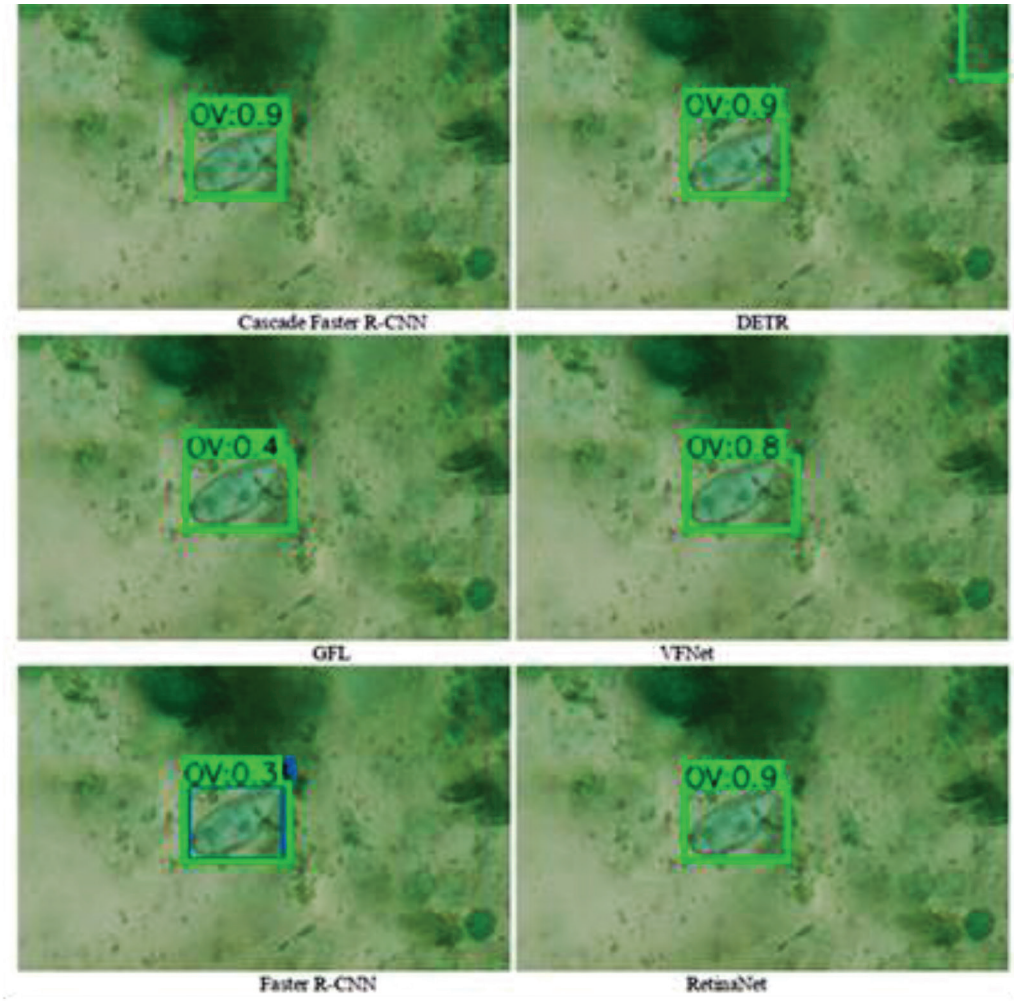

Fig. 5. The comparison of object detection techniques on an OV egg

We also experimented with the effectiveness of pre-trained models. Because most modern and high-performance backbones only had pre-trained weights available for the backbones (all of the ones we chose were pre-trained from the ImageNet dataset [8]), not the detector. So we trained another set of models for each backbone if pre-trained weights for the detector were available (all of them were pre-trained from the MS COCO dataset [9]) by using every layer except the ones that output bounding boxes and classes from COCO weight. The diagram of the experimental methodology is shown in Fig. 3.

A. ResNet

ResNet from the paper "Deep Residual Learning for Image Recognition" by Kaiming He, Xiangyu Zhang, Shaoqing Ren, and Jian Sun from Microsoft Research published in 2015. It is one of the major breakthroughs of machine learning by introducing the use of residual connection which neutralizes the "vanishing gradient" problem while training very deep models. With sufficient accuracy and a lot of flexibility, it is the de facto standard image classification and is also widely used as the backbone of most object detection after 2015, such as Faster R-CNN [10], Cascade R-CNN [3], RetinaNet [2], and DETR [4].

We selected the intermediate size ResNet 50 and ResNet 101 for the task. They are small enough to be able to run at a reasonable speed on a personal computer while also being accurate enough for our use.

With ResNet being the baseline backbone for Cascade R-CNN originally, pre-trained weights of the object detectors were available for both ResNet 50 and ResNet 101. We trained 2 models for each depth, one using only ImageNet pre-trained backbone with the rest of the detector part randomized, and another one with the entire detector pre-trained on the MS COCO dataset with only the detection layers randomized.

All models were trained using Stochastic Gradient Descend (SGD) optimizer with a base learning rate of 0.005, weight decay of 0.0001, and momentum of 0.9.

B. ResNeXt

ResNeXt from the paper "Aggregated Residual Transformations for Deep Neural Networks" by Saining Xie, Ross Girshick, Piotr Dollár, Zhuowen Tu, Kaiming He from Facebook AI Research [11]. It is the follow-up work of ResNet by increasing the cardinality of the model, the technique is more efficient than increasing the depth or width of bigger models.

As the technique relies on making ResNet bigger, we chose a depth of 101 like the deeper model of ResNet we chose previously, and 2 cardinality sizes of 32x4 and 64x4.

As ResNeXt also had MSCoco pre-trained weights like ResNet, we trained 2 sets of models with ImageNet and MSCoco pre-trained weights. All models were trained with the same setup as the ResNet.

C. ResNeSt

ResNeSt or "Split-Attention Networks" [12]. The technique utilized Attention Layers on the model that is essentially a ResNeXt. With Attention mechanism significantly improve the accuracy of the model without much speed decrease.

We chose 2 models with 50 and 101 depths, much like the ResNet.

Only ImageNet weights were available for ResNeSt. Both models were trained using the same setup as ResNet.

D. PVT

PVT or Pyramid Vision Transformer from the paper "Pyramid vision transformer: A versatile backbone for dense prediction without convolutions" [13]. The original Vision Transformer (ViT) [24] was specifically designed for the image classification task and typically yields lower resolution outputs and was not suitable to be used as the backbone of object detection, segmentation, or similar models. PVT solved that by performing dimensional reduction similar to standard convolutional neural networks.

The models were then trained using the Adaptive Moment Estimation optimizer with weight decay (AdamW). We used a base learning rate of 0.0001 and a weight decay of 0.0001.

E. Swin

Swin from the paper "Swin Transformer: Hierarchical Vision Transformer using Shifted Windows" [14]. It is a vision Transformer technique that improves the memory consumption of attention layers by using shifted windows and computing only non-overlapping areas.

The models were then trained using the Adaptive Moment Estimation optimizer with weight decay (AdamW). We used a base learning rate of 0.0001 and a weight decay of 0.0001.

F. PVT v2

An improved version of Pyramid Vision Transformer by the same authors [15]. The technique made improvements with the addition of overlapping patch embedding, the use of convolution layers within the transformer block, and linear-complexity attention layers.

Although the technique offers many different sizes of the model ranging from the smallest B0 to the biggest B5, B3 is the biggest we can use in our environment. Thus, 2 models were chosen, the smallest B0 and B3.

Both models were trained using the same setups as the original PVT.

V. Comparative Results

We evaluated the accuracy of the trained models using the mean Average Precision (mAP) metric on the laboratory data and measured the processing time per image processed on an Nvidia GTX1080 GPU with a batch size of 1. The mAP and speed comparison is shown in Table II.

We also measured the models' specificity (true negative over the total number of pictures without an object) and sensitivity (true positive over the total number of pictures with at least an egg) scores. The results are shown in Table III.

Originally we did not plan to use COCO weights as only a few backbones had full pre-trained detectors and instead, we chose to standardize at ImageNet weights for the backbones and train the detection part from scratch. Although using the pre-trained weights generally give better result than training from scratch especially for small dataset. But with the detection part of an object detection model being much smaller than the backbone part we did not expect much difference. The results however showed otherwise. The one model that we have tested before with COCO weights, Cascade Faster R-CNN with ResNet 101 as the backbone, significantly underperformed when trained with only ImageNet weights on the backbone part and training the detection part from scratch. Thus, we decided to include COCO weights whenever possible.

A. Lab Data

We evaluated the precision of the trained models using the mean Average Precision (mAP) score on 772 validation images. The score was computed by the ratio between the true positive (correctly predicted an object) over the total number of objects. The predicted boxes were considered true positive when the area overlapped with the ground truth boxes more than a certain threshold, this is called Intersection Over Union (IOU). We select 4 IOU thresholds, 0.3, 0.5, 0.7, and 0.9. We also measure the models' inferencing speed using GTX 1080 GPU with 1 image per batch. The speed was measured using only the average of the models' processing time of all images.

As shown in Table II. All Vision Transformer models significantly outperformed the original ResNet and ResNeXt when using ImageNet weights. PVT V2 B0 actually had more precision with ImageNet weights than ResNet with COCO weights on top of being fractionally faster than ResNet 101. Note that ResNeXt had more precision than ResNet when trained using COCO weights but worse than ResNet when trained with ImageNet weights.

We then evaluate the sensitivity and specificity scores of the trained models. The sensitivity score is calculated by using true positive over the total number of pictures with at least an egg while specificity is calculated by true negative over the total number of pictures without an object. More sensitivity means fewer parasite eggs were left undetected while more specificity means fewer false alarms. The results are shown in Table III.

TABLE II
Accuracy in Mean A Verage Precision and Inference Speed of Each Technique.

Backbone	**Pre-trained Dataset**	**Mean Average Precision (mAP)**				**Speed (images/sec)**
		0.3	0.5	0.7	0.9	
ResNeXt 101-32	ImageNet	0.730	0.674	0.578	0.134	3.944
ResNeXt 101-64	ImageNet	0.742	0.681	0.592	0.127	3.085
ResNet 50	ImageNet	0.745	0.685	0.595	0.157	5.221
ResNet 101	ImageNet	0.752	0.691	0.605	0.157	4.506
ResNeSt 50	ImageNet	0.816	0.765	0.671	0.170	3.441
ResNeSt 101	ImageNet	0.826	0.771	0.674	0.200	3.014
PVT Tiny	ImageNet	0.830	0.800	0.732	0.340	4.346
Swin Tiny	ImageNet	0.865	0.820	0.733	0.398	4.010
Swin Small	ImageNet	0.866	0.831	0.742	0.386	3.332
PVT Small	ImageNet	0.844	0.805	0.745	0.359	2.766
ResNet 50	**COCO**	**0.873**	**0.838**	**0.756**	**0.472**	**5.134**
ResNet 101	COCO	0.874	0.850	0.772	0.482	4.441
PVT V2 B0	**ImageNet**	**0.880**	**0.847**	**0.775**	**0.340**	**4.547**
PVT V2 B3	ImageNet	0.885	0.852	0.780	0.417	2.535
ResNeXt 101-64	COCO	0.883	0.862	0.788	0.493	3.133
ResNeXt 101-32	COCO	0.887	0.864	0.792	0.497	3.736

The table is sorted by mAP at IOU 0.7. The technique highlighted in bold fonts is the ones with highest score of speed multiplied by mAP at IOU 0.7 for each dataset.

TABLE III
SENSITIVITY AND SPECIFICITY SCORE OF EACH TECHNIQUE

Backbone	Pre-trained dataset	MIF		OV	
		Sensitivity	Specificity	Sensitivity	Specificity
ResNeXt 101-32	ImageNet	0.753	0.941	0.766	0.593
ResNeXt 101-64	ImageNet	0.786	0.947	0.801	0.622
ResNet 50	ImageNet	0.782	0.958	0.805	0.639
ResNet 101	ImageNet	0.804	0.945	0.826	0.659
ResNeSt 50	ImageNet	0.841	0.963	0.840	0.676
ResNeSt 101	ImageNet	0.863	0.964	0.826	0.684
PVT Tiny	ImageNet	0.876	0.981	0.840	0.801
Swin Tiny	ImageNet	0.892	0.965	0.851	0.819
Swin Small	ImageNet	0.914	0.973	0.840	0.830
PVT Small	ImageNet	0.884	0.978	0.833	0.789
ResNet 50	COCO	0.927	0.996	0.858	0.901
ResNet 101	COCO	0.937	0.987	0.862	0.908
PVT V2 B0	ImageNet	0.908	0.991	0.865	0.836
PVT V2 B3	ImageNet	0.929	0.980	0.837	0.805
ResNeXt 101-64	COCO	0.943	0.993	0.872	0.918
ResNeXt 101-32	COCO	0.949	0.991	0.862	0.924

B. Real-World Data

We select some images that each technique predicts differently. For the ImageNet pre-trained models, the same technique with different model sizes all had an interesting tendency to predict roughly the same result as shown in Fig. 7 to Fig. 9. Although the ImageNet models in general sometimes struggle to predict anything at all as shown in Fig. 6 compared to the same image predicted by the COCO models in Fig. 10. The other results of the ImageNet model compared to the COCO model are shown in Fig. 10 to Fig.13.

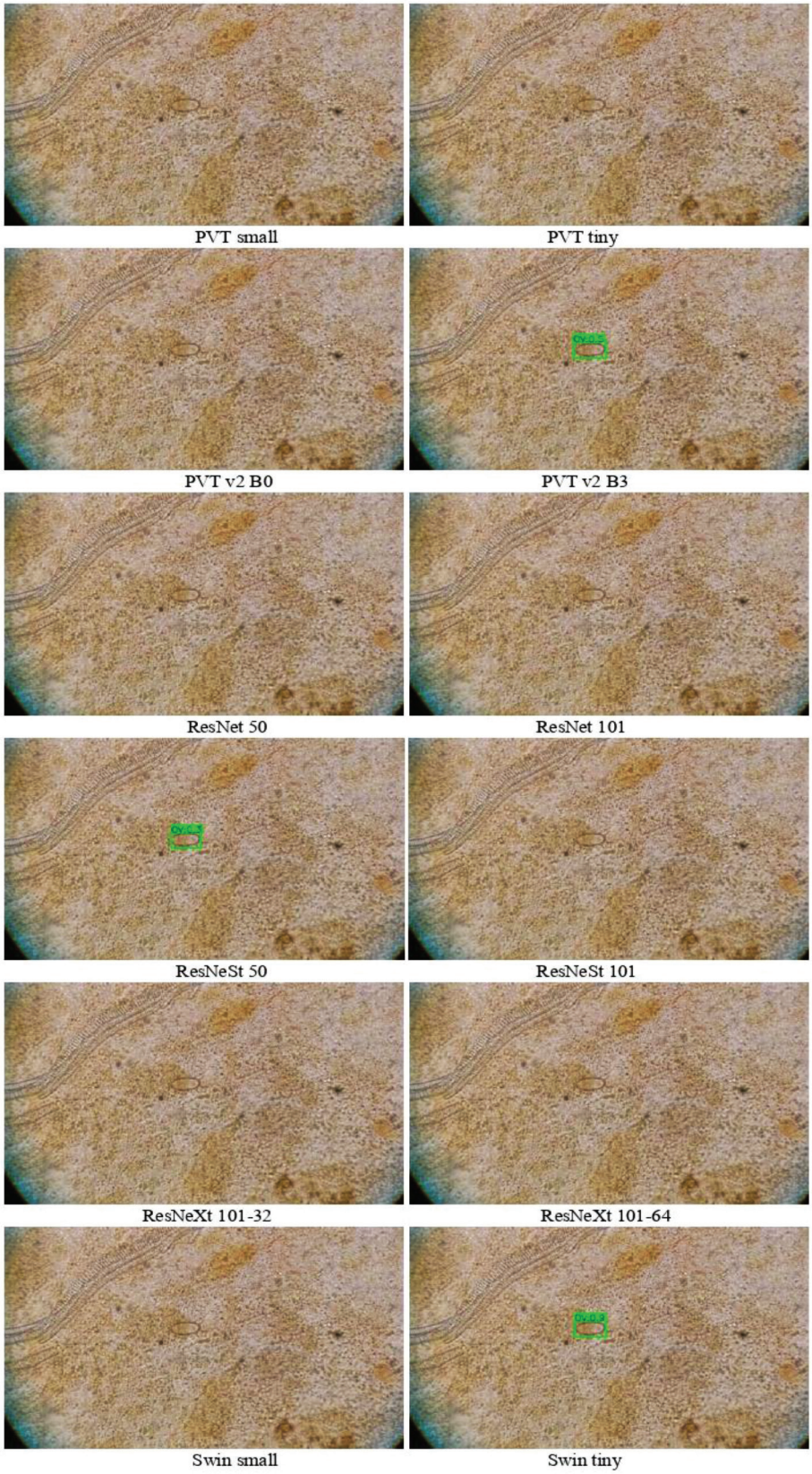

Fig. 6. Example results of an image with a MIF egg from ImageNet models

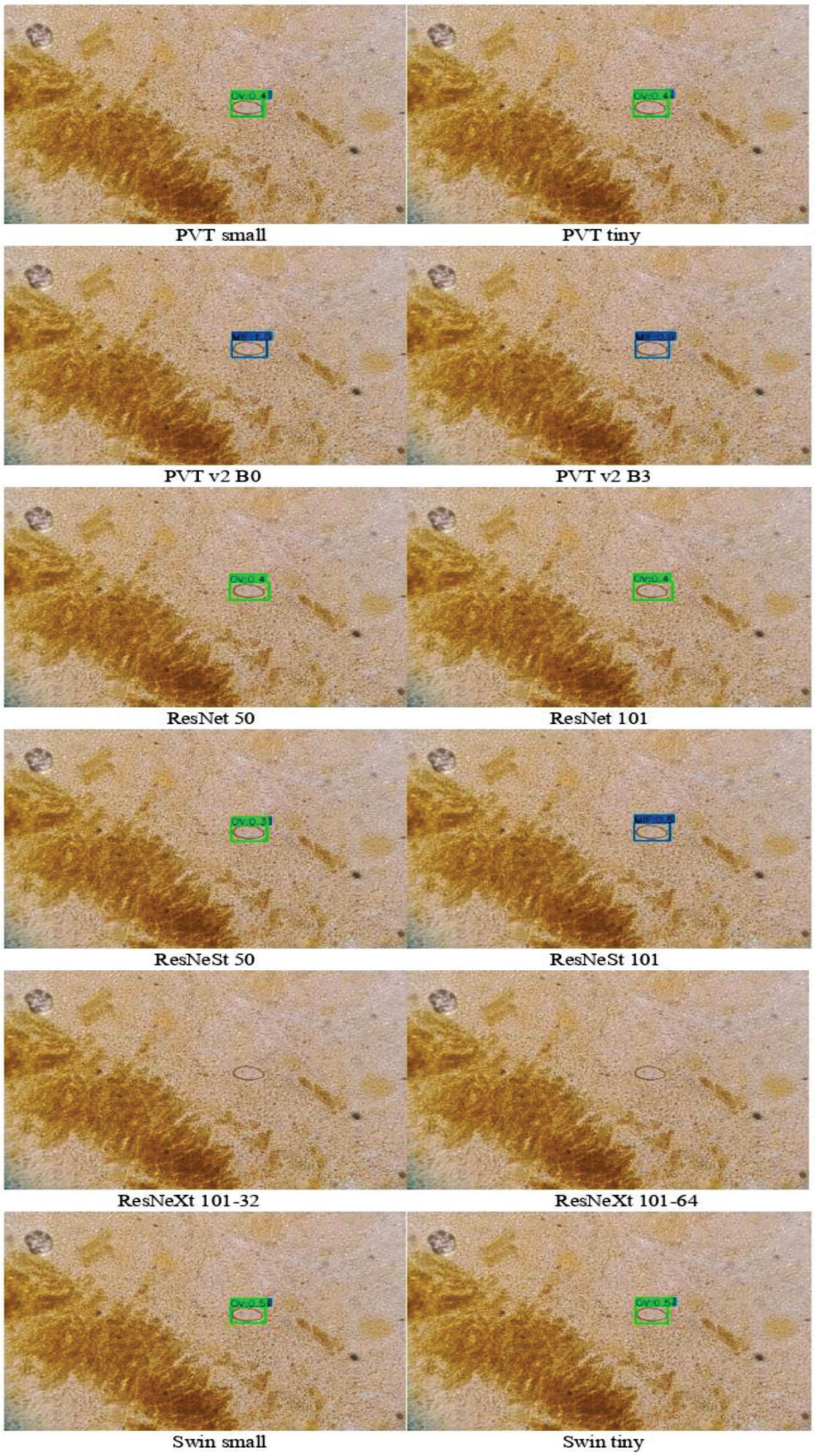

Fig. 7. Example results of an image with a MIF egg from ImageNet models

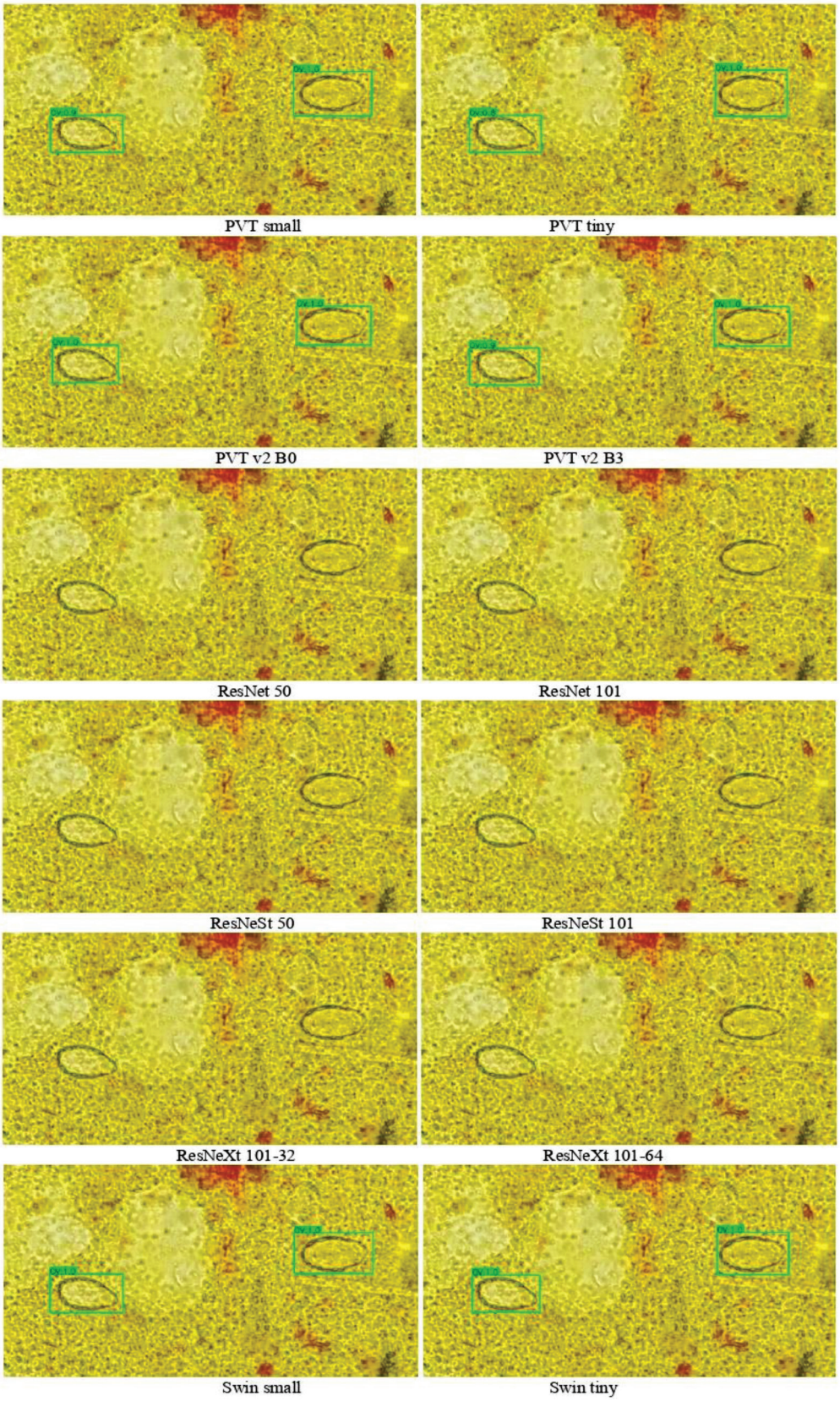

Fig. 8. Example results of an image with OV eggs from ImageNet models

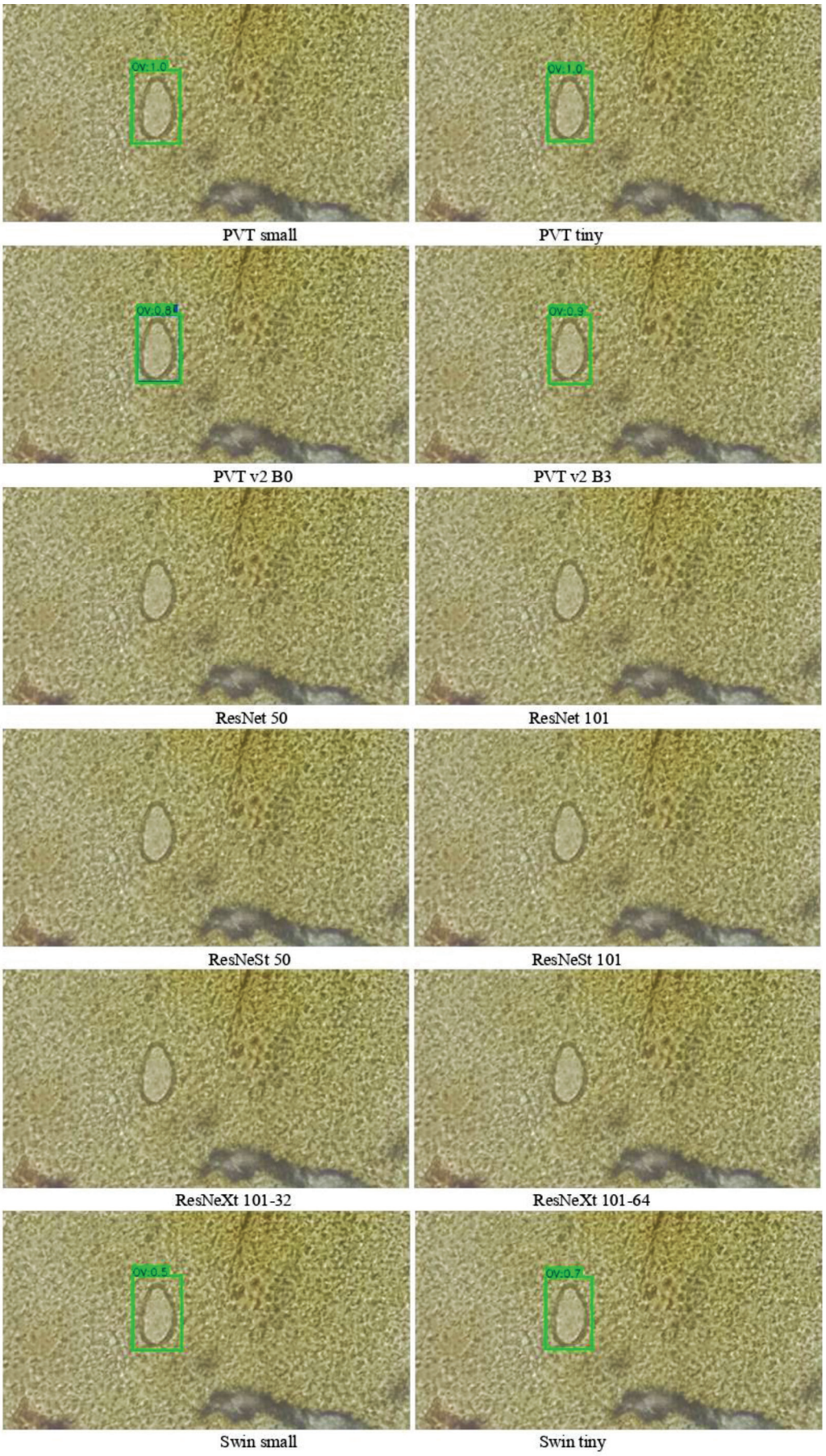

Fig. 9. Example results of an image with an OV egg from ImageNet models

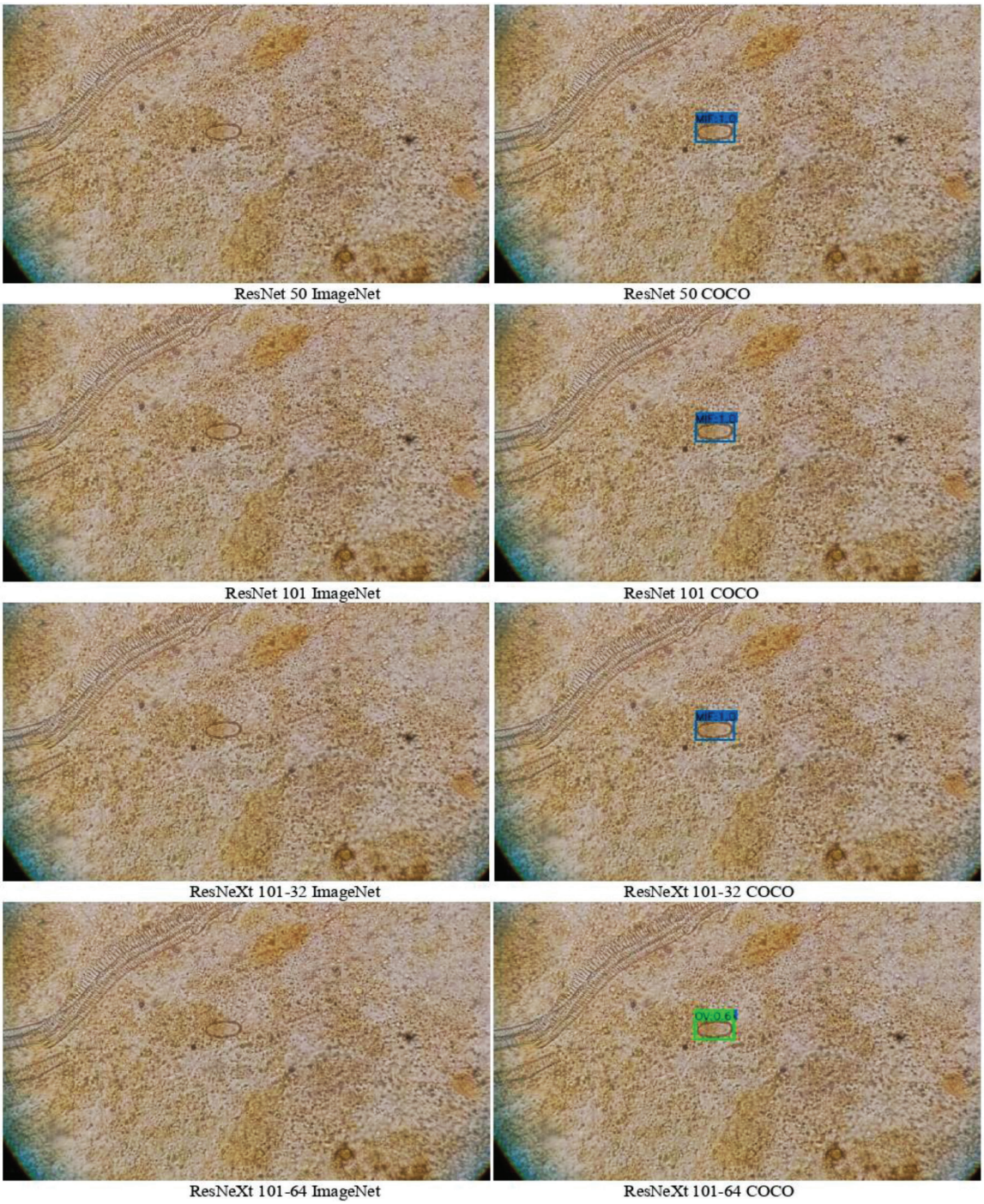

Fig. 10. Comparison result of a MIF egg between only ImageNet pre-trained backbones with randomized detector weight on the left and the entire model pre-trained on MS COCO on the right

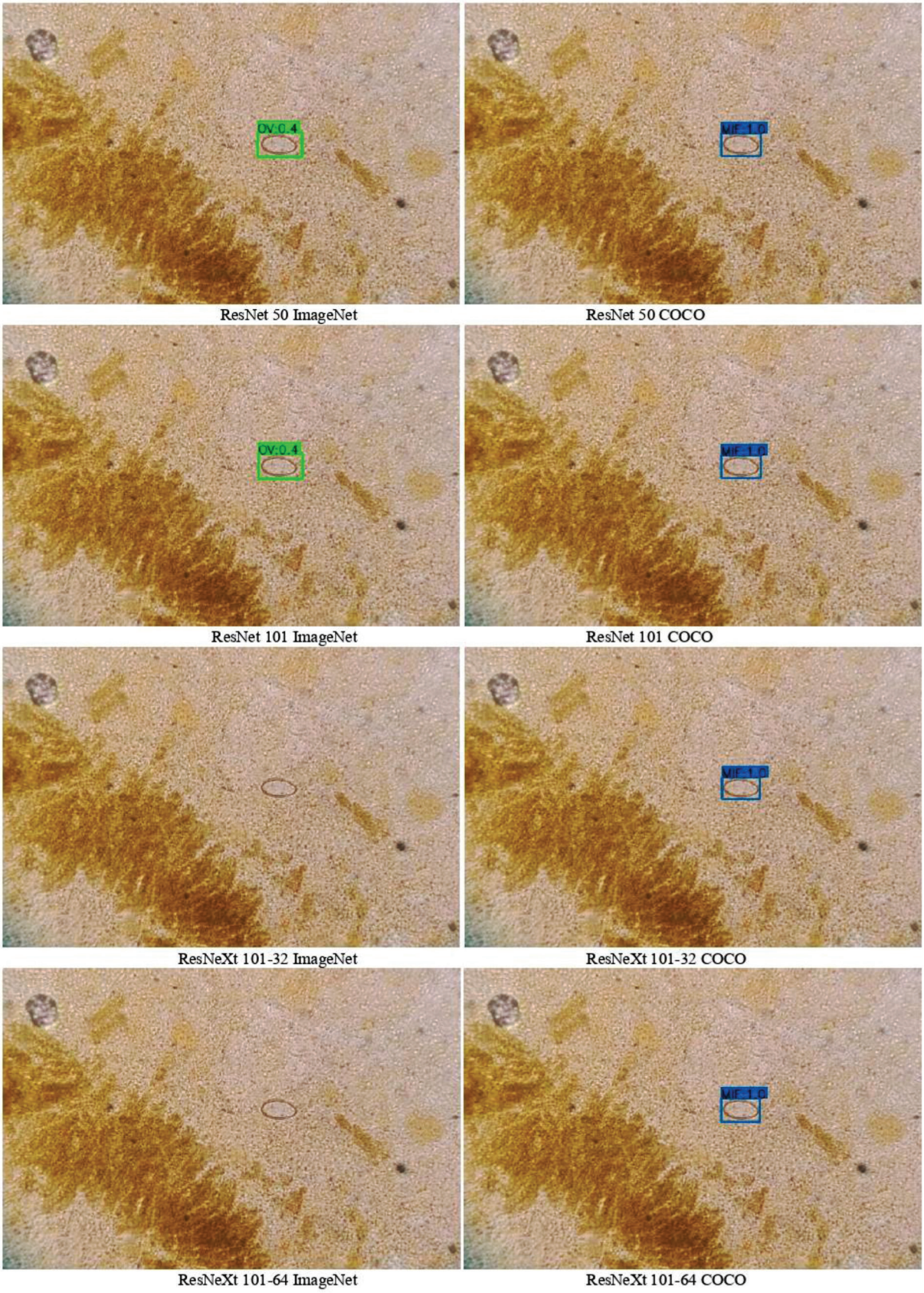

Fig. 11. Comparison result of a MIF egg between only ImageNet pre-trained backbones with randomized detector weight on the left and the entire model pre-trained on MS COCO on the right

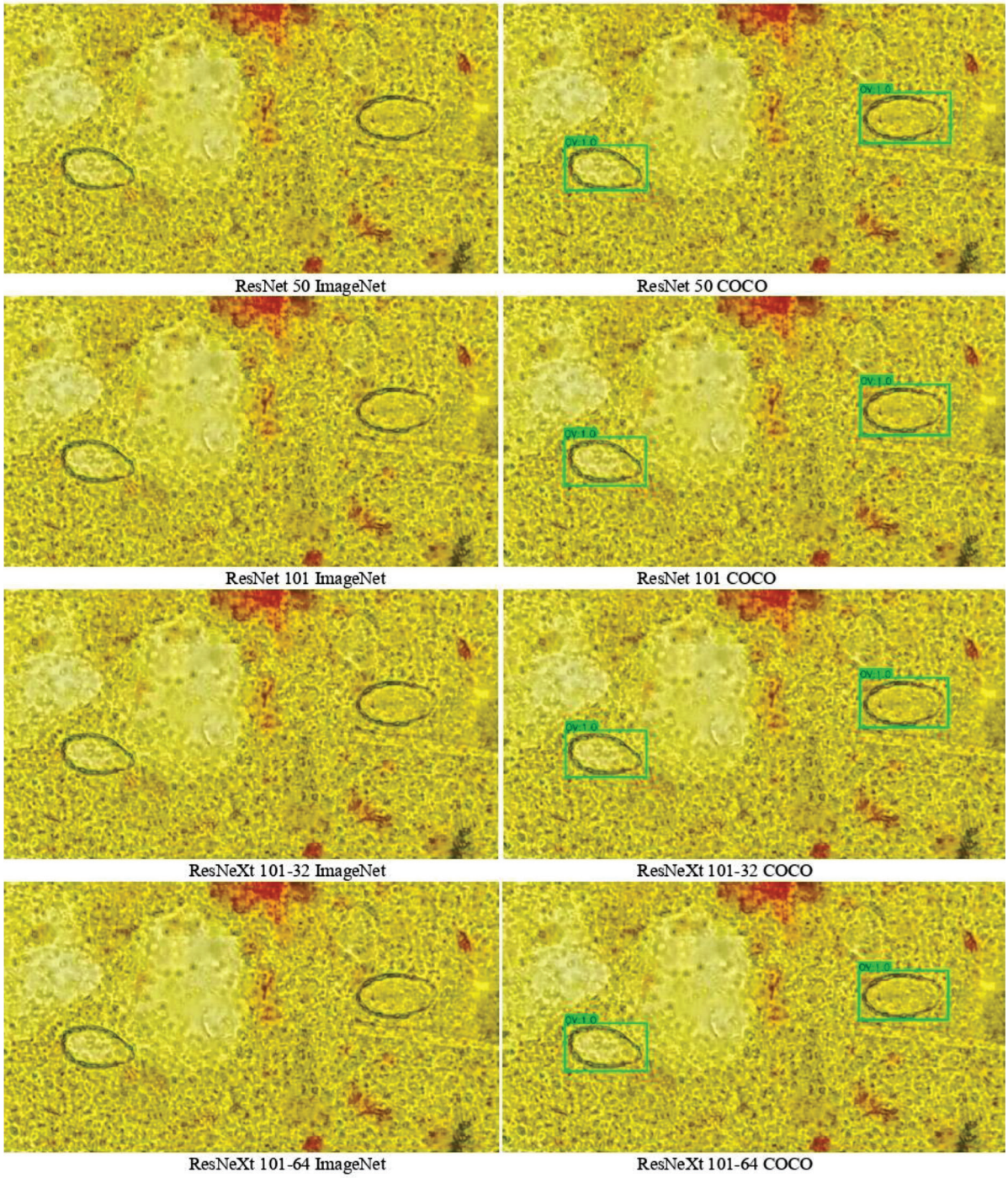

Fig. 12. Comparison result of OV eggs between only ImageNet pre-trained backbones with randomized detector weight on the left and the entire model pre-trained on MS COCO on the right

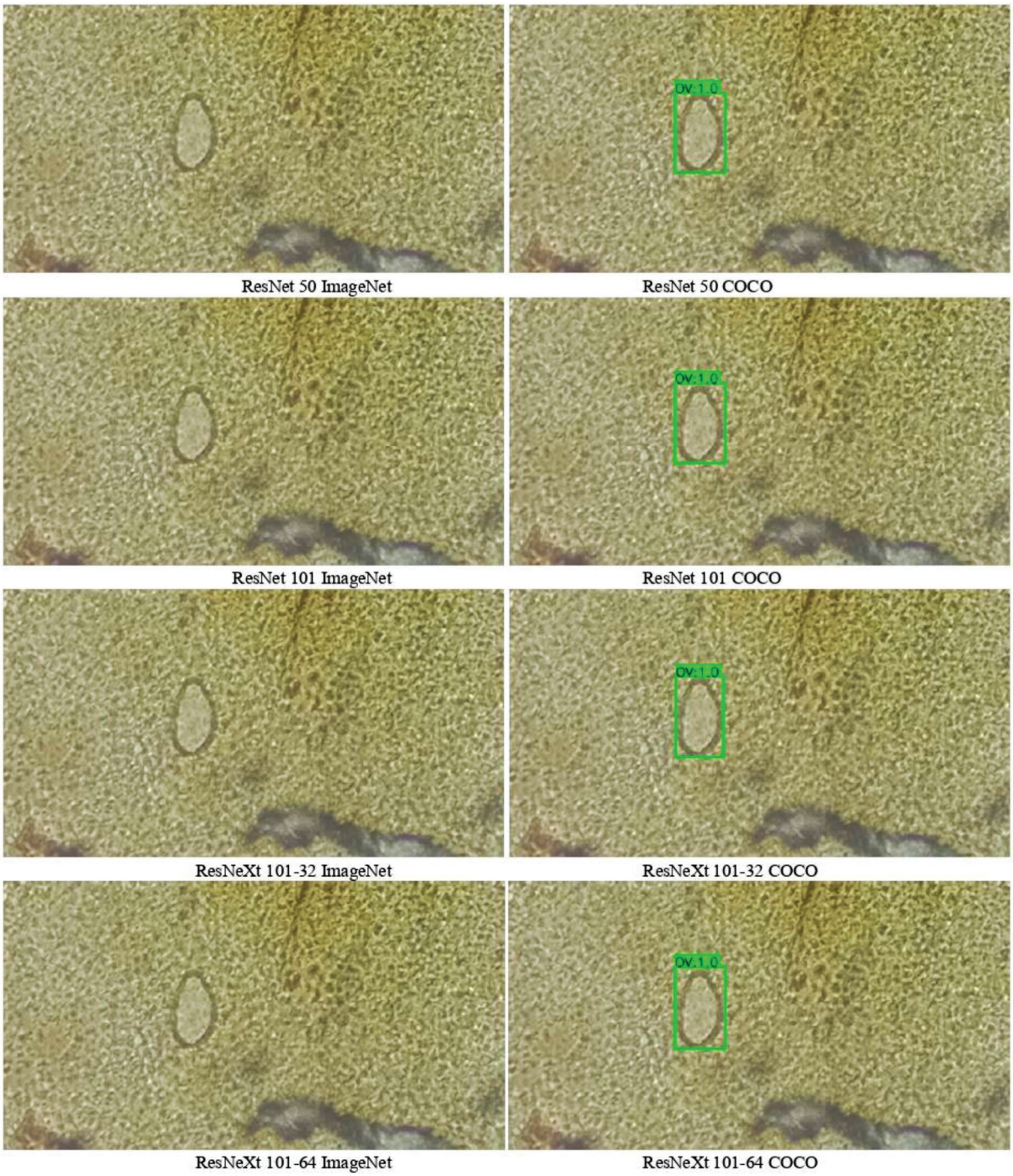

Fig. 13. Comparison result of an OV egg between only ImageNet pre-trained backbones with randomized detector weight on the left and the entire model pre-trained on MS COCO on the right

Like in the lab data, Vision Transformer models were significantly better than the original ResNet and ResNeXt. PVTv2 in particular showed good classification accuracy on top of, most of the time, correct object localization even without pre-trained weight on the detector part. PVT and Swin also had good localization but not so much for classification.

VI. Conclusions

Both results from lab data and real-world data showed that using a higher-performance backbone can significantly improve the performance of the detector. But for backbones with a similar level of performance like ResNet 50 and ResNet 101, the complete pre-trained weights are much more important than a little bigger backbone.

While all Vision Transformer models outperformed the original ResNet. The fact that the ResNeXt actually had less precision than ResNet with just ImageNet while performing better with COCO weights suggests that the use of pre-trained weights gives different performance increases for each backbone. Thus, the result between Vision Transformers themselves may be inconclusive. Pre-trained weights for the entire detector for each backbone would be needed for more complete results.

ACKNOWLEDGMENT

Scholarship received from Thailand Graduate Institute of Science and Technology (TGIST) of the National Science and Technology Development Agency (NSTDA). Scholarship ID SCA-CO-2562-9836-TH.

REFERENCES

[1] F. Bray, J. Ferlay, I. Soerjomataram et al. (2018, Sep). Global Cancer Statistics 2018: Globocan Estimates of Incidence and Mortality Worldwide for 36 Cancers in 185 Countries. *CA: A Cancer Journal for Clinicians*. [Online]. *68(6)*, pp. 394-424. Available: https://acsjournals. onlinelibrary.wiley.com/doi/abs/10.3322/caac.21492

[2] T. Y. Lin, P. Goyal, R. Girshick et al. (2018, Aug). *Focal Loss for Dense Object Detection. Computer Vision Foundation*. [Online]. *1*, pp. 2980-2988. Available: https://arxiv.org/abs/1708.02002

[3] Z. Cai and N. Vasconcelos. (2019, Nov). Cascade R-CNN: High-Quality Object Detection and Instance Segmentation. *IEEE*. [Online]. *43(5)*, pp. 1483-1498. Available: http://dx.doi.org/10.1109/tpami.2019.2956516

[4] N. Carion, F. Massa, G. Synnaeve et al. (2020, May). *End-to-End Object Detection with Transformers. European Conference on Computer Vision*. [Online]. *12346*, pp. 1-17. Available: https://arxiv.org/abs/2005.12872

[5] D, Bolya, C, Zhou, F, Xiao et al. (2019, Apr. 4). YOLACT: *Real-Time Instance Segmentation. Computer Vision and Pattern Recognition*. [Online]. Available: https://arxiv.org/abs/1904.02689

[6] A. Dosovitskiy, L. Beyer, A. Kolesnikov et al. (2022, Jan. 10). *An Image is Worth 16x16 Words: Transformers for Image Recognition at Scale*. [Online]. Available: https://arxiv.org/abs/2010.11929

[7] K. Chen, J. Wang, J. Pang et al., (2022, Jan. 10). *Mmdetection: Open MMlab Detection Toolbox and Benchmark*. [Online]. Available: https://arxiv.org/abs/1906.07155

[8] O. Russakovsky, J. Deng, H. Su et al. (2022, Jan. 10). *ImageNet: A Large-scale Hierarchical Image Database*. [Online]. Available: https://ieeexplore.ieee.org/document/5206848

[9] T. Y. Lin, M. Maire, S. Belongie et al. (2022, Jan. 15). *Microsoft coco: Common Objects in Context*. [Online]. Available: https://arxiv.org/abs/1405.0312

[10] S. Ren, K. He, R. Girshick et al. (2022, Jan. 15). *Faster R-CNN: Towards Real-Time Object Detection with Region Proposal Networks*. [Online]. Available: https://arxiv.org/abs/1506.01497

[11] S. Xie, R. Girshick, P. Dollár et al. (2022, Jan. 15). *Aggregated Residual Transformations for Deep Neural Networks*. [Online] Available: https://arxiv.org/abs/1611.05431

[12] H. Zhang, C. Wu, Z. Zhang et al. (2022, Jan. 15). *ResNeSt: Split-Attention Networks*. [Online]. Available: https://arxiv.org/abs/2004.08955

[13] W. Wang, E. Xie, X. Li et al. (2022, Jan. 15). *Pyramid Vision Transformer: A Versatile Backbone for Dense Prediction without Convolutions*. [Online]. Available: https://arxiv.org/abs/2102.12122

[14] Z. Liu, Y. Lin, Y. Cao et al. (2021, Jan. 15). *Swin Transformer: Hierarchical Vision Transformer Using Shifted Windows*. [Online]. Available: https://arxiv.org/abs/2103.14030

[15] W. Wang, E. Xie, X. Li et al. (2022, Jan. 15). *PVTv2: Improved Baselines with Pyramid Vision Transformer*. [Online]. Available: https://arxiv.org/abs/2106.13797

Natthaphon Hongcharoen received his B. Eng. degree from the Department of Computer Engineering, Faculty of Engineering and Technology, Panyapiwat Institute of Management in 2019. He has experience in internships at the National Electronics and Computer Technology Center (NECTEC), and the National Science and Technology Development Agency (NSTDA) in the Image Technology Research Laboratory. And won a gold medal at Super AI Engineer Camp Season 1 by the Artificial Intelligence Association of Thailand (AIAT). His research areas include Machine Learning, Image processing, and Computer Vision.

Parinya Sanguansat is an Associate Professor in Electrical Engineering and head of Computer Engineering and Artificial Intelligence at Panyapiwat Institute of Management (PIM), Thailand. He graduated B.Eng., M.Eng., and Ph.D. in Electrical Engineering from Chulalongkorn University. His research areas include Machine Learning, Image processing, and Computer Vision. He got many research grants from both private and public organizations. He has written several books about Machine Learning and MATLAB programming.

Sanparith Marukatat graduated in Computer Science in 1998 from the University of Franche-Comté, Besançon, France. In 2004, he completed his doctoral thesis on online handwriting recognition at the University of Paris 6, France. Currently, he is Principal Researcher in the AI Research Group at the National Electronics and Computer Technology Center (NECTEC). Dr. Marukatat's research interests include machine learning, pattern recognition using statistical tools, and deep learning.

Comparison of Keywords Extraction Techniques in Kickstarter and Indiegogo Projects

Woottikarn Hongwiengchan[1] and Jian Qu[2]

[1,2]Faculty of Engineering and Technology, Panyapiwat Institute of Management, Nonthaburi, Thailand
E-mail: Woottikarnhon@ pim.ac.th, jianqu@pim.ac.th

Received: October 28, 2021/ Revised: January 1, 2022/ Accepted: February 21, 2022

***Abstract*— there are many fake projects on Kickstarter and Indiegogo, and they are usually hard to distinguish from real projects. This research is a pioneer study to try to find a way for helping humans to identify possible fake projects. We propose to extract keywords from the projects, the extracted keywords would give the user a better understanding of the project. We compared keyword extraction for crowdfunding projects by using RAKE, NLTK, LIAAD/YAKE, BERT, and Gensim models. We measured the keyword extraction performance of each model using the precision, recall, and F1 scores. According to the results, the NLTK model is the most efficient, with a precision of 54.40% and an F1 of 70.47%.**

***Index Terms*—Kickstarter Projects, Indiegogo Projects, NLTK, Keyword Extraction**

I. Introduction

There are many projects on the official Kickstarter and Indiegogo websites, and more projects are being added each day. Some people use these projects to deceive others into investing. Even the project has no way of being able to succeed. According to Kickstarter's latest statistics, as of 2021, the average project failure and investor fraud rate is 60.78%, and the project success rate is only 39.22%. No published works are currently focused on research investigating fake projects on Kickstarter and Indiegogo because it is very difficult to detect and determine if they are fake or fraudulent projects that cannot be fulfilled. It is necessary to use relevant professional knowledge to examine and understand the project to determine the likelihood of success rates.

The data in Fig. 1 shows based on the statistics for 2019[1], 2020[2], and 2021[3]. We have found that the success rate of Kickstarter projects is low and the failure rate is higher than the project completion rate.

To reduce the number of scams from fake projects, we wanted to understand and learn more about the project by extracting keywords from project articles on Kickstarter and Indiegogo. Keyword extraction is the process of collecting words and phrases from the text. Generally, a keyword is a word that contains important information or the text that is the essence of the article, while some article keywords can be single words or consist of multiple words [1]. Keyword retrieval is a very complicated task. In Natural Language Processing (NLP) research, there are many methods of extracting core principles. Therefore, in this research, we try to find the most optimal way to extract keywords for Kickstarter and Indiegogo projects. The keywords will be used to find more information like theoretical principles that correspond to or support that the work in a project can be made and it really works. Thus, investors will make better decisions.

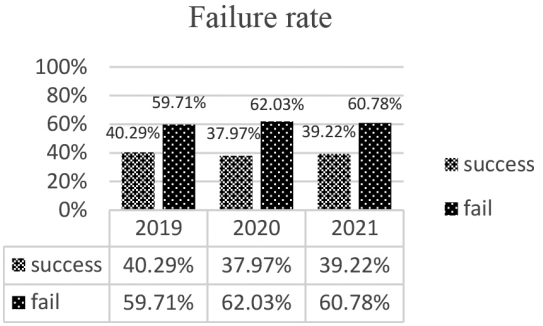

	2019	2020	2021
success	40.29%	37.97%	39.22%
fail	59.71%	62.03%	60.78%

Fig. 1. The failure rate of Kickstarter projects

II. Related Studies

When we read an article, sometimes we only want to know the main idea or the article's essence. Reading every text in the article will take quite a long time to understand the content, sometimes we are buried by information from many texts and loss the focus on the main ideas of the article. Therefore, by extracting

[1] https://www.shorturl.asia/wlv0n (last accessed on 15 October 2021)
[2] https://www.crowdcrux.com/kickstarter-statistics-in-2020/(last accessed on 15 December 2021)
[3] https://www.kickstarter.com/help/stats (last accessed on 15 December 2021)

keywords from the article with techniques in NLP, we can easily understand the main idea faster. There are many techniques used for keyword extraction in NLP. We have studied and applied five techniques for research: NLTK [2], RAKE [3], Gensim [4], YAKE [5], and BERT [6]. All five techniques are highly efficient keyword extraction algorithms and the library of each algorithm can be easily imported for use on Python platforms. Each technique uses a different algorithm. For example, RAKE has a list of stop words, phrase separators, and word separator sets. While RAKE is extracting keywords from the text when the system detects a match for the stop word list. Those words are excluded because they are considered meaningless. Words that are considered to carry meanings are associated with the text being described as bearing content and referred to as content speech. The input parameters section for the RAKE algorithm includes a list of stop words and a set of phrase separators and word separators. Use stops word and phrase separators to separate text from a document into important words or sentences. Most of these optional keywords help researchers to isolate the exact keywords needed to get information from the document. But no matter what technique, most N-gram, TF-IDF [7] word frequencies are used as statistical properties in keyword selection. Word frequency (TF) and inverse document frequency (IDF) are used to evaluate the effectiveness and importance of keywords in a document. After the assessment, TF-IDF removes any irrelevant or unsuitable words for keywords. NLP researcher Onan et al. proposed a machine-learning method and additional statistical properties for keyword separation [8]. Jian Qu et al. also proposed a method that combines statistical properties and adaptive rules to separate keywords [9]

Another technique widely used among researchers is KeyBERT, an easy-to-use keyword extraction technique. KeyBERT is a keyword extraction library from BERT embedding to get keywords that are most representative. KeyBERT has recently been proposed as a replacement for Word2Vec [10]. The concept of word2vec is to create a classifier to predict whether the context word which is likely to occur close to the target word selected. After that, Word2Vec takes the weights obtained from the classifier as word embedding, but BERT is different because it has its model and depends on the transformer library [11]. BERT operates in two steps including pre-training and tuning during pre-training. First, BERT models are trained without data labels. For customizing the BERT model start with pre-trained parameters and all parameters are fine-tuned using labeled data from the destination application. A distinctive feature of BERT is its unified architecture for tasks. Therefore, there is a difference between pre-training architecture and final downstream architecture.

However, all techniques used to extract words still need to be optimized and compared to human word extraction. Overall, the efficiency of automatic word extraction for English data of each technique is quite good, but it can also improve the accuracy and keyword selection criteria used to separate keywords from articles.

III. Our Approach

For this research, we used information from the official website of Indiegogo and Kickstarter. We select projects from a high investment amount of 150 projects, divided into 50 completed projects and 100 unsuccessful projects to learn about fake project information. We choose the number of unsuccessful projects over successful ones because there are many types of unsuccessful projects. For example, a project that can be accomplished has a theory to support its creation but suddenly stops, and projects do not continue. Some projects can create pieces and have a theory to support them, but they can't be used in real work. We will use the information of each project obtained from the search on the website for keyword extraction from multiple techniques to get good keywords and suitable ones. We applied five models, NLTK [2], RAKE [3], Gensim [4], LIAAD/YAKE [5], BERT [6], and we then compare them with the keyword extracted by ten students, nine of them are undergraduates and one graduate.

A. NLTK

NLTK (Natural Language Toolkit) [2] is an open-source software and API for NLP (Natural Language Processing) platform available for Python. It is a powerful tool for processing text data, parsing, classification, interception, tagging, semantic reasoning, and other computational linguistics. Installing the NLTK Module requires downloading and installing an additional bundle that will download dictionaries and other language and grammar frameworks required for full NLTK functionality. NLTK fully supports English.

Stop words do not have a clear meaning like 'and', 'a', 'it', and 'they' these have a meaningful impact when we use them to communicate, but these terms may mean nothing with computer analysis keyword extraction. Stop words are left in the entire data system and not included in NLTK text analyses because it is considered meaningless. Sometimes, using the NLTK module to extract words from informal articles, for example, from the internet, might be a problem. Therefore, we need to train these models on new datasets with informal languages first.

B. RAKE

RAKE [3], also known as Rapid Automatic Keyword Extraction, is a highly effective keyword extraction technique.

RAKE is based on the observation that common keywords consist of multiple words with standard punctuation marks or pauses. Alternatively, we can say interchangeable words like 'and', 'of', and 'that'. First, the text in the document is split into an array of words separated by specific words. Secondly, the array is divided again into successive sequences of phrase-separated words and stop-word positions. Finally, the word location is determined. Then, we will combine words in one location and select them as keywords.

C. Gensim

Gensim [4] consists of several sub-technical extraction techniques such as Word2Vec, FastText, and Latent Semantic Indexing. Gensim automatically searches for keywords by examining statistically occurring patterns within its own dictionary. Furthermore, the techniques within Gensim are unsupervised. This means that as long as we have the dictionary, we can easily apply it to other texts.

D. YAKE/ LIAAD

YAKE [5] is a way to extract keywords based on text attributes automatically. It is a keyword extraction tool in Pyth. This method also provides an end-to-end keyphrase extraction pipeline to extract keywords from text documents. It uses a statistical text feature extracted from a single document to select the most important text keywords. YAKE's systems do not require training on a specific set of documents, language, and domain size.

E. BERT

BERT [6] uses a mechanism of relational learning between words of text in the form of a transformer. The details of the operation of the Transformer are described by Google [12].

The core principle of BERT is in Transformers, a new neural network architecture for linguistic understanding.

Transformers are word-processing models that involve other words in a sentence. Instead of verbatim processing, BERT can determine the full context of a word by looking at the words that come before and after them. It's especially useful for understanding the intent behind a search query. Fig. 2 shows the procedure of extracting keywords with BERT pre-training.

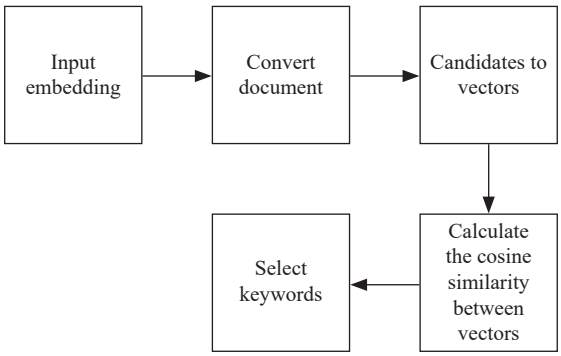

Fig. 2. Procedure of extracting keywords with BERT pre-training

F. Compare Keywords

In this research, we will manually generate five keywords to create a ground truth equal to the number of automatic keywords obtained from each model to compare with automatic keyword extraction. Human-generated keywords are done by ten students, including one undergraduate and one graduate. We analyzed and selected keywords based on their meaning, main content of the project, nature of work, type of work, and benefits.

Table I shows an example of a keyword extraction with ten students using the method of reading from each project article. If a student reads and does not understand the content, he or she will go find more information regarding the project, whether it's through the website, books, or others to understand the content or the algorithm that is required for decision-making and selection of keywords. We have a keyword extraction process as follows: First, we had nine undergraduate students read the article and select the right word or benefit for the project. In the second step, one graduate will compare all the keywords received from the nine undergraduate students, and in the last step, one graduate will select five suitable keywords. Keywords selection is primarily based on the keywords that are the essence of the content.

TABLE I
AN EXAMPLE OF MANUAL KEYWORDS EXTRACTION

Number	Manual Keyword
1	Wheel Reflector
2	Reflector With 360-degree
3	Reflective Power
4	Overlapping Design
5	Gapless Shining

In Fig. 3 shows a flow chart of the sequence of steps of keyword extraction with five techniques and Table II to Table VI shows an example of a keyword extraction by five techniques: NLTK, RAKE, YAKE/ LIAAD, Gensim, and BERT.

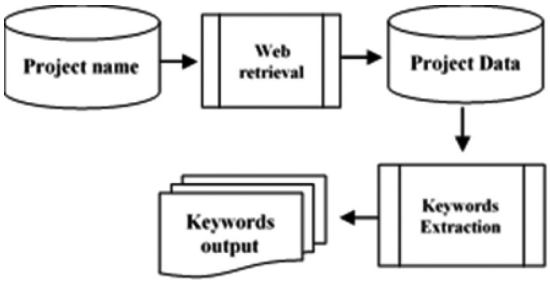

Fig. 3. Flow chart of extracting keywords by five techniques

TABLE II
AN EXAMPLE OF KEYWORDS EXTRACTION WITH RAKE

Original Text	FLECTR 360 OMNI – Edition 2020. The wheel reflector with 360-degree visibility! FLECTR 360 reflects car headlights wherever they come from. Sideways, from behind or in front – simply from ANY direction! It magically turns your rims into gapless shining retro-reflectors. Its overlapping design also doubles its reflective power. FLECTR 360 OMNI fits oval, round & sharp-edged rims from 26" and above with a maximum of 32 spokes. Exclusion: caliper brake wheels without a minimum curvature of 15 mm above the brake flank.
Output	**"Calliper brake wheels",** "Flectr 360 omni fits oval", "Round & sharp-edged rims", "Flectr 360 reflects car headlights", "Gapless shining retro-reflectors"

TABLE III
AN EXAMPLE OF KEYWORDS EXTRACTION WITH YAKE/ LIAAD

Original Text	FLECTR 360 OMNI – Edition 2020. The wheel reflector with 360-degree visibility! FLECTR 360 reflects car headlights wherever they come from. Sideways, from behind or in front – simply from ANY direction! It magically turns your rims into gapless shining retro-reflectors. Its overlapping design also doubles its reflective power. FLECTR 360 OMNI fits oval, round & sharp-edged rims from 26" and above with a maximum of 32 spokes. Exclusion: caliper brake wheels without a minimum curvature of 15 mm above the brake flank.
Output	**"Feflector 360 reflects car headlights",** "Feflector 360 reflects car headlights come", "Omni edition 2020 wheel reflector 360 degrees", "Degree visibility reflector 360 reflects car headlights", "Visibility reflector 360 reflects car headlights come"

TABLE IV
AN EXAMPLE OF KEYWORDS EXTRACTION WITH GENSIM

Original Text	FLECTR 360 OMNI – Edition 2020. The wheel reflector with 360-degree visibility! FLECTR 360 reflects car headlights wherever they come from. Sideways, from behind or in front – simply from ANY direction! It magically turns your rims into gapless shining retro-reflectors. Its overlapping design also doubles its reflective power. FLECTR 360 OMNI fits oval, round & sharp-edged rims from 26" and above with a maximum of 32 spokes. Exclusion: caliper brake wheels without a minimum curvature of 15 mm above the brake flank.
Output	**"Reflects",** "Brake", "Reflective", "Sharp", "Shining"

TABLE V
AN EXAMPLE OF KEYWORDS EXTRACTION WITH BERT

Original Text	FLECTR 360 OMNI – Edition 2020. The wheel Reflector with 360-degree visibility! FLECTR 360 reflects car headlights wherever they come from. Sideways, from behind or in front – simply from ANY direction! It magically turns your rims into gapless shining retro-reflectors. Its overlapping design also doubles its reflective power. FLECTR 360 OMNI fits oval, round & sharp-edged rims from 26" and above with a maximum of 32 spokes. Exclusion: caliper brake wheels without a minimum curvature of 15 mm above the brake flank.
Output	**"FLECTR",** "Edition", "OMNI", "Degree visibility", "Wheel reflector"

TABLE VI
AN EXAMPLE OF KEYWORDS EXTRACTION WITH NLTK

Original Text	FLECTR 360 OMNI – Edition 2020. The wheel reflector with 360-degree visibility! FLECTR 360 reflects car headlights wherever they come from. Sideways, from behind or in front – simply from ANY direction! It magically turns your rims into gapless shining retro-reflectors. Its overlapping design also doubles its reflective power. FLECTR 360 OMNI fits oval, round & sharp-edged rims from 26" and above with a maximum of 32 spokes. Exclusion: caliper brake wheels without a minimum curvature of 15 mm above the brake flank.
Output	**"Flectr 360 reflects car headlights wherever",** "Flectr 360 omni – edition 2020", "Flectr 360 omni fits oval", "Overlapping design also doubles", "Calliper brake wheels without"

G. Matching Keywords

Keyword matching is where the keywords obtained from five algorithms are compared with the keywords made by ten students. Using the following conditions: a keyword that matches 100% manual keyword will get one score point; if it matches 75%, it will get 0.75 points; if it matches 50%, it will get 0.50 points; if it matches 25%, it will get 0.25 points.

TABLE VII
AN EXAMPLE OF MATCHING KEYWORDS

Number	Manual Keyword	NLTK
1	Wheel Reflector	"Flectr 360 Reflects Car Headlights Wherever"
2	Reflector With 360-degree	"Flectr 360 Omni – Edition 2020",
3	Reflective Power	"Flectr 360 Omni Fits Oval",
4	Overlapping Design	"Overlapping Design Also Doubles",
5	Caliper Brake Wheels	"Caliper Brake Wheels Without"

From Table VII the result of the keyword matching is 2 points. There are two valid keywords: "overlapping design" and "caliper brake wheels".

H. Precision and Recall

To compare each model that was searched for keywords, we will use precision and recall as a measure. Precision is the number of keywords that match the keywords we generate divided by the total number of keywords we generate. The recall is the total number of keywords coming out of each model divided by the number of keywords we define.

$$recall = \frac{|\{Manual\ keyword\} \cup \{retrieved\ keyword\}|}{\{Manual\ \ keyword\}} \quad (1)$$

A recall is a manually generated fraction of a keyword successfully retrieved.

$$precision = \frac{|\{Manual\ \ keyword\} \cap \{retrieved\ keyword\}|}{\{retrieved\ keyword\}} \quad (2)$$

Precision is the ratio of Manual keywords to retrieved keywords.

$$F - score = \frac{2 * precision * recall}{(precision + recall)} \quad (3)$$

Traditional F measurements are harmonic that combine precision and recall.

IV. Results and Discussion

A. Results

In this research, keywords are automatically obtained by extracting keywords from various modeling algorithms and are compared with the keywords given by the 10 students, with nine undergraduate students reading the paper and choosing the right or useful word for the project, then one graduate compares the keywords all received from nine undergraduate students and five of the appropriate keywords were selected.

We compare it with the keywords obtained from each algorithm. The data in Table VIII shows the total number of keywords retrieved from each algorithm number of valid keywords and the number of invalid keywords.

TABLE VIII
ALL RETRIEVED KEYWORDS, VALID KEYWORDS, AND INVALID KEYWORDS OF DIFFERENT MODEL

List	All Keywords	Valid Keyword	Invalid Keyword
RAKE	750	333	417
NLTK	750	408	342
YAKE/LIAAD	750	314	436
Gensim	750	227	523
BERT	750	391	359

The data in Table IX shows the results the precision, recall and F-score of different model: RAKE, NLTK, YAKE/LIAAD, Gensim and BERT.

TABLE IX
THE PRECISION, RECALL, AND F-SCORE OF DIFFERENT MODEL.

List	Precision	Recall	F-score
RAKE	44.40%	100%	61.50%
NLTK	54.40%	100%	70.47%
YAKE/LIAAD	41.87%	100%	59.03%
Gensim	30.27%	100%	46.47%
BERT	52.13%	100%	68.53%

The data in Fig. 4 shows the results precision, and F-score rate of different models: RAKE, NLTK, YAKE/LIAAD, Gensim, and BERT.

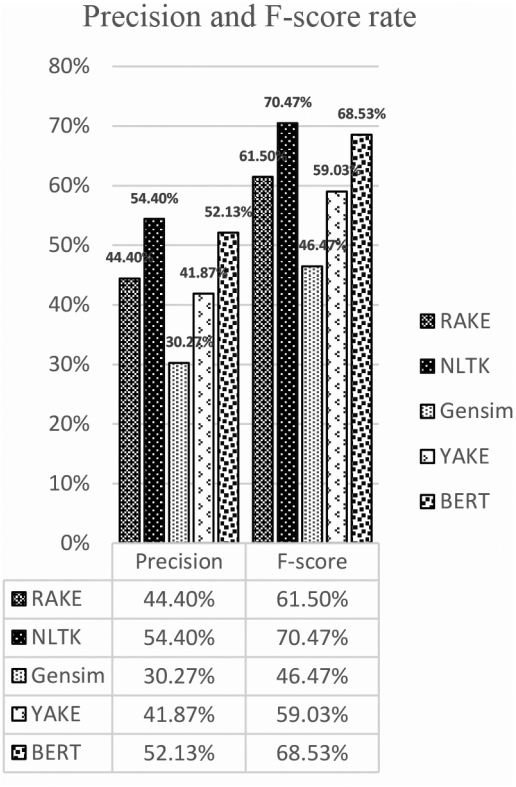

	Precision	F-score
RAKE	44.40%	61.50%
NLTK	54.40%	70.47%
Gensim	30.27%	46.47%
YAKE	41.87%	59.03%
BERT	52.13%	68.53%

Fig. 4. The Precision and F-Score of Different Methods

B. Discussions

When we applied five algorithms: RAKE, NLTK, LIAAD/YAKE, GENSIM, and BERT, to extract keywords from a total of 150 projects. We studied and compared five techniques to find the model that extracts the best keywords, we also studied the behavior of keyword extraction in each model and compared all the keywords extracted in the same model. We have found the keyword extraction characteristics of each model: RAKE model the extracted keywords will focus on the topic, traits, and abilities mentioned by the article. NLTK model will focus on the key traits, components, abilities, models, or versions. LIAAD/YAKE model focuses on the capabilities and specific words of the content. The gensim model will focus on a single word that describes abilities or traits, and finally, the BERT model will focus on thematic content. It will extract the keywords into long sentences. It discusses topics, potentials, and sentences that describe the nature of the equipment or objects the project will create.

V. Conclusion and Future Work

There are many projects on Indiegogo and Kickstarter. Unfortunately, it is not easy to identify unsuccessful projects. To identify possible fake information in each project, we need to isolate the keywords for each project and further analyze the data for each project. Currently, there are several ways to extract keywords from the English text. Therefore, we have compared the effectiveness of keyword extraction methods for various Indiegogo and Kickstarter projects through experiments in this research.

To get information about the various factors of the fake project. So we take the data of 150 projects for experimentation. There are both successful and unsuccessful projects. In our experiment, we compared the keywords extracted from ten students to the keywords extracted from each algorithm to find an algorithm that extracts the keywords closest to the students. We found the NLTK model to be more efficient than other keyword extraction methods. It has a precision rate of 54.40% and a 70.47% F score, with BERT coming in second with a precision rate of 52.13% and a 68.53% F score.

The extracted keywords will make it easier for investors to search for more information, learn about the details and theories that support the project, and help make investment decisions easier. When analyzing the information obtained, we can determine that the project is likely to be successful. Such as Project Titan. As we read about the project, we will focus on artificial gill technology and size. When we take this information into further research, we can see that in theory it can actually be done. However, due to the small size of the artificial gum, it cannot be used for artificial respiration for 45 minutes, so this project is a fake project. The method of separating keywords from project data is the solution to help investors not be scammed into investing in fake projects.

This research is a pioneer study to try to find a way for helping humans to identify possible fake projects, In the future, we will improve the model and train algorithms to improve the efficiency of keyword extraction and we may extend this research by creating modules to examine projects on Kickstarter and Indiegogo for identifying possible fake projects.

Acknowledgements

The first author studied a keyword extraction algorithm, experimented, and co-drafted the manuscript. The last author gave advice, suggested an experimental method, and co-drafted the manuscript. The first and second authors contribute 50% equally to this work.

The first author would like to thank the scholarship sponsor from CP ALL.

References

[1] F. Bayatmakou, A. Ahmadi, and A. Mohebi, "Automatic Query-Based Keyword and Keyphrase Extraction," in *Proc. 2017 Artificial Intelligence and Signal Processing Conference*, 2017, pp. 325-330.

[2] E. Loper and S. Bird, "NLTK: The Natural Language Toolkit," in *Proc. The ACL Interactive Poster and Demonstration Sessions*, 2020, pp. 62-69.

[3] S. Rose, D. Engel, and N. Cramer, *Automatic Keyword Extraction from Individual Documents*. John Wiley & Sons, Inc., New Jersey, 2010, pp. 1-20.

[4] M. M. Haider, M. A. Hossin, H. R. Mahi et al., "Automatic Text Summarization Using Gensim Word2Vec and K-Means Clustering Algorithm," in *Proc. IEEE Region 10 Symposium*, 2020, pp. 283-286.
[5] R. Campos, V. Mangaravite, A. Pasquali et al., "YAKE! Keyword Extraction from Single Documents using Multiple Local Features," *Information Sciences*, vol. 509, pp. 257-289. Jan. 2020.
[6] N. Karacapilidis, N. Kanakaris, and N. Giarelis, "A Comparative Assessment of State-of-the-Art Methods for Multilingual Unsupervised Keyphrase Extraction," in *Proc. IFIP International Conference on Artificial Intelligence Applications and Innovations*, 2021, pp. 635-645.
[7] C. Zhang, "Automatic Keyword Extraction from Documents using Conditional Random Fields," *Journal of Computational Information Systems*, vol. 4, no. 3, pp. 1169-1180, Jun. 2008.
[8] A. Onan, S. Korukoğlu, and H. Bulut, "Ensemble of Keyword Extraction Methods and Classifiers in Text Classification," *Expert Systems with Applications*, vol. 57, pp. 232-247, Sep. 2006.
[9] J. Qu, NL. Minh, A. Shimazu, "Web Based English-Chinese OOV Term Translation Using Adaptive Rules and Recursive Feature Selection," in *Proc. The 25th Pacific Asia Conference on Language, Information and Computation*, 2011, pp. 1-9.
[10] T. Mikolov, K. Chen, G. Corrado et al., "Efficient Estimation of Word Representations in Vector Space," *arXiv*, no. 1301.3781. pp. 1-10. Jan. 2013.
[11] J. Devlin, M. W. Chang, K. Lee et al., "BERT Pre-training of Deep Bidirectional Transformers for Language Understanding," *arXiv,* no. 1810.04805v2, pp. 1-16. May. 2019.
[12] A. Vaswani, N. Shazeer, N. Parmar et al., "Attention is All You Need," in *Proc. Advances in Neural Information Processing Systems*," 2017, pp. 5998-6008.

Woottikarn Hongwiengchan is currently studying for the Master degree of Engineering (Engineering and Technology), Panyapiwat Institute of Management, Thailand. Him research interests are natural language processing and AI.

Jian Qu is a full-time lecturer at the Faculty of Engineering and Technology, Panyapiwat Institute of Management. He received Ph.D. with Outstanding Performance award from Japan Advanced Institute of Science and Technology, Japan, in 2013. He received B.B.A with Summa Cum Laude honors from the Institute of International Studies of Ramkhamhaeng University, Thailand, in 2006, and M.S.I.T from Sirindhorn International Institute of Technology, Thammasat University, Thailand, in 2010. His research interests are natural language processing, intelligent algorithms, machine learning, machine translation, information retrieval, and image processing.

Design and Development of a Carry-On Bag to Support Women in Work-and-Travel Activities

Suchada Rianmora[1], Thorfan Netkueakun[2], and Nutthamon Samorhom[3]
[1,2,3]School of Manufacturing Systems and Mechanical Engineering
Sirindhorn International Institute of Technology, Thammasat University
Pathumthani, Thailand
E-mail: suchada@siit.tu.ac.th[1], thorfan.net@gmail.com[2], nutthamon.sam@gmail.com[3]

Received: March 28, 2023 / Revised: May 3, 2023 / Accepted: May 9, 2023

***Abstract*—Design under constraints can be accomplished properly with the assistance of Product Design and Development (PDD). Presented in this study is the development of durability, flexibility, and accessible briefcase-style bag for work-and-travel activity. Target customers are set as women who, mostly, require some details that lead the designers to comprehend some hidden issues. Providing enough space and a strong body to store many stuffs, and preserving items in good condition are the key considerations. A solid-based baggage cover can provide a shock-absorption structure, and its size must not exceed - 40cm x 20cm x 25cm. The weight of the bag plus stuff is determined around 4 kg, which is the key parameter for Finite Element Analysis (FEA). Force distribution around the bag is simulated for safety purposes; when a 1000 N of the external force (or impact force) delivers a shock or high impact in a relatively short period of time on the front/back area of the bag, the developed bag still in a usable condition; no crack found. Polycarbonate (PC) - Acrylonitrile Butadiene Styrene, or ABS plastic material is applied to the main body of the bag. All analyzed results can be applied as the key guidelines for the manufacturers or customers to assist work-and-travel activity with happiness.**

***Index Terms*—Design and Development, Carry-on Bag, Finite Element Analysis, Conceptual Design, Usefulness of Products.**

I. Introduction

Over the past three years, during the COVID-19 pandemic, people have made the decision to pay less attention to going out for doing some activities, and some have stayed at home almost all the time where online foods and products are the choice and key tool for supporting their basic needs [1]-[5]. However, some might feel not comfortable living like that as a twenty-four-seven platform. Besides, as the stay-at-home lifestyle is prolonged in many parts of the country, people are getting more about experiencing worry, unease, or nervousness; typically, about an imminent event or something with an uncertain outcome. For instance, if people live in an area where nonessential travel is advised against, it would not be a good idea to drive to an outdoor space. A great way to release these stresses and problems, outdoor activities are the choice to get a change of environment. Since, at this particular moment, people are facing on-and-off services in the middle of the coronavirus pandemic, not all outdoor activities are allowed to do as a full option/version. Some outdoor activities are not engaged right now; luckily, some are safe, which can help give people a much-needed mental reset. Traveling is a good choice and is recommended as one of the popular activities to do. For supporting this activity, proposed in this study is about how to provide an easy-to-access product with durability plus flexibility where a "carry-on bag" is applied as the case study.

Since, "Quality of life" can be expressed as an individual's perception of their position in life in the context of the culture and value systems in which they live and in relation to their goals, expectations, standards, and concerns. For supporting this issue, current, many researchers have tried to provide specific concepts and approaches for supporting the COVID-19 pandemic to enhance the quality of life of people in various fields; fundamental needs, logistics, medical services and facilities, traveling issues, automotive, and transportation [8]-[11]. When the day-to-day of our lives is already super-stressful, people have tried to find ways for reducing stress by doing outside activities where traveling and visiting nature experienced can greater decrease stress than those who perform either indoor activities or who watch nature programming on visual reality platforms for the same amount of time. From the obtained results, someone who is depressed may have mood swings, changing environment can make their mood improve more. These have led to the proposed approach to introduce an alternative design of a carry-on bag, which can support users who would like

to perform tasks while traveling where the conditions or the item(s) inside can be preserved as the original conditions.

II. Research Background

In order to extract and reveal the blind spot of business, gender is the most powerful determinant of how to see everything in the world – different viewpoint, different gender. With this keyword – "gender", it is more significant than age, income, ethnicity, or geography. Recently, for creating and developing a new design of the product, a design team has started with launching a set of questionnaires to both men and women (target) customers [12], even if some products are emphasized to sell to men such as clothes, shoes, socks, shaving, or sportswear. Since women have a multiplier effect. They are multiple markets in one. Because women serve as primary caregivers for children and the elderly in virtually every society in the world, women buy on behalf of the people who live in their households, as well as for extended family (such as older parents and in-laws) and friends.

A. The Status of Women in Society

There are 1.4 million more women who are licensed to drive than men. Women also tend to purchase more new cars than used ones, with 62% of new cars in the country being purchased by women [13]. Women influence 7 trillion dollars of spending annually and influence 83% of all consumer spending [14]. From this viewpoint, it can convey and imply the trend of work-and-travel platforms in women that is growing up day by day. Moreover, as a growing number of women are buying cars, it is now crucial for entrepreneurs to create facilities or special items to support women's needs to work with a smile while traveling. In Thailand in some areas like downtown – metropolitan areas, people have spent more time traveling on the road because of traffic jams. Some minor activities are raised and performed during that situation. The situation is better when people drive on a clear road at night. There is a steady stream of oncoming traffic. However, the national speed limit applies. Thus, daytime activity is taken into consideration as the reference for creating a drafted design of a product proposed in this study.

B. Concerning the Issue When Women Keep Stuff in Bags

The target group of customers, in this study, is considered "the female of age group ranging 15-64 years", since this range is the main consumer of the handbags market [15]. In general, women can express their feelings with a clearer view than men; some hidden issues can be revealed such as the key considerations of the desired product that should provide durability, reliability, safety, and affordability characteristics. Whereas, from the men's viewpoints, they are more drawn to interior layout, exterior styling, technology, and ruggedness. Women define a successful transaction as getting the exact product they want, while men are more about negotiating the best deal [16]-[17].

Normally, the lady keeps the cosmetic in a bag (purse), and a small container at home that provides stability at room temperature is required and it is considered as one of the basic needs of women. This requirement is, also, imprinted as perception where the case or container required for containing sensitive stuff inside needs to provide some functions and space like this case.

Illustrated in Fig. 1 [18] is an example of a cosmetic box that is available in the market and it contains many slots plus functions such as light-dimming brightness application attached to the mirror or compact size of the drawers. The style of this product type, which is about the combination between a round-shaped structure and easy-to-use characteristics of the product, is mainly constructed based on the knowledge and skills to enable customers to feel relaxed and at ease, confident, and assured that their expectations will be met - even better when exceeded.

Fig.1. The main components of the cosmetic box [18]

However, in the real life and situation of working women, women, sometimes, forget and put their makeup sets in the wrong place such as a car or high-temperature weather environment, which is a nightmare for the lady.

Comparing among various types of cosmetic items (e.g., lipstick, blush, foundation, face powder, eye shadow eyeliner, and mascara) that women need to own, "lipstick" is the winner, since its concepts are about "available anywhere, anytime, and to anyone". However, it is reported that the structure and chemical properties are considered the most sensitive product [19]-[23].

For supporting the design stage of this proposed study to design a carry-on bag for supporting work-and-travel activity, the lipstick plus its characters (i.e., both physical and chemical terms) are studied and reviewed as the key component with the assumption that if the lipstick can maintain its shape and property

under the provided conditions inside the developed carry-on bag, the other products can be preserved their original conditions.

C. Key Factors to Make Customers Feel Comfortable

The design team had found the bright direction to create the criteria and constraints of the space (room) with compartments inside the bag, materials used for making and covering a whole bag, and the main structure like bag skeleton for supporting force applied during traveling. However, some hidden issues such as customer feelings and requirements for the bag are needed to be revealed in a systematic way. Sometimes, the target customers do not want to answer long and too much texts questionnaires since, in their perception, doing this for unknown people like a self-administered survey wastes their time. This style of the questionnaire is designed explicitly to be completed by a respondent without an interviewer's assistance (or bias). Self-administered surveys are widely used for collecting quantitative research data. From the known-to-known platform, one of the most common types of self-administered surveys is mail-in questionnaires. Online questionnaires sent out to respondents via email invitations are another example of a self-administered survey. Apart from paper and online forms, self-administered surveys also come in the form of oral tests [24].

However, currently, even if a digital platform and an easy-to-access application have become famous and necessary for better living, with this digital platform, some drawbacks are indicated via distorted details and wrong instructions since "copy-and-paste" style can make a new document file in second from an unknown group of people. They just start to consider which social media channels of whom contain many followers and have become famous influencers. Then, the illegal groups tried to copy the identity of those people to be theirs by using personal information, pictures, a product of interest, or an address for selling prod-up products to innocent target customers. The forbidden websites or social media platforms do not exist in terms of registration by known persons. After they receive money from bank transactions, they are gone and leave the recent social platform(s), then they have started a new account with a new name of another famous influencer [25]-[26].

D. Reasons and Factors Influence Women to Purchase

Recently, the majority of marketing victim who has decided to purchase product(s) from illegal websites are women [27]-[29]. To understand more about some hidden issues plus the reasons why they have made a decision like those recorded data, the key factors are taken into consideration.

Factor 1: Reliability, Empathy, and Trust

Once the customers know that the design team or manufacturers are interested in meeting their needs rather than selling a product, their comfort level will increase. The following statements are the key tools that will support the design team and manufacturers to meet customer satisfaction.

1) Taking time to find out what customers really need and want by considering facial expressions or ways to answer questions is the priority to do. Next, show them how the design team can meet those desires. This kind of respect engenders comfort and trust – this can link to the reliability of the product and business.

2) The manufacturers must consider are about "acknowledge and respect diversity", since women are as diverse a group as they come. Moreover, during the 21st century, women are strong and independent when compared to historical times. Modern women enjoy having their strength, even after marriage and having children. Having strength is socially accepted now because a woman is doing things for herself as well as others, like working and or furthering their education while raising children. They can do many things and almost everything they want to do.

3) A woman's strength is very important to her because that is part of what self-confidence is built upon. This leads to many strong women achieving goals and accomplishing dreams only to create new ones that reach even higher. Many women during this century are strong in the fact that they are an entrepreneur/workers as well as a mother, wives, daughters, and sisters/aunts, among many other titles/roles. The products launched to this target group should contain "durability, flexibility, and safety function".

4) Historically, women were not socially accepted in the ways that they are now. The best example is the fact that women can serve in any military branch, political office, or even any business capacity. Thus, these can reveal the trend of products that should be provided with "boyish" which is a style that blends masculine and feminine trends, and it is considered as a younger look and more casual than a "mannish one". For "Mannish style", is quite similar to the "boyish style"; however, the "Mannish style" is a masculine (i.e., having qualities or an appearance traditionally associated with men or boys) focused fashion most often worn by women with a professional look. It features masculine items and oversized items and is meant to accentuate femininity with masculine clothing.

In summary, when companies or manufacturers understand the background and respect the roles or titles of women in a systematic way, and in return, they will appreciate the respect and the way to afford them. This might show the good and bright future that they will choose a brand, service, or product made by those manufacturers who can maximize customer loyalty with a smile.

Factor 2: Classic Requirements from Women's Viewpoint

This factor is considered as a classic set of data that are about the tool for supporting the design and development of a new product. The marketing and sales strategies for women consumers are also included in this topic where the "secret" to why women buy and why they do not. Listed things to keep in mind when marketing and selling to women are [30]-[33]:

1) Women are considered the world's most powerful consumers, and their impact on the economy is growing every year.

2) Around 70-80% of all consumer purchasing is driven by women, through a combination of their buying power and influence. Influence means that even when a woman is not paying for supporting herself, she usually acts as the influencer behind someone else's purchase.

3) The concept of "shades of pink or everything about pink", sometimes, is not the right choice for setting as the key strategy. When a product is offered in only one color, and that color is pink, it conveys a limited message to the target customers who are assumed as women or a smaller group compared to providing varied ranges and shades of color. Not all women do like the pink item(s). Versatile with flexible products can increase the selling volume.

4) Service is a key tool and identifier for making customer retention. Since women tend to change their minds at critical moments such as seeing bad service occurred to other customers who are purchasing the same item from the same manufacturers or service provider, they decide to quit and leave immediately. Since they have higher expectations for customer service. Thus, when manufacturers decide to elevate the experience for women, this means that they have been trying to elevate it for everyone with the same standard.

5) Prices tell about the quality, according to an e-commerce study, consumers often fall for prices and miss out on other facts. This usually gives a bad experience to the customers. We all must have heard the saying "Good things come at a good price". Thus, if we see a good collection of outfits at a very low price then there is a chance that the quality will be degraded.

6) Women are getting married at older ages, and women (and men) are having fewer children than in previous generations. This implies that they have more potential to buy something without concerning much about financial stress.

In summary, the key point results obtained from this section are about creating a bag to support work-and-travel activity; four classic requirements from women's viewpoints are addressed: *durability, flexibility, safety, easy-to-access, and attractive details.*

III. Research Concept

In order to create a conceptual design and platform of a new product, the key considerations are "*durability, flexibility, and easy-to-access concepts*" where the concept of Product Design and Development (PDD) is applied. PDD consists of five main stages concept development, system-level design, detailed design, testing and refinement, and production ramp-up, as shown in Fig. 2.

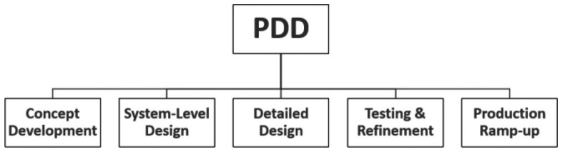

Fig. 2. Five phases of PDD for creating a new product

A. Concept Development Stage

For supporting the design team to create a drafted model of a carry-on bag, the combination of water-proof cooler food storage (thermo-bag style) (Fig. 3) and a briefcase-design platform with a small size is applied as the reference model (Fig. 4). Besides, in order to accomplish creating a drafted design of a new bag, the concept called "3Fs – Form, Fit, and Function" is applied. Moreover, after identifying the drafted ideas about the direction to go for creating a carry-on bag, the proper number of respondents who are the target customers, the classic method that is sample size analysis is discussed.

Fig. 3. Waterproof-cooler food storage (thermo-bag style) for supporting outdoor activity with insulated pouch accessories item [34]

Fig. 4. Small compact 4-wheeled briefcases with 3.231-kg weight [35]

- *Form/Fit/Function-Guidelines for A New Design*

The form is expressed the physical characteristic or looking of the future product expected to be made

by a design team. The proper references (i.e., the existing products available in the real market) are raised and extracted into main components.

For the waterproof-cooler food storage illustrated in Fig. 3, the outer surface of the main body is made from EVA material plus Oxford cloth, which can support waterproof characteristics and provide lightweight, and stylish. However, the cushion material is not found in this bag. Carrying a digital device or tablet with this bag style is not a choice.

For the small compact 4-wheeled briefs, the design and function provided can match the work-and-travel platform since some digital gadgets and devices can be properly supported compared to the previous style – soft thermo-bag design. However, the weight of the 4-wheeled briefcase, which is made from poly-carbonate and polyester materials, is the main concern – that women might feel worried about it.

Moreover, for supporting traveling activity via airline channels, the size of the bag is the main concern. Carry-on baggage allowance can vary according to the airline, the cabin class customers are traveling in, and even the size of the aircraft. As a general guide, carry-on baggage should have a maximum length of 22 in (56 cm), a width of 18 in (45 cm), and a depth of 10 in (25 cm) [36]. Illustrated in Fig. 5 is an example of baggage restrictions announced by airlines [37]. For the hand baggage, all customers are permitted to carry one piece of hand luggage and one small item (handbag/ laptop) on board. Hand luggage must not exceed 56cm x 45cm x 25cm, and the small item must be no bigger than 40cm x 30cm x 15cm. Both items can weigh up to 23 kg each.

This information is conveyed to the customers to avoid paying for fees, if the hand baggage exceeds the limit, it will be checked into the hold. This can be added to the customer's checked baggage allowance. However, if it exceeds this, the customer will be charged the airport's excess baggage fees [37].

Fig. 5. Baggage restrictions [37]

- *Sample Size Analysis*

The sample size is the number of completed responses the survey receives. The sample size of this research represents part of the group of the people or target population. This research focuses on work-and-travel supportive bags where conducting the surveys of women's favorite activities with the assistance of a statistically significant sample size can help to find out what issues are a greater concern [38]. In general, considering customer perceptions and behaviors from their experiences cannot obtain the exact direction of answers – biases are found. The biases are mentioned as beliefs, which are not initiated by known facts about someone or about a particular group of individuals [39]. For surveying the favorite activities performed by women, the measures of satisfaction level can be expressed as facial emotions or mood-and-tone during the conversation; however, when an online-questionnaire platform has become a vital technology and popular, the total time spent answering question set is taken into consideration as a tool for measuring and showing a willingness to work on the assigned task. When the respondents submit the question set with too fast or too slow, these imply about lack of concentration or consciousness to perform the task. Besides, this can imply consciousness which is a function of mind, understanding, reasons, emotion, and instinct interacting with memory. The conscious ability can be improved by gaining more information in memory through learning and experiencing new things. Thus, the proper way to inform the target customers before answering questionnaires is to provide "a storytelling of carry-on bag" to them in concise words - 5 to 7 sentences. For providing a whole frame of research to motivate their concentration. They will then use their intellect to override their emotions following the contents provided. Thus, they can focus on the task at hand. Whereas less key information is provided as the preface details, a lack of concentration occurs. Age, culture, place to live, educational background, carrier, and salary are the basic demographic variables that are included in the surveys [40].

The researchers have studied the perceptions and behaviors of people who live in the capital city (i.e., the Bangkok metropolitan region) and the survey questions were constructed to assess how people feel about favorite activities. The researchers did not have much information on the subject to begin with, so assumed that half of the respondents decide to travel and bring assigned task to do at that moment; this gave us maximum variability - Equation (1) is applied [41], [42]:

Equation 1:

$$\left(\frac{(Z)^2 \, x \, p \, x \, q}{(e)^2}\right) = n, \qquad (1)$$

where

e is the desired level of precision (the margin of error, or confidence interval)

p is the estimated proportion of the population that has the attribute in question

q is *1-p.*

Therefore, in this study, $p = 0.5$ indicates 95% confidence, and at least 5%—plus or minus—precision. A 95% confidence level gave Z values of 1.96, per the normal tables, giving

$$\left(\frac{(1.96)^2 \, x \, 0.5 \, x \, 0.5}{(0.05)^2}\right)$$

From the calculated value, it was found that a random sample of 385 respondents in the target population was enough to give the confidence levels needed. In practice, around 500 online-link of questionnaires were distributed to the target customers. At this initial stage of the concept development phase, 400 respondents returned their answers; these obtained data were extracted and translated into a conceptual model of the carry-on bag – 3D CAD model. Besides, the key points, which are used as the supportive information plus reasons to select the proper materials used for creating a carry-on bag, are "the monthly income" (Table I), and "the favorite activity" (Table II) of the target customers. The resulted presented in Table I presented that the first and second groups of the monthly income are considered as the major group of the target customers where the range of salary is around 35,000 - 100,000 THB (1058.14 - 3023.16 USD). This implies some key points that they can support work-and-travel platform with less stress comparing to the average salary in Thailand, which is 24,500 THB (734 USD) [43].

TABLE I
MONTHLY INCOME OF THE RESPONDENTS

Monthly Salary		No. of Respondents (400)	(%)
(THB)	(USD*)		
< 15,000	453.47	36	9
15,001 - 25,000	453.50 - 755.79	56	14
25,001 - 35,000	755.82 - 1058.11	68	17
35,001 - 50,000	1058.14 - 1511.58	108	27
50,001 - 100,000	1511.61 - 3023.16	104	26
> 100,000	> 3023.16	28	7

* Foreign Exchange Rates as of 19 January 2023 - Exchange Rate = 33.078 THB/US Dollar [43]

From Table II, the first four activities that women would like to do when they have free time are listed as *Traditional Shopping, Travelling, Communication with Family & Friends,* and *Outdoor Exercise*, respectively. These can show the bright direction for the design team to go and continue the task – since "Traveling" is counted as one of the popular things women like to do.

TABLE II
MONTHLY ACTIVITIES OF THE RESPONDENTS

Favorite Activities	No. of Respondents (400)	(%)
Traditional Shopping	67	16.75
Travelling	63	15.75
Communication with Family & Friends	59	14.75
Outdoor Exercise	46	11.5
Cooking	43	10
Housecleaning	40	10
Online Shopping	23	5.75
Religious Activities	16	4
Indoor Exercise	15	3.75
Singing	13	3.25
Embroidery	6	1.5
Gardening/Planting	4	1
Language Learning	2	0.5
Musical Activities	1	0.25
Watching TV/Movies	1	0.25
Working	1	0.25
Art Activities	0	0

Two alternative design concepts as shown in Fig.6 and Fig. 7 are taken into consideration where their designs are suitable for carrying many types of stuffs and they are quite popular as the favorite styles that women want to use in daily life – as everyday bag.

For **"Design A"** (Fig. 6) – this bag contains waterproof-insulated material and a gusset on the bottom area with a trapezoidal prism-shaped design of a main body.

For **"Design B"** (Fig. 7) – this bag provides a solid structure of the main frame, which is similar to the concept of a briefcase and hand baggage style with a small size. Handle with finger grooves is provided; however, this fixed finger grooves structure might make the users feel not comfortable and hurt during grabbing after a while, since the space between a concave-up (curve) is not a universal design that is available for all sizes of fingers and hands – not for everyone. Thus, it would be better to provide the straight-line design of the handle as a universal design concept, all sizes of fingers and hands can be supported.

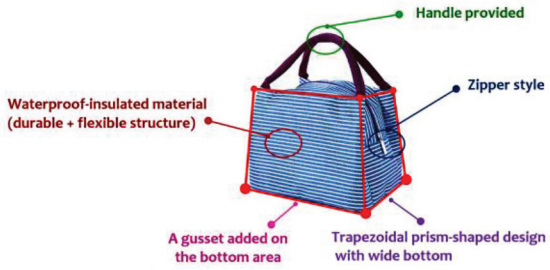

Fig. 6. Main components of the carry-on bag – *Design A*

Fig. 7. Main components of the carry-on bag – *Design B*

For **"Design C"** (Fig. 8 to Fig. 10) – this style has been introduced as the original design of a carry-on bag that provides the solid structure of the main frame, which is similar to the concept of briefcase and hand baggage style with a small size (Design B). For the handle, since the fixed finger grooves structure as present in Design B might make the users feel not comfortable during grabbing after a while, since the space between a concave-up (curve) is not a universal design that is available for all sizes of fingers and hands – not for everyone. Thus, it would be better to provide a straight-line or arched trunk handle for the briefcase bag; this illustrates more on universal design concept where the various scales of palms, hands, and fingers hands can be supported.

Fig. 8. Original design of "Design C" – carry-on bag inspired from classic briefcase baggage – Design B, (left) Isometric view, (right) Transparent display of isometric view

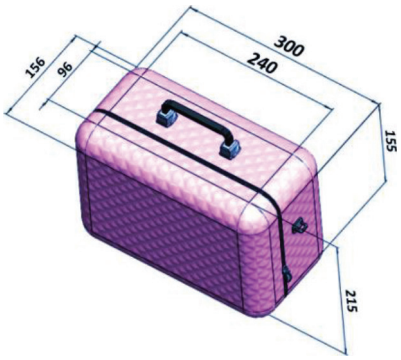

Fig. 9. Original design of "Design C" – isometric view with dimension

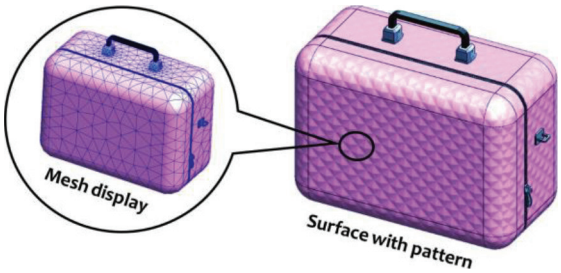

Fig. 10. Design C – printed pattern provided on the body's surface; mesh model showing smooth surface without texture

Recently, in 2021, the *"Keep It Cool" Smart Bag by the Internet of Things (IoT) for better living with the alternative design* proposed by Rianmora and Seng [44] was introduced (Fig. 11). The key concept of this reference is about presenting "a smart bag" that can support the people to keep the sensitive cosmetic products in a good condition for traveling to another province/place where the temperature inside the bag can be adjusted, and controlled the temperature and humidity conditions inside the bag easily and properly via a smartphone application. Besides, applying this will not damage and destroy the physical or chemical properties of the products compared to the traditional insulated bags. This research mentioned that the "internet of thing – IoT can make the world and life easier with simple settings and convenient functions applied while requiring less effort and investment cost.

Fig. 11. "Smart bag" prototype propsed by S. Rainmora, and S. Seng [44]

Since from the key points mentioned earlier, which are the solid-profile structure like briefcase bag, the minimal design of handle, the zipper closure platform, and the air ventilation unit with small fan for keeping items inside back with preserving the original condition, the proposed design (**Design - D**) contains these key points to create the conceptual model as shown in Fig. 12 and 13. The optional function – air ventilation with automatic fan unit, is added to the original style of briefcase-like platform – ***Design C***.

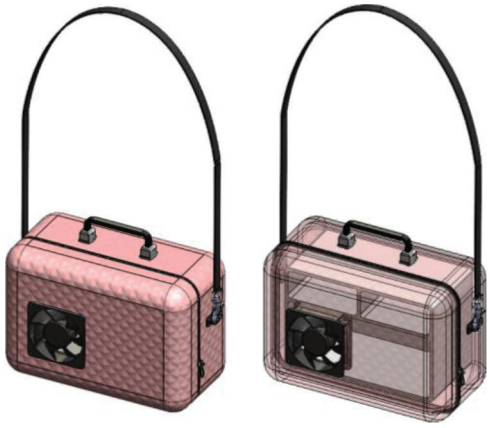

Fig. 12. Main components of the carry-on bag – Design D, (left) Isometric view, (right) Transparent display of isometric view

However, in the recent research (Rianmora and Seng [44]), the force distribution or weight of the items stored inside plus the bag itself have not been mentioned in details. This would be a bright direction to study more on the issue of load applied and design the mainframe (body) of the briefcase-like bag. Therefore, these have led to the proposed research where the design and development of a briefcase-like bag with air ventilation unit (i.e., small fan attached to the frontal area of the bag) has been studied and simulated by using Finite Element Analysis – FEA, which will be discussed in Section D – Testing and refinement stage.

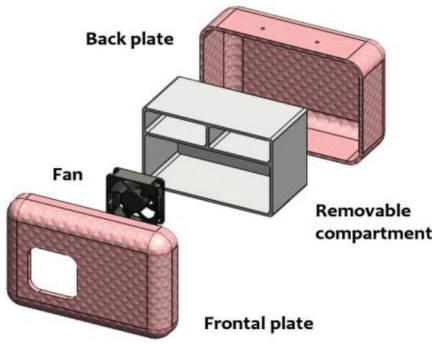

Fig. 13. Revealing the body components of the carry-on bag – Design D

B. System-Level Design Stage

This sub-section is required for classifying the carry-on bag of Design D into main components and sub-components. In general, there are many components to a bag depending on the its style and configuration. In general, there are three key elements that apply to most bags, which are body and compartment, closure and opening, and strap and handle.

• *Body and Compartment*

Body size is considered around 40 x 30 x 15 (unit in cm) with zipper (or other with easy-to-access style) – the users can access it whenever they want, and clasp locker, which is a commonly used device for binding together two edges of fabric or other flexible material. A gusset can be added and applied as a bracket strengthening an angle of a bag structure. It is like a panel, either triangular or diamond in shape, that is inserted into a garment or flexible material to help shape and reinforce key points. A bag might have feet on their flat bottoms to protect the bag if it stands on the ground. Besides, the materials used for the bag (both exterior and interior) can be guided by both function and style. Materials used are also critical to the relative sustainability of a handbag.

Keys: Function and form are both determining factors in this design decision. If a bag is meant to hold a computer, it might not be round; however, bags with unique shapes can be great ways to express style of the designer. For the bottom area of bag, if the bag needs to hold more, or stand up on its own, the bag might have a boxed bottom plus studs or feet or have a gusset on the bottom (and usually the sides).

Guidelines: In this study, material used for this area is waterproof-like fabric or polymer. To make bag durable for supporting work-and-travel platform, some high-tech plastics are recommended: polyethylene, ABS, and polycarbonate, which are lightweight and durable. ABS is lighter, but polycarbonate is more durable. The most durable, but also the heaviest, is aluminum [45]. Moreover, the interior and exterior pockets add to the functionality, and change the look of the bag.

• *Closure and Opening*

This element is the most important part of a bag, since a bag opening must provide good function to secure belongings, makes access easier or harder depending on customer's needs. Moreover, the design and pattern of this element have direct effect on the physical look of a bag. However, closure options for bags are limitless – drawstrings, carpet bag hardware, snaps, magnets, turnbuckles, or zippers.

Keys: A zipper can support easy-to-use and access by users; however, sometimes, it will not stick together. Either the head has been broken, and the teeth are

misaligned, some of the zipper stitching has slipped, causing the teeth to be misaligned, or the head and pull tab have broken or warped, causing the teeth to malign when the users pull the tab of the zipper. A larger size zipper will fail just as quickly as a smaller one. Zippers can be an indication of the overall quality of the bag. A YKK zipper is widely believed in the industry to be the most reliable zipper on the market [46].

Guidelines: In this study, for keeping stuffs safely inside bag where easy-to-access concept is applied. For the traditional zipper style, it is very useful and recommended for applying to make bags where the lock function is added. Zippers come in two types: chain, and coil. A chain zipper contains two sets of interlocking teeth, usually made of metal. It is better and stronger than a coil one, which slides on two parallel coils usually made of polyester. The key benefit of chain zippers is shown through being much more difficult to break into than coil zippers, which can be pulled apart with a ballpoint pen and reclosed.

- *Strap and Handle*

This is considered a critical element of a bag since it determines how users carry the handbag, and how much users can (or should) carry. The weight of the bag and its contents (items inside) are supported, by the body, wherever the strap/handle makes contact. The load can be made comfortable by how it is carried (e.g., in the hand, over one shoulder, across the body, or around the waist).

Keys: The specific characteristics of the strap and handle are described in the following statements:

1) *Strap Width:* For the wider straps, they can distribute larger loads better than narrower ones of the same material and pattern. Under a heavy load, the wider strap can be more comfortable. The key design depends upon the size of the bags, the small bags do not have the loading of laptops or heavy items or cross-body bags. Thus, straps can be narrow and delicate, while remaining comfortable and good feeling.

2) *Strap Length:* The key consideration of length design is dictated primarily by function during using where the style and pattern (adjustable padded shoulder strap with swivel snap hooks).

Guidelines: Material types for straps can imply the strength and comfort of a bag since some textiles need to be doubled (or more) over and stitched for giving enough strength to the strap, while material like leather or webbing is strong enough to be used as a single layer strap - high stiffness value. Styles of the strap can be defined as:

1) *Adjustable strap:* making it easy to change the length as needed is the key point that adds convenience and flexibility.

2) *Removable strap:* it can be attached in different ways, allow crossbody bags to be easily converted into belt bags, shoulder bags, or even backpacks.

3) *Fixed strap:* it is mounted directly into the handbag itself (it is not attached with hardware). This can be a striking design feature, and can give peace of mind with added security and fewer connections. However, this type of strap needs to be sized correctly for best fit.

For *Handle:* it might be the main way and be often applied for carrying a small handbag. They can also be striking design elements when they are made from a contrasting material (e.g., wood, acrylic, polymer, or metal).

After extracting the key considerations and guidelines of all key elements that apply to most bags, the researchers have tried to list and assigned the main components of the bag – for both styles (Fig. 6 and Fig. 7) for supporting the "detailed design stage" where the proper specific characteristics on the new design of carry-on bag can be assigned quickly without trial-and-error.

Summary: The main frame and function of the carry-on bag are constructed according to "Design D". Three key elements are classified as body, closure/open, and handle. The details of each are explained in the following statements.

Body: Trapezoidal-prism shaped (i.e., pyramid-like platform) plus round-corner design with the a wide bottom are applied. A removable compartment is provided inside the bag for providing flexibility to the users. The waterproof material is applied on the solid structure where the bag can stand by itself without a gusset.

Closure and open: A chain zipper type with a ring for attaching straps is applied.

Handle: Round-and-thick style is applied where the curve of the handle will be provided with ergonomics consideration.

C. Detailed Design Stage

In order to identify the specific details of a bag product that can be applied for carrying stuff, the key considerations are raised first via two issues; *what are the common items (or popular items) inside a woman's bag, and how to find the weight of bag after putting items inside.* Some everyday items are required by women, which are mentioned in many articles from easy-to-access online resources (Table III). These items are (mostly) carried in women's purses as products they would like to work into their daily routine [47]-[80]. However, carrying these items can cause some pains around the forearm and shoulder-bone or muscle between the shoulder and the elbow.

For identifying the force applied to the bag, the researchers have tried to find the key factors and issues, which have a direct effect on the bag during carrying every day. One of the factors is "the stuff/ items inside the bag". Thus, lists of popular items stored inside women's bags are presented in Table III. All 31 items were listed and researched from various sources: both online (articles posted on the websites) [81]-[87], and offline (direct interviewed data) platforms. After identifying the handbag essentials that every modern woman carries in her purse, the total weight of items inside the bag is around "3,200 g (or 3.2 kg)". This is amazing information found from this research, and it can imply that women must carry loads of two main sources: bag (itself-200 to 500 g), and stuff inside the bag. Illustrated in Table V are the FEA results obtained from the SolidWorks application. The areas affected by the load distribution are shown as the front and back areas plus the handle portion.

For **Design A**, since this design is provided with waterproof-insulated material (fabric) and a water-resistant bottom-folding tote bag, the weight is around 99-115 g.

For **Design B**, the design is provided with a solid structure with zippers and finger-grooves handle like a small briefcase where the weight is around 1 kg.

For **Design D** (Fig. 12), the design contains the main body, removable compartment (as partitions inside the bag-interior design), universal-design handle (straight-line handle), and strap. Besides, air ventilation with a small fan is applied according to the controlling system proposed by Rianmora and Seng (2021).

Illustrated in Fig.14 are the body components of the developed design of the carry-on bag – Design D. This model will be used in FEA simulation for studying force/load distribution applied around the front, back, top, and bottom areas of the bag.

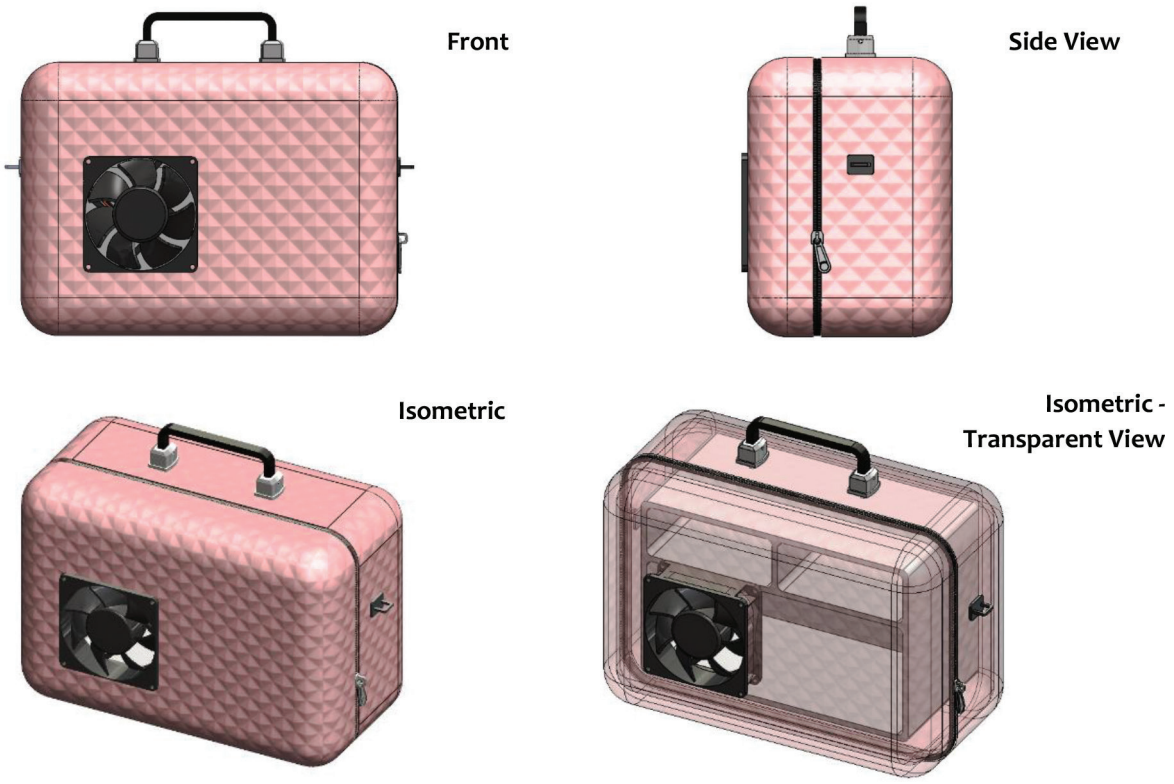

Fig. 14: Four views of the carry-on bag – Design D

D. Testing and Refinement Stage

To minimize the risk of pain in the shoulder and arm that is often due to muscle, tendon, or ligament damage from holding and carrying a load all the time or every day. These have led to the next sub-section which is about the study of loads, which are from the bag itself and the stuff carried. For studying the effect of loads carried on the shoulders [88]-[90], the researchers have tried to extract the weight of each item and combine all to be the reference for the design of load contribution activity – "testing and refinement" by the application of Finite Element Analysis (FEA) method [91]-[96].

The key reason for applying FEA in this design study is to determine the amount of external force-impact force, which is a force that delivers a shock or high impact in a relatively short period of time. It occurs when two entities collide, and this collision is the result of any object falling onto, or slamming into, the developed bag.

TABLE III
HANDBAG ESSENTIALS EVERY MODERN WOMAN CARRY IN HER PURSE

No.	Item	Weight (unit in "g")	Source
1	Battery case or portable cellphone charger/ Portable Charger	125-620	[47]
2	Tablet	460-470	[48]
3	Earphones or air pods	38.3	[49]
4	Diary / notebook / notepad	190	[50]
5	Mobile phone	130-200	[51]
6	Nail file	13	[52]
7	Wallet (Leather)	28.35-85.05	[53]
8	Hand cream (100 mL)	86- 90	[54]
9	Hand sanitizer	190	[55]
10	Mask (Extra Masks)	12.5 g/pc	[56]
11	Lipsticks, lip gloss, or lip balm	2.5-4.3 (Avg. 3.4)	[57]
12	Sunscreen (88 ml)	85.05	[58]
13	Face moisturizer (50 mL)	96.4	[59]
14	Handkerchief/Tissues: wet wipes (small pack – 25 wipes)	160	[60]
15	A period (a sanitary) pad	4.7-14.1	[61]
16	Zippered pouches	40.5	[62]
17	Reusable Bag (HDPE)	5.5 g/pc	[63]
18	Breath freshener/ Mint or any chewing gum	240	[64]
19	Aromatherapy pulse point oil/ Travel-size perfume bottle (88 mL)/ Deodorant	85.05	[65]
20	Hair stuff: hair brush, scrunchies, rubber bands, hair bands, clips, or clutches	5- 8	[66]
21	Sleek compact mirror – (48 x 48 x 6 inches)	109	[67]
22	Makeup Kit (travel-sized set)	80	[68]
23	A Pen (1 g[69]) & Paper (one A4 paper- 5 g[70])	6	[69] , [70]
	Medication	0.5-2.4 g/pc	[71]
24	Blister packs (10 pills/pack) (unit-dose packaging for pharmaceutical tablets)	3 g/10 pills/pack (0.3 g/dose)	[72]
25	Plasters (50 g – 60 pcs.)	0.83 g/pc	[73]
26	Sunglasses or Reading glasses (40 g[74]) and its case (47 g[75])	87-90	[74] , [75]
27	Business cards / Cardholder	30	[76]
28	A Key	7	[77]
29	Safety pins	0.1 g/pc	[78]
30	Foldable umbrella	120	[79]
31	Candy/ Chocolates/ Snack Bar	28	[80]

The key components, which are required as the inputs for the simulation, are the *type of material used for each element (component) of the bag*, the direction of load applied on the bag, and the type of motion applied. Moreover, the setting of commands applied in the simulation are the same; except for the fixed geometry, force, and mesh size, which will be changed according to the area of interest. Table IV is the type of material that is used for making each component of a carry-on bag; these are assigned according to the experiences of the design team and exerts who are now working on a similar type of business. Each type of material is then used for identifying "Young's modulus (E)" value [92],[93].

Young's modulus (E) is a property of the material that tells about how easily it can stretch and deform and is defined as the ratio of tensile stress (σ) to tensile strain (ε). The stress is the amount of force applied per unit area ($\sigma = F/A$) and strain is extension per unit length ($\varepsilon = dl/l$) [92],[93].

TABLE IV
TYPE OF MATERIAL REQUIRED FOR MAKING EACH ELEMENT OF A CARRY-ON BAG

No.	Part	Material	Young's Modulus (MPa)*
1	Outer Shell	ABS PC	2410
2	Handle	ABS PC	2410
3	Handle Hook	Aluminum 1060 Alloy	69000
4	Side-Hook	Stainless Steel	200000
5	Interior Compartment	Low-Density Polyethylene (LDPE)	172
6	Strap	Rubber	6.1
7	Swivel Strap Hook	Stainless Steel	200000

Source: * Young's Modulus of each material is the default value provided in SolidWorks [91].

For *Finite Element Analysis* (FEA), four areas of interest are studied (Table V) where the simulation with commands was performed in the *SOLIDWORKS* program - to identify the von Mises stress of each area. The *static / stress* is selected to calculate displacements, reaction forces, stresses, strains, and factors of safety distribution of the model. Using this simulation can support the design team to avoid failure or crack due to high stresses where four failure criteria are considered. The simulation process can be done by setting the following steps: *Part > Connections > Fixture > External Load > Mesh > Run.*

Steps required: the *SolidWorks* simulation is used for all areas where the external load of 1000 N is applied to the *handle* and to the *front*, *back, left,* and *right sides of the model*.

Firstly, setting proper material for each part of the bag in "*Part Property Manager*" is performed when all materials used for this design are provided in the library of software (Table IV).

Secondly, "*Connections Property Manager*" is done by setting "*Component Interactions and Local Interactions*". The *Component interaction* is used to specify the interaction conditions that control the action of the selected components during simulation while "*Local interaction*" is used to define interactions between sets of geometric entities of solids, shells, and beams. In addition, *Local interactions* settings override component-level interactions.

Thirdly, the *Fixture Property Manager* is used to define displacements on vertices, edges, or faces of the model. The *Reference Geometry, On Cylindrical Face,* and *Fixed Geometry* commands are used to assign value, and location is dependent upon the area of interest.

Fourthly, the *Distributed Mess, Gravity,* and *Force* commands in the *External Loads Property Manager* are used in the simulation. The *Distributed mess* of 4 kg is assigned at the inner bottom area of the interior compartment and acts as the weight of the handbag essential in the purse. In this case, the distributed mass plus the weight of the stuff inside the bag (from Table III) are applied. At the center of the model, the *gravity force* is applied. Moreover, the *force* assigned to each area is depended upon the area of interest.

Fifthly, in the *Mesh application*, the *blended curvature-based mesh* is used with a mesh size of 35 mm.

Finally, the program starts to simulate the conditions assigned where the time spent for simulation depends upon the mesh size, no. of interesting areas, and size of the virtual model. In this study, the range of time indicated around 30 minutes to 1 hour for each simulating process.

During the analysis of the Finite Element (FE) part, it was assumed that the objects inside the bag were fixed to each other, which established the contact conditions among them. A total of 152,661 elements were used in the analysis.

Results: for the handle, the results showed that the maximum von Mises occurred on the strap is 5.641 MPa. In the second area, the front and the back sides of the outer shell, the maximum von Mises occurred in these areas is 1.741 MPa. In the third area, the left and right side of the outer shell, the maximum von Mises occurred in these areas is 3.933 MPa.

Discussion: The Finite Element (FE) part of the analysis has some limitations that should be noted, including:

1. Although the strap was made of rubber, a "linear elastic" behavior in the analysis was assumed. This may not accurately reflect the material's true behavior.

2. The design team did not perform a convergence test to ensure the accuracy of our results.

3. The analysis was conducted under static conditions, while the 1000-N load we used was an assumption of an "impact load". To accurately simulate an impact load, a dynamic explicit analysis should be performed".

TABLE V
FEA SIMULATION ON "DESIGN - D" OF THE PROPOSED DESIGN

Area of Interest	External Force (N)	Max von Mises (MPA)	Result
Handle	1000	5.641	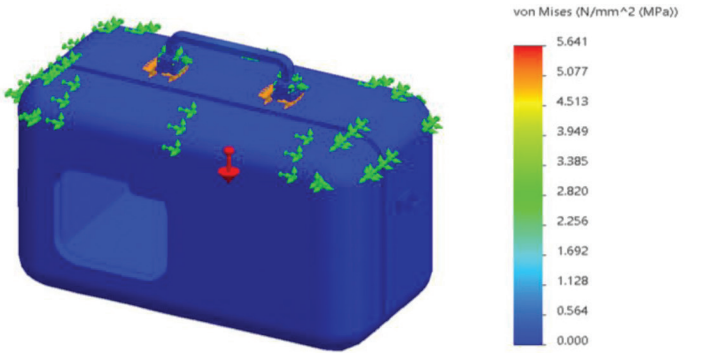
Front And Back Sides of The Outer Shell	1000	1.741	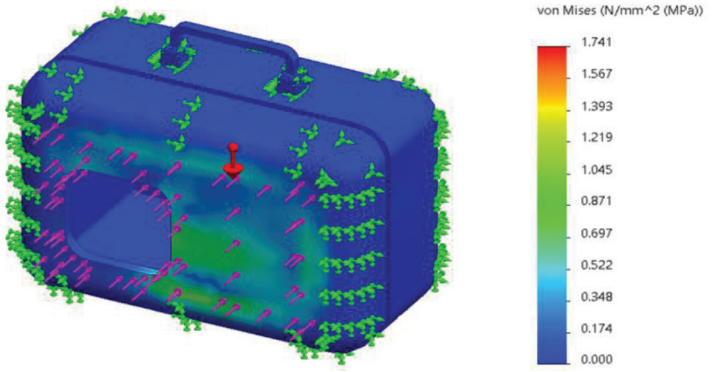
Left and Right Sides of The Outer Shell	1000	3.933	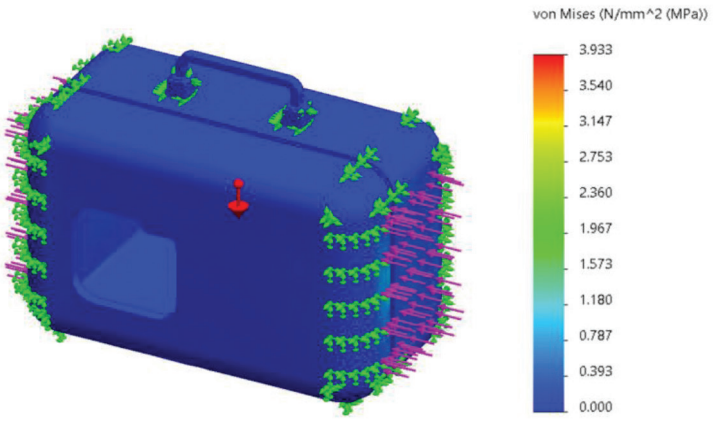
Side Hook	100	67.492	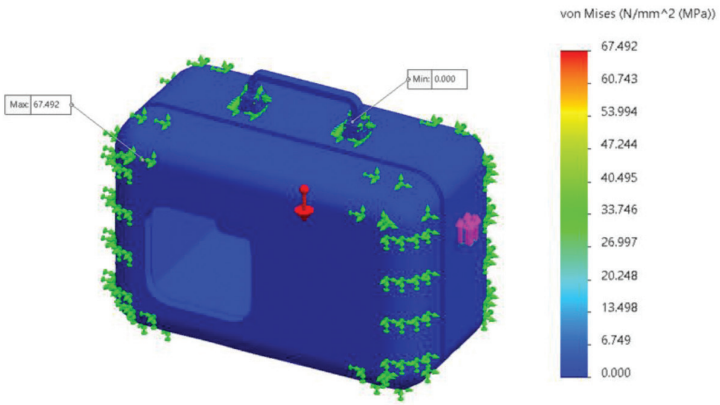

In conclusion: from the three areas where the same material is applied: (Poly Carbonate/Acrylonitrile Butadiene Styrene - PC/ABS), the maximum von Mises occurs is not exceed the yield strength or Young's modulus of the ABS PC which means that these areas will not break with the load of 100 kg or 1000 N. For the last area, *the side hook*, the results showed that the maximum von Mises occurs is around 67.492 MPa, which does not exceed the yield strength or Young's modulus of the stainless steel, which means that these areas will not break with the load of 10 kg or 100 N

E. Production Ramp-up Stage

In order to support the platform of the start-up companies who ramp up once they leave the prototype stage and begin regular production for the market, essentially, ramp-up implies bringing the company's capacity utilization close to maximum.

The key concept of this stage: Considering "the right person, the right place, and the right time" is applied. A sudden increase in resource requirement is known as ramp-up. Simply saying that the resource manager identifies and allocates the appropriate resources to fulfill the resource requests. Ramp-up occurs during the "execution" stage when additional resources are needed to complete different tasks.

Background: After obtaining the guidelines for designing a 3D virtual model of a carry-on bag, some specific elements; body structure, handle, and closure functions are suggested in detail where easy-to-maintain functions are raised; applying water-proof-polymer surface cover can make water or rain roll off the surface immediately, and safety condition relating to force (load) distribution on the bag during carrying and traveling.

Guidelines: In practice, the calculation about the "usefulness of products" can be used for supporting "two stages" of PDD; *concept development* – to identify and select one proper design from two or more alternative ones, and *production ramp-up* – to recheck and verify about the decision made by a design team whether that decision is correct and follows a good pattern of the design stage. Like in this study, two references of bags are compared and checked the trend of the selected design can match the target customers.

Limitations: However, in research, the physical prototype (a real manufactured part) has not been created yet, only graphical shapes via artworks and 3D CAD models are applied. The alternative designs (i.e., Design A and Design B) are considered to use as the reference prototype – the design team must make a decision on which one is the best or the most suitable one. Applying the "usefulness of products" method can see which component(s) of the product(s) should be considered and selected to be modified and used as the reference(s) for a new design and development [97].

How to do: Usefulness can be defined as an effective concept, which describes an item or new technology for helping someone to do something with appropriateness and socially valuable. The actual use of a product is the key consideration for the "Usefulness (U)" calculation [98]. In order to apply Table VI to select the importance level of the product, the concept of "needs" by "Maslow's Hierarchy of Needs" [99] is asked for supporting the design team to select the suitable value; however, making a decision by a group of people is quite suggestive. The potential members with skills or experiences in that product are required to suggest and discuss this issue in a systematic way. In this study, bags or containers used for storing stuff are considered as basic and safety needs according to as shown in Fig.15. Thus, from the importance level (Table VI), bags can be considered as "Very High" level where the main benefits can be implied about supporting essential for daily activities, and compulsory daily activities.

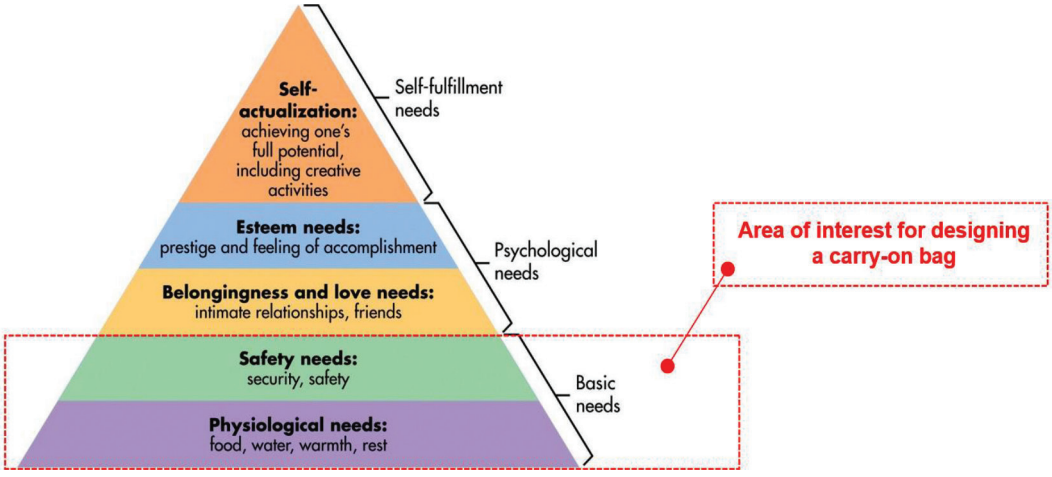

Fig. 15. Maslow's Hierarchy of Needs [99]

The key components of "usefulness of products" can be expressed as:

1) Important Level

The "importance of use" can be described as the impact of a product on people or users' lives. The product, which has more impact on society, should have a higher value of usefulness. The level of importance of products depends on how much a product has an impact on user life. Some items are essential to human life, but some are not. Five levels of importance of use have been identified (Table VI).

TABLE VI
LEVEL OF IMPORTANCE OF PRODUCTS [99]

Code	Points on a Scale of 5	Level of Importance	Type of Importance	Product Examples
A	5 (>4.0 - 5.0)	Extreme	• Life-saving drugs, life support systems • Patient life support system • Medical equipment, medicine	Mechanical ventilator or Equipment, Defibrillator, Heart/Lung bypass machine (Oxygen Cylinder, Pacemakers)
B	4 (>3.0 - 4.0)	Very high	• Essential for daily activities • Compulsory daily activities	Water, Taking food, Using restroom, Vehicles, Bags, or Containers to carry stuff safely
C	3 (>2.0 - 3.0)	High	• Accommodation • Social communication • Banking transactions	House, Clothes, Internet, Computer, Smartphone, EDC Machine, Pen, Belt, Spectacles, Shoes
D	2 (>1.0 - 2.0)	Medium	• Household appliances • Machines for daily needs	Air-conditioning system, refrigerator, Washing machine
E	1 (0.0 - 1.0)	Low	• Recreation activities • Entertainment systems • Recreation systems	Television, Comics, Books, Computer games, Bowling, Go-carting

From Table VI, the level of importance of products can be modified and adapted due to the current situation and conditions required by the people who are living in the society in that period. Since new technologies have the potential to change and elevate the human condition – the quality plus standard of life. Ways to modify the importance of products are mentioned as considering how technology or invention applied for creating some products becomes more important and necessary for living compared to the results or performance of itself in the past, that thing is referred to and considered as "high level". For example, "Internet and banking transactions". In the past, banking transactions – as online applications, can only be done and executed only at the local branch service area of the bank compared to the present where customers can perform banking transactions such as transferring money, paying bills and especially, card-less cash withdrawal that can be done in seconds by using mobile banking application on a smartphone with internet connection.

2) Popularity of Use

The key consideration of this "popularity of use" is how often people prefer to use a product launched by a company named "A", compared to others (a product from a company named "B"), which is counted in a similar group. If a product from "A" company has often been used by many people, that product from "A" company should be considered more useful and popular than another (product from "B" company) that is used by fewer people. It defines as the rate of popularity within a certain time.

However, the concept of "product differentiation" is required for supporting the analysis of "popularity of use", since "product differentiation" is the process of identifying and communicating the unique qualities of a brand compared to its competitors. Currently, some open sources of digital forums and comments can easily convey wording data speedily. This has a direct effect on the reason why people prefer brands as compared to products. Since customers require comfort, happiness, and satisfaction in their lives, and they get it in part through the products they purchase. If the brands they use consistently deliver or provide a positive experience, customers form an opinion that the brand is trustworthy, which gives them peace of mind when buying.

In summary, the key factors that customers choose one brand of a product instead of a different brand of the same product are *service quality, customer experience, brand awareness, association,* and *brand perceived quality*.

3) Usage Duration

"Usage duration" is one of the key factors, which have a direct effect on "product usefulness". Simply saying that a product of "A" company has been used for a long period, and this is longer than a same product of a different brand (i.e., from "B" company). This situation can be considered more useful compared with others. In practice, the usage duration can be considered in units of "hour per day".

4) Assessing Product Usefulness

Equation 2:

Usefulness (U) = Important level (L) × Popularity of use (R) × Usage frequency (F) × Usage duration (D)

The unit should be the same for all factors in the equation such as day, month, or year. For a seasonal product such as a sweater or swimsuit, product demand changes significantly over a seasonal period, then a large unit of time such as a year should be considered. For products that demand does not fluctuate over the period, any unit of time can be selected for the calculation.

Case A: Usefulness Calculation for "Design A: Waterproof-Insulated Storage with Oxford cloth"

Based on customer feedback, it was found that some customers prefer to use other items or materials instead of small-scale bags. However, for carrying fresh fruits, foods, or beverages that require more space, the waterproof-insulated style shown in Fig. 16 was developed. This style, which is similar to Design A, is considered as one of the alternative containers for carrying items during the day. The importance of "Design A" was rated as 3.7, indicating that it is still a popular choice among customers due to its affordable price.

The time spent for carrying or holding this bag style is "around 4 hours". From the customers' experiences (228 out of 400-57%), they said that it is not comfortable for carrying this bag, even if it is a lightweight bag, since when "electronic devices or digital gadgets" are contained inside, there is no supportive element provided. They decided to use it like the on-and-off pattern-it is not a "continuous usage" type. The rate of use is identified as 4 hours per day or 24 hours (4/24).

Calculation of Design A: Waterproof-insulated storage with Oxford cloth

Importance of use (L): **Very high (Code B) = 3.7/5 (3.7 scale from the maximum - 5 scales)**

Rate of popularity for use (R): **278/400** (ratio of number of target users who have experience with the waterproof-insulated storage/total number of people who could potentially use it)

Rate of use (F × D): **3/24** (ratio of number of hours of use/total number of hours in a day)

Therefore, applying *Eq. 2* can determine the *Usefulness (U) of Design A:*

Usefulness (U) = Important level (L) × Popularity of use (R) × Usage frequency (F) × Usage duration (D) ***Eq.2***

= (3.7/5) × (228/400) × (4/24)

= **0.0703**

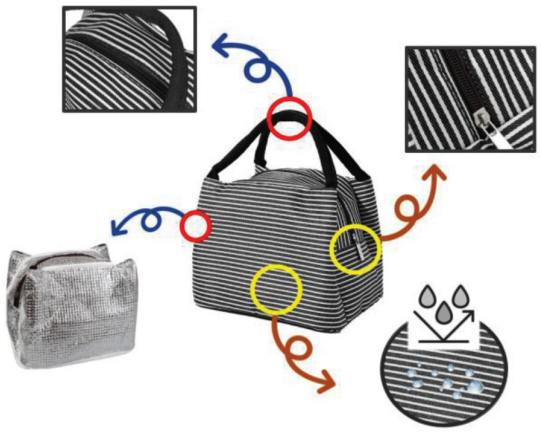

Fig. 16. Key considerations from customer perceptions on waterproof-insulated storage with Oxford cloth

Case B: Usefulness calculation for "Design B: Small briefcase-like style with strap"

For considering the assessing the usefulness of Design B: a "small briefcase-like style with strap" (Fig. 17), from the customer's viewpoint, this style can preserve and protect some stuff inside rather than using soft fabric or synthetic material as seen in Design A, even if the weight of the solid structure is higher than Design A. Besides, with the structured plastic handle that is curved ergonomically fits the balm during holding or carrying, this style is choice and easy to grab while traveling during rush hour. Therefore "4.0" is selected as the point for representing the important level of Design B. From the customers' experiences (172 out of 400-43%) –the price of Design B was higher than Design A's. This implied less selling volume for Design B compared to Design A. Moreover, time spent using this type of cane was considered around 3 hours per day or 24 hours (6/24), even if the weight is the main concern, the customers decided to apply and use this style almost all-day during working–some digital gadgets required for work can be properly carried and saved in this briefcase-like bag.

Calculation of Design B: A Small briefcase-like style with a strap

Importance of use (L): **Very high (Code B) = 4/5 (4 scales from the maximum- 5 scales)**

Rate of popularity for use (R): **172/400** (ratio of number of target users who have experiences with the simple walking cane/total number of people who could potentially use it)

Rate of use (F × D): **6/24** (ratio of number of hours of use/total number of hours in a day)

Therefore, applying *Eq. 2* can determine *Usefulness (U) of Design A:*

Usefulness (U) = Important level (L) × Popularity of use (R) × Usage frequency (F) × Usage duration (D) ***Eq.2***

= (4/5) × (172/400) × (6/24)
= **0.086**

Fig. 17. Key considerations from customer perceptions on small briefcase handbags

Discussion – Assessment of the Usefulness of a Product

After calculating the value of usefulness of two different styles – waterproof-insulated bag and small briefcase bag, the discussion activity has been raised where four main areas are taken into consideration.

Analysis of selecting value: for distinguishing among very similar products with the same range of level of importance, in this study, the importance level of a bag/container/storage is "Very high" or 4 (>3.0 - 4.0) scale – since this type of product is necessary for carrying, storing, or keeping some important stuffs for everyday life. Assigning intermediate points to the "level of importance" could be beneficial. Even if, there is a higher popularity and easy-to-use involved in applying "Design A – waterproof-insulated bag with a lightweight design that a briefcase-style – Design B. However, with the foldable material characteristic presented in Design A, users feel so worried about carrying electronic or digital items inside – since there are no supportive layers like a shock absorber provided. Thus, the importance level of Design A (3.7 from 5) should be less than the of Design B (4 from 5).

From customer perceptions, the bag, which contains a solid structure plus a zipper-locking system with a lightweight body, can produce the stuff inside safely and it is suitable for traveling. With proper sections or compartments provided inside the bag, some items are organized and easy to access and find a thing. Besides, shock-absorber material is provided, the users can bring digital gadgets or tablet everywhere they want and they can enjoy a work-and-travel platform.

However, the weight of a briefcase-style bag even the small one is around 1 kg. The users might feel fatigued carrying during the day.

Suggestions: however, this method could also be based on user preferences and the perspective of a design team. Using various methods such as user surveys or research articles – data analysis or optimization can support the way to make a decision.

Findings: for the conclusion of this phase, the researchers could obtain the guideline about assessing the ratio of the usefulness of these products as the usefulness of "Design A" (a waterproof-insulated bag): usefulness of "Design B" (A small briefcase bag) = 1: 1.22. This value can be applied to the trend of selling volume when the manufacturers would like to start creating or developing a new product. This can support the assumptions raised by a design team about the choice or reference bag that might fit to the customer's requirements. In this study, a briefcase-style bag with a small size is the proper choice, and its characteristics are interesting to be developed for supporting more activities in various conditions of the situation.

IV. Conclusion

In order to provide a proper design structure, Product Design and Development (PDD) with the assistance of finite element analysis (FEA) are applied. At the initial stage of this study, the customer perceptions and the market survey of a bag that is popular for women were considered and the obtained results could support the researchers for making the analysis of the market for a particular bag, which includes the investigation into customer feelings,expectations, and requirements. The durability, flexibility, universal design concept, easy-to-access, and easy-to-use function are the key points extracted from target customers. *For the conceptual design stage*, the researchers first started to reveal the hidden issues of the bag structures of waterproof-insulated and briefcase bags where a high percentage of usage (found from waterproof-insulated bags) may be inappropriate since only the price is the key to purchasing decisions.

For *assessment of the usefulness of a product*, distinguishing among very similar products with the same level of importance can be identified and studied by using the "usefulness (U)" formula. The guideline of this calculation can convey information about "identifying which design should be selected?" or "checking the reference style of the bag selected by designers is proper enough for supporting the design and development stage". However, the scale of importance of a product ranging from 0 to 5 will be assigned by the judgment of the researchers; that is quite subjective. Using various methods such as user surveys or research articles can support the way to make decisions. For *material selection and final design obtained*, "durable, flexible, portable, and

waterproof concepts are required as the key consideration. Therefore, ABS PC, Aluminum 1060 Alloy, Stainless Steel, Low-Density Polyethylene (LDPE), Rubber, and Stainless Steel are applied. The virtual model of the bag is provided with air ventilation (FAN) to maintain the original condition of the stuff inside the bag. The load-distribution simulation (FEA) is applied to that 3D model where the critical part was shown through the corner-slot area of the fan since it was not the flat surface for a whole frontal plate.

V. Contribution

Some designs of the bag can provide and serve as a decorated platform where the fashion accessory such as a colorful handle, strap, protective case (covering coat), or extraordinary handle-curve design is introduced. For self-defense purposes, the durability, stability, and force distributed on the front and back areas plus the handle of the bag are the key considerations, the applications of FEA can be used to support the ways to identify the proper material used. Moreover, the strength of structures of equal cross-sectional area loaded in tension is independent of the shape of the cross-section. The "tensile stress" is the key consideration where it is the stress state caused by an applied load that tends to elongate the material along the axis of the applied load, in other words, the stress caused by pulling the material.

VI. Recommendation

In order to develop a new design for work-and-travel bags based on customer needs, the conceptual design of the product should concern with dimension, shape, size, and material usage for the manufacturing process. Those factors have a strong positive correlation with the weight of the product. The Finite Element Analysis (FEA) technique has been applied in this study to determine the suitable material for a bag. However, the results obtained from this study are applied and suitable for being as one of the main guidelines and considerations for the manufacturers or customers to select the proper design and material for making a "fancy bag" with the simple-and-minimal design concept.

Acknowledgment

The authors would like to offer our gratitude to the School of Manufacturing Systems and Mechanical Engineering, Sirindhorn International Institute of Technology, Thammasat University. We really appreciate the provided instruments and greatly assisted to finish this paper.

Conflict of Interest

The authors of this publication declare there is no conflict of interest.

Funding Agency

This research received no specific grant from any funding agency in the public, commercial, or not-for-profit sectors.

References

[1] C. Xianglan, H. Yuanyuan, D. Yachao et. al., "Gender and Culture Differences in Consumers' Travel Behavior During the COVID-19 Pandemic," *Sustainability*, vol. 15, no. 2, Jan. 2023.

[2] S. Gössling, D. Scott, and C. M. Hall, "Pandemics, Tourism and Global Change: A Rapid Assessment of COVID-19," *Journal of Sustainable Tourism*, vol. 29, no.1, pp. 1-20, Apr. 2020.

[3] R. Rastegar, F. Higgins-Desbiolles, and L. Ruhanen, "COVID-19 and a Justice Framework to Guide Tourism Recovery," *Annals of Tourism Research*, vol. 91, no. 103161, Feb. 2021.

[4] R. Rastegar, S. Seyfi, and S. M. Rasoolimanesh, "How COVID-19 Case Fatality Rates Have Shaped Perceptions and Travel Intention?" *Journal of Hospitality and Tourism Management*, vol. 47, pp. 353-364. Jun. 2021.

[5] S. M. Rasoolimanesh, S. Seyfi, R. Rastegar et al. (2021, Sep.). Destination Image During the COVID-19 Pandemic and Future Travel Behavior: The Moderating Role of Past Experience. *Journal of Destination Marketing & Management*. [Online]. *21*, p. 100620. Available: https://doi.org/10.1016/j.jdmm.2021.100620

[6] Measuring Quality of Life. (2012, Mar. 1). *The World Health Organization Quality of Life (WHOQOL)*. [Online]. Available: https://bit.ly/3ZzeRDE

[7] P. Supsermpol, S. Olapiriyakul, and N. Chiadamrong, "Reverse Logistics Network Design for Infected Medical Waste Management in Epidemic Outbreaks Under Uncertainty: A Case Study of COVID-19 in Pathum Thani, Thailand," *International Scientific Journal of Engineering and Technology*, vol. 6, no. 2, pp. 66-82, Dec. 2022.

[8] P. Parthasarathy and S. Vivekanandan, "An Extensive Study on the COVID-19 Pandemic, an Emerging Global Crisis: Risks, Transmission, Impacts and Mitigation," *Journal of Infection and Public Health*, vol. 14, no. 2, pp. 249-259, Feb. 2021.

[9] S. Srivastava, T. Pareek, S. Sharma et al., "Determinants of Restaurant Experience During the on-Going Pandemic Scenario in India," *Journal of Foodservice Business Research*, vol. 26, no.2, pp 208-224, Apr. 2022.

[10] E. T. Njoya, "Assessing the Poverty Impact of the COVID-19-Induced Tourism Crisis in Tanzania: A Social Accounting Matrix Microsimulation Analysis," *Journal of Sustainable Tourism*, vol. 31, no.3, pp. 801-820, Jan. 2022.

[11] H. M. Hajiabadi, V. N. Hamed, and H. Hamideh, "COVID-19 and Tourism: Extracting Public Attitudes," *Current Issues in Tourism*, vol. 26, no. 4, pp. 547-553, Jul. 2022.

[12] M. Burke. (2021, Jul. 6). *Men vs Women Shopping Statistics, Behaviors & Other Trends*. [Online]. Available: https://bit.ly/3ZiIUQz

[13] A. Boyle. (2022, Dec. 19). *Men vs. Women: The Gender Divide of Car Buying.* [Online]. Available: https://bit.ly/3SZA47L

[14] Catalyst. (2020, Apr. 27). *Buying Power (Quick Take).* [Online]. Available: https://www.catalyst.org/research/buying-power/

[15] Businesswire. (2019, Aug. 2). *Global Handbags Market Report 2019-2024*. [Online]. Available: https://bwnews.pr/3ZvY8Sj

[16] M. Mark. (2014, Nov. 11). *Car Buying by Women Driven by Different Reasons Than Men.* [Online]. Available: https://bit.ly/3VrTQKy
[17] K. J. Parkin. (2017). *Women at the Wheel: A Century of Buying, Driving, and Fixing Cars. University of Pennsylvania Press.* [Online]. Available: https://bit.ly/41SGmtQ
[18] Shopee. (2022, Aug. 15). *Cosmetic Storage Box*. [Online]. Available: http://bitly.ws/BcYi
[19] C. G. Marcado and A. M. Krog. (2022, Dec. 20). *Lipstick Formulation and Method*. [Online]. https://patentimages.storage.googleapis.com/31/1a/bd/0548e3068a1d72/EP0195575A1.pdf
[20] Galmatic. (2007, Nov. 11). *Why You Shouldn't Keep Beauty Products in the Car.* [Online]. Available: https://www.galmatic.com/shouldnt-keep-beauty-products-car/
[21] S. M. Mawazi, N. A. B. A. Redzal, N. Othman et al., "Lipsticks History, Formulations, and Production: A Narrative Review," *Cosmetics*, vol. 9, no.1, p. 25, Jan. 2022.
[22] Laura. (2020, Jun. 17). *What is Lipstick Made of? A Visual Guide (Present, Past, & Future)*. [Online]. Available: https://makeupscholar.com/what-lipstick-made-of/
[23] S. Pan and N. Germann. (2019). "Thermal and Mechanical Properties of Industrial Benchmark Lipstick Prototypes," *Thermochimica Acta*, vol. 679, no. 178332, Sep. 2019.
[24] J. S. M. Belisario, J. Jamsek, K. Huckvale et al., (2015). Comparison of Self-Administered Survey Questionnaire Responses Collected Using Mobile Apps Versus Other Methods. *Cochrane Database of Systematic Reviews*, no. 7. Jul. 2015.
[25] N. Malleson and M. A. Andresen, "The Impact of Using Social Media Data in Crime Rate Calculations: Shifting Hot Spots and Changing Spatial Patterns," *Cartography and Geographic Information Science*, vol. 42, no. 2, pp. 112-121, 2015.
[26] S. Aghababaei and M. Makrehchi, "Mining Social Media Content for Crime Prediction" in *Proc. 2016 IEEE/WIC/ACM International Conference on Web Intelligence (WI)*, 2016, pp. 526-531.
[27] G. Dina. (2015, Jan. 8). *How People Buy and Sell Illegal Stuff*. [Online]. Available: https://cnb.cx/3Ln7iwj
[28] H. T. Milhorn. (2007). *Cybercrime: How to Avoid Becoming a Victim*. California, U.S.A.: Universal-Publishers, 2007, pp. 1-324.
[29] S. He, Y. He, and M. Li, "*Classification of Illegal Activities on the Dark Web*," in *Proc. the 2nd International Conference on Information Science and Systems*, 2019, pp. 73-78.
[30] S. Bakshi, "Impact of Gender on Consumer Purchase Behaviour," *Journal of Research in Commerce and Management*, vol. 1, no. 9, pp. 1-8, Aug. 2012.
[31] M. Barletta, "*Marketing to Women*. Chicago: Dearborn Trade, 2003, pp. 1-253.
[32] R. T. Green and I.C. Cunningham, "Feminine Role Perception and Family Purchasing Decisions," *Journal of Marketing Research*," vol. 12, no. 3, pp. 325-332, 1975.
[33] L. Irigaray. *The Logic of the Gift*. Routledge: New York, 1997, pp.174-189.
[34] AliExpress. (2022, Dec. 10). *Waterproof-Cooler Food Storage (Thermo-Bag Style) for Supporting Outdoor Activity with Insulated Pouch Accessories Item*. [Online]. Available: http://bitly.ws/BfBW
[35] TUMI. (2022, Dec. 25). *Universal Wheel Briefcase - Business Briefcase*. [Online]. Available: http://bitly.ws/BfD3
[36] M. Alisha and G. Elina. (2022, Jun. 21). *Airline and TSA Carry-On Luggage Size Restrictions.* [Online]. Available: http://bitly.ws/BfDK
[37] My Baggage. (2023, Feb. 14). *British Airways 2023 Baggage Allowance*. [Online]. Available: http://bitly.ws/BfEa
[38] J. M. Morse. (2000), "Determining Sample Size," *Qualitative Health Research*, vol. 10, no. 1, pp. 3-5.
[39] V. A. Zeithaml, A. Parasuraman, and L. L. Berry, *Delivering Quality Service: Balancing Customer Perceptions and Expectations*. New York: Simon and Schuster, 1990.
[40] S. R. Jaeger, A. V. Cardello, and H. G. Schutz, "Emotion Questionnaires: A Consumer-Centric Perspective," *Food Quality and Preference*, vol. 30, no. 2, pp. 229-241, Dec. 2023.
[41] G. D. Israel, "Determining Sample Size. Qualitative Health Research," *Sage Journal*, vol. 10, no. 1, pp. 1-5, Jan. 2000.
[42] D. Iacobucci, "Structural Equations Modeling: Fit Indices, Sample Size, and Advanced Topics," *Journal of Consumer Psychology*, vol. 20, no. 1, pp. 90-98. Jan. 2010.
[43] S. Jordan. (2023, March 4). *Average Salary in Thailand: What's a Good Monthly Wage?* [Online]. Available: http://bitly.ws/BfQB
[44] S. Rianmora and S. Seng, "Keep it Cool Smart Bag by Internet of Thing (IoT) for Better Living with Alternative Design," *International Scientific Journal of Engineering and Technology*, vol. 5, no. 2, pp. 38-54, Dec. 2021.
[45] S. Popovics. (1992). *Concrete Materials: Properties, Specifications, and Testing.* New York: William Andrew, 1992, p. 661.
[46] G. Emily. (2022, Nov. 27). *If Your Zipper Says YKK, this is What it Means.* [Online]. Available: https://www.rd.com/article/zippers-letters-ykk/
[47] R. Gilmore. (2023, Jan. 14). *10 Best Portable Chargers & Power Banks.* [Online]. Available: https://bit.ly/3IMWZyq
[48] A. Walloga. (2015, Sep. 11). *14 Things Every Modern Woman Should Carry in Her Purse.* [Online]. Available: https://bit.ly/3y1mxDb
[49] Apple.com. (2020, Jan. 11). *AirPods (2nd Generation).* [Online]. Available: https://www.apple.com/airpods-2nd-generation/specs/
[50] Product Weight. (2020, Jan. 11). *Ideal to Note Down Your Weight Loss Progress, Ideal as Gift for Birthday or Christmas (German Edition).* [Online]. Available: https://amzn.to/3kNNFlQ
[51] B. Cohen. (2022, Dec. 4). *How Much Does a Smartphone Weigh?* [Online]. Available: https://bit.ly/3YdM46G
[52] Skolko-Vesit. (2023, Jan. 15). *How Much Does a Nail File Weigh?* [Online]. Available: https://bit.ly/3mnK4vd
[53] Liberty Leather Goods. (2023). *A Handy Guide to Leather Thickness & Weigh-With a Chart.* [Online]. Available: https://bit.ly/3EMpStC
[54] Skolko-Vesit. (2023, Jan. 15). *How Much Does It Weigh?* [Online]. Available: https://bit.ly/3IMtlJw
[55] Himalaya. (2023, Feb. 14). *Item-Weight of Himalaya Pure Hands Hand Sanitizer, 100 ml.* [Online]. Available: https://amzn.to/3meA5bD
[56] Roccer. (2023, Feb. 14). *Item-Weight of Disposable Face Mask With 3 Layers Protection (50 pcs)*. [Online]. Available: https://amzn.to/3SXtC1j
[57] Elixery. (2017, Jun 8). *Do You Really Eat Four Pounds of Lipstick in Your Lifetime?* [Online]. Available: https://bit.ly/3m84Xuj
[58] Neutrogena. (2023, Feb. 14). *Neutrogena, Ultra Sheer Dry Touch Sunscreen, SPF 55, 3 fl oz (88 ml)*. [Online]. Available: https://bit.ly/3ZtG0Ia
[59] CeraVe. (2023). *Light-Weight Face Lotion with Hyaluronic Acid and Fragrance Free.* [Online]. Available: https://amzn.to/3Fds91d
[60] Johnson's Baby. (2017, May 10). *Johnson's Baby Disposable Hand & Face Cleansing Wipes, Pre-Moistened Wipes Gently Remove 99% of Germs & Dirt from Delicate Skin, Paraben-, Phthalate- & Alcohol-Free, Hypoallergenic, 25 ct.* [Online]. Available: https://amzn.to/3SMsJsk
[61] S. Sasidaran, P. Kachoria, A. Raj et al., "Physical Properties of Menstrual Hygiene Waste as Feedstock for Onsite Disposal Technologies," *Journal of Water, Sanitation and Hygiene for Development*," vol.11, no.3, pp. 474-482, May. 2021.
[62] AdotecGear. (2023, Feb. 14). *Wide-Floor Zipper Pouch*. [Online]. Available: https://bit.ly/3ZBZ7Qz
[63] A. van Leeuwen. (2013, Mar. 4). *Shopping Bag Quantity Assumptions*. [Online]. Available: https://bit.ly/3mkABVG

[64] Hugs. (2023, Feb. 14). *Hugs Mint Chewing Gum Mint Flavour.* [Online]. Available: https://amzn.to/3yaJZ0w
[65] Amazon.Com. (2023, Feb. 14). *Item Volume of Travel Size Spray Bottle – 88mL (3 Ounce).* [Online]. Available: https://amzn.to/3KPThXq
[66] Walgreens. (2023). *Barrettes & Hair Clips-Hair Brushes & Accessories.* [Online]. Available: https://bit.ly/3J6Z4GV
[67] VrHere MirriM. (2023, Feb. 14). *Makeup Pocket Mirror with 10x Magnification Glass Plus Plain Mirror.* [Online]. Available: https://amzn.to/3ZC3KtV
[68] Beauty, Dream Life. (2017, Apr. 3). *A Look at the Weight of Our Makeup: Travel Tips for Women*. [Online]. Available: https://bit.ly/3Y9X5pH
[69] Inkbeta. (2022, Apr. 19). *Much Does a Pen Weigh in Grams?* [Online]. Available: https://bit.ly/3mmshVb
[70] D. Munk. (2020). *How Many A4 Sheets Does it Take to Make 1 kg?* [Online]. Available: https://bit.ly/3KQgby7
[71] M. Otsuka, Y. Akizuki, K. Otsuka et al., (2007). "A Comparison of the Technical Quality of American and Japanese Ranitidine Tablets," *Dissolution Technologies*. vol. 14, pp. 22-28, Aug. 2007.
[72] Sean. (2022, Nov. 21). *Blister Pack or Bottle? How to Choose Drug Packaging.* [Online]. Available: https://bit.ly/3ZnbtfK
[73] Band-Aid. (2023, Apr. 19). *Band-Aid, Tru-Stay, Adhesive Bandages, Plastic Strips, 60 Bandages.* [Online]. Available: https://bit.ly/3IDKGV8
[74] Koalaeye. (2021, Mar. 25). *How Much Do Sunglasses Weigh?* [Online]. Available: https://bit.ly/3EMLs16
[75] Baooyoweily. (2023, Apr. 20). *Leather Glasses Case.* [Online]. Available: https://bit.ly/3IHJX5u
[76] Generic. (2023, Jan, 22). *Leather Card Wallet.* [Online]. Available: https://bit.ly/3ZBCU5c
[77] Velyrhorde. (2022, May 8). *How Many Grams Does a Key Weigh?* [Online]. Available: https://amzn.to/3Yg1U0F
[78] Faroutguides. (2023, Feb. 19). *The Ideal Sewing Kit for Your Thru-Hike.* [Online]. Available: https://bit.ly/3YkcnrH
[79] MUJI. (2022, May 8). *Light-Weight All Weather Foldable Umbrella.* [Online]. Available: https://muji.lu/3EPOcdS
[80] Milk Chocolate Nougat Bar. (2023, Feb. 14). [Online]. Available: https://bit.ly/3kJfsUM
[81] N. Allam. (2022, May. 22). *17 Things Every Woman Should Have in Her Bag*. [Online]. Available: https://bit.ly/3ZDhlBf
[82] A. Walloga. (2022, May. 22). *14 Things Every Modern Woman Should Carry in Her Purse*. [Online]. Available: https://bit.ly/3y1mxDb
[83] S. Stroitelev. (2022, May. 22). *Photos of the Fascinating Things Women Keep in Their Bags*. [Online]. Available: https://bit.ly/3ybKQhv
[84] Admin Zatchels. (2021, Mar. 2). *10 Handbag Essentials Every Woman Should Carry in 2021*. [Online]. Available: [Online]. Available: https://bit.ly/3ER1YgB
[85] G. Nilakshi. (2021, Sep. 6). *21 Things Every Woman should Carry in Her Handbag*. https://bit.ly/3kzcNwV
[86] B. Stafferton. (2022, Jan. 28). *10 Handbag Essentials Every Woman Should Have in 2022*. [Online]. Available: https://bit.ly/3y3WVFt
[87] L. D. Almeida. (2022, Dec. 19). *Top 5 Travel Purses for Women Exploring the World in 2023*. [Online]. Available: https://www.pilotplans.com/blog/travel-purses
[88] H. W. Mackie, J. M. Stevenson, S. A. Reid et al., "The Effect of Simulated School Load Carriage Configurations on Shoulder Strap Tension Forces and Shoulder Interface Pressure," *Applied Ergonomics*, vol. 36, no. 2, pp. 199-206, Mar. 2005.
[89] M. Holewijn, "Physiological Strain Due to Load Carrying," *European Journal of Applied Physiology and Occupational Physiology*, vol. 61, pp. 237-245, Oct. 1990.
[90] J. J. Vacheron, G. Poumarat, R. Chandezon et al., "The Effect of Loads Carried on The Shoulders," *Military Medicine*, vol. 164, no. 8, pp. 597-599. Aug. 1999.
[91] T. J. Hughes, *The Finite Element Method: Linear Static and Dynamic Finite Element Analysis*. Massachusetts: U.S.A: Courier Corporation, 2012, p. 704.
[92] L. J. Segerlind. (1991). *Applied Finite Element Analysis*. New Jersey, U.S.A.: John Wiley & Sons, 1985, pp. 1-448.
[93] Solidworks. (2022, Jan. 28). *Solidworks Materials Web Portal.* [Online]. Available: Matereality.com: https://bit.ly/3rKdqRG
[94] G. Zhao, H. Wang, L. Wang et al., "The Biomechanical Effects of Different Bag-Carrying Styles on Lumbar Spine and Paraspinal Muscles: A Combined Musculoskeletal and Finite Element Study," *Journal of Orthopaedic Surgery*, vol. 15, no. 1, Jan. 2023.
[95] L. Gómez , C. A. Díaz, G. A. Orozco et al., "Dynamic Analysis of Forces in the Lumbar Spine During Bag Carrying," *International Journal of Occupational Safety and Ergonomics*, vol. 24, no. 4, pp. 605-613, Sep. 2017.
[96] B. Szabó and I. Babuška (2021). *Finite Element Analysis: Method*. New Jersey: Wiley & Sons, 2021, pp. 1-357.
[97] S. Rianmora and K. Poulpanich, "Concept Development in a Walking Assistive Device: Offset Handle With a Small Base Area," *International Journal of Knowledge and Systems Science*, vol.13, no.1, pp. 1-39. Sep. 2022.
[98] P. Sarkar and A. Chakrabarti, "Assessing Design Creativity," *Design Studies*, vol. 32, no. 4, pp. 348-383, Jul. 2011.
[99] S. McLeod, "Maslow's Hierarchy of Needs," *Simply Psychology*," vol. 1, pp. 1-18, Apr. 2007.

Suchada Rianmora is a lecturer in School of Manufacturing Systems and Mechanical Engineering, Sirindhorn International Institute of Technology, Thammasat University, Thailand. She received her D. Eng from Asian Institute of Technology, Thailand. Her research interests are reverse engineering, rapid prototyping, design and development, and manufacturing processes.

Thorfan Netkueakun received her Bachelor of Technology in Industrial Engineering Program from School of Manufacturing Systems and Mechanical Engineering, Sirindhorn International Institute of Technology, Thammasat University, Thailand. Nowadays, is a full time Master degree student in Logistics Supply Chain System Engineering at the same school. Her research interests are product design and development, and manufacturing processes, supply chain and marketing strategy.

Nutthamon Samorhom is a received her Bachelor of Technology in Industrial Engineering Program from from School of Manufacturing Systems and Mechanical Engineering, Sirindhorn International Institute of Technology, Thammasat University, Thailand. Currently, she is research assistant. Her research interests are reverse engineering, rapid prototyping, manufacturing process design, and instrument process and control.

Study of Effects of Inlet Wind Velocity and Direction on Airflow around the Buildings Using CFD Turbulence Models: A Case Study of Rajamangala University of Technology Rattanakosin (Salaya Campus), Thailand

Jirapol Klinbun[1], Tipapon Khamdaeng[2], and Numpon Panyoyai[3]

[1]Department of Mechanical Engineering, Faculty of Engineering, Rajamangala University of Technology Rattanakosin Salaya Campus, Nakhon Pathom, Thailand
[2,3]Faculty of Engineering and Agro-Industry, Maejo University, San Sai, Chiang Mai, Thailand
E-mail: jirapol9@hotmail.com, tipapon@mju.ac.th, numpon@mju.ac.th

Received: Feb 8, 2022 / Revised: March 21, 2022 / Accepted: April 18, 2022

***Abstract*—This research investigates of the effects of inlet wind velocity and inlet wind direction on airflow around the buildings of Rajamangala University of Technology Rattanakosin (Salaya), Thailand using Computational Fluid Dynamics (CFD) turbulence models. The evaluation of a CFD model's performance and validation of its predictions with high-quality experimental data is necessary before the model is used in practice. In this study, there are 2 Models. Model 1 is the simulation for an inlet wind velocity of 0.5 and 1.5 m/s in the west direction. Model 2 is the simulation for an inlet wind velocity of 0.5 and 1.5 m/s in the south direction. The results were found that the higher inlet wind speeds at the inlet flow boundary would lead to a higher increase in the average speed of air around the building. In addition, the combined wind speed and inlet flow direction were affected to where the maximum wind speed occurs. The data obtained from this study will serve as a future basis for the construction of buildings in the university to provide better natural ventilation.**

***Index Terms*—Airflow, Numerical Model, Wind Speed, Wind Direction**

I. Introduction

The university land area which is consisting of a lecture building, operating buildings, offices, stadiums, libraries, etc. They should have open spaces for outdoor activities, and the area should also be good air ventilation. Surrounding infrastructure and buildings play an important role in the airflow around the buildings. In addition, controlling the direction of air and the speed of air flowing into the building and the living space surrounding the building provides a consistent wind speed and is suitable for activities in that part of the area [1]- [3]. Current analysis of airflow dynamics surrounding the building has become an integral part of the planning of the project or construction. This is because the energy of the airflow is an important factor that contributes to thermal comfort both indoors and outdoors [4]-[7]. The study of airflow around the building simulation is a new matter to help in this area. It can be performed in two ways: (a) physical model and (b) computer simulation. By the way, the computer simulation will yield faster results and a lower budget than the actual building model. However, the right choice and compromise between the accuracy and cost associated with modeling wind flow around buildings is essential in meeting practical engineering needs. The airflow around buildings has been studied for several purposes, such as (a) determination of wind surface pressure distribution on building envelopes, (b) turbulent dispersion of airborne contaminants, and (c) pedestrian comfort. There are three widely used numerical approaches for analyzing outdoor turbulent flow using Computational Fluid Dynamics (CFD) based on Reynolds Averaged Navier-Stokes (RANS) equation, Large Eddy Simulation (LES), and Direct Numerical Simulation (DNS) [8]-[10]. Many previous researchers have studied the flow around a single building (bluff body) or multiple buildings [7], [11]-[15]. The literature review revealed that there are limited studies available for intermediate cases, in which the buildings are close enough and the flow around the building is strongly affected by adjacent buildings.

The main objective of the present study is to provide a faster, yet reliable and simple modeling tool for simulations of outdoor airflow around multiple buildings. The intent is to improve the 2D k-ε turbulence models mainly developed and used for modeling airflow in indoor environments. The measurement airflow around the building at the Rajamangala University of Technology Rattanakosin (Salaya campus) has been

carried out to provide the base for input data in the simulation. Then, the effects of inlet wind velocity and direction on airflow around the buildings were obtained.

II. Material and Methods

The Rajamangala University of Technology Rattanakosin (Salaya campus) has been selected for investigation of the airflow around the buildings. There are 25 buildings in the area, as seen in Fig.1. In order to fit the model with the similarity analysis of incoming flow, modeled buildings have been scaled to a 1:100 ratio.

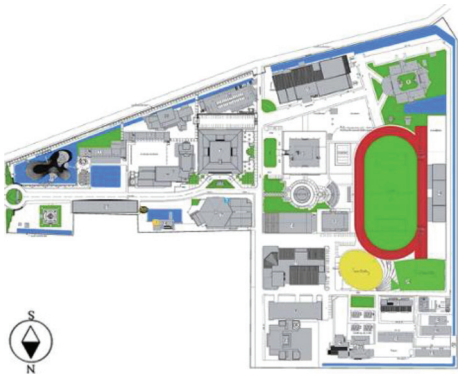

(a)

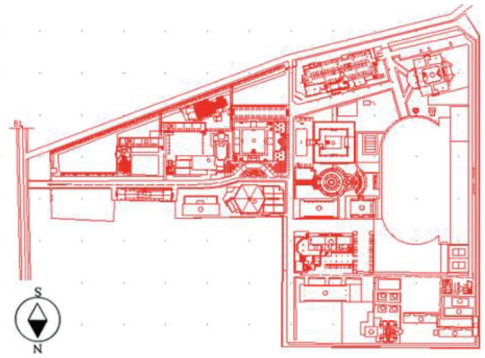

(b)

Fig. 1. Modeled buildings in area of the Rajamangala University of Technology Rattanakosin (Salaya campus) (Ref. https://building.rmutr.ac.th)

A. Numerical Models

For a systematic study of the effects of wind inlet direction and wind speed on airflow, the application of computational fluid dynamics offers considerable advantages over field measurements and wind-tunnel experiments [16]. However, a main disadvantage of CFD is that it can be computationally expensive when increasing the resolution of the computational mesh and/or the size of the computational domain [17]. From Fig. 1, a model is drawn to calculate the airflow around the building as seen in Fig. 2.

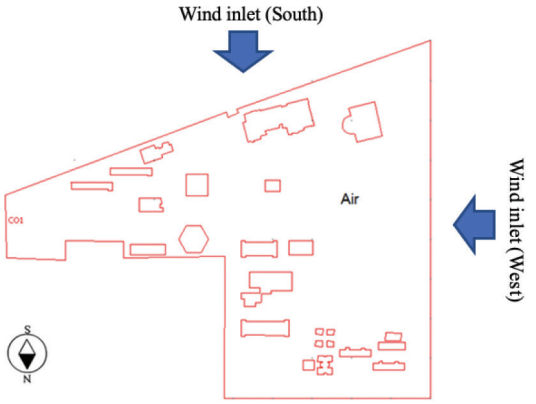

Fig. 2. Calculation domain

In this study, a numerical model is developed using COMSOL Multiphysics (Version 4.4), which is CFD software. The details of the numerical model including governing equations, turbulence modeling, boundary conditions, and initial condition are presented on the following topics.

Assumption: (a) Flow field is two-dimensional and steady. (b) All thermal properties are constant. (c) Air is an incompressible fluid.

Continuous equation [18]:

$$\nabla \cdot U = 0 \tag{1}$$

Navier–Stokes equations [18]:

$$\rho U \cdot \nabla U = \nabla \cdot \left[\left(\eta + \rho \frac{c_\mu k^2}{\sigma_k \varepsilon} \right) \cdot \left((\nabla U) + (\nabla U)^T \right) \right] - \nabla P \tag{2}$$

Where ρ is the fluid density [kg/m^3], U is the average velocity [m/s], η is dynamics with a viscosity [Ns/m^2] P is pressure [Pa], k is the kinetic energy of turbulence [m^2/s^2], ε is the diffusion rate of the kinetic energy of the turbulence [m^2/s^3].

The k-ε turbulence model:

$$\rho U \cdot \nabla k = \nabla \cdot \left[\left(\eta + \rho C_\mu \frac{k^2}{\varepsilon} \right) \nabla k \right] + \frac{1}{2} \rho C_\mu \frac{k^2}{\varepsilon} \left((\nabla U) + (\nabla U)^T \right)^2 - \rho \varepsilon \tag{3}$$

The equation can be distributed as follows:

$$\rho U \cdot \nabla \varepsilon = \nabla \cdot \left[\left(\eta + \rho C_\mu \frac{k^2}{\varepsilon} \right) \nabla \varepsilon \right] + \frac{1}{2} \rho C_{\varepsilon 1} k \left((\nabla U) + (\nabla U)^T \right)^2 - \rho C_{\varepsilon 2} \frac{\varepsilon^2}{k} \tag{4}$$

Where σ_k = 1.00, σ_ε = 1.30, $C_{\varepsilon 1}$ = 1.44, $C_{\varepsilon 2}$ = 1.92, C_μ = 0.09 are the standard values proposed by Spalding and Launder [19].

B. Boundary and Initial Conditions

All calculation setting is shown in Table I.

TABLE I
CALCULATION CONDITIONS

Inlet: $u=u_{input}$ m/s v=0.0 m/s $u=u_0$ $k=(3I_T^2/2)(u_0\cdot u_0)$, $\varepsilon=C_\mu^{0.75}\left((3I_T^2/2)(u_0\cdot u_0)\right)^{1.5}/L_T$
Outlet: P=0 Pa $\rho=\rho_0$ $n\cdot\nabla k=0, n\cdot\nabla\varepsilon=0$
Side wall: $n\cdot u=0$, $\left[(\eta+\eta_T)\left(\nabla u+(\nabla u)^T\right)\right]n=\left[\rho C_\mu^{0.25}k^{0.5}/\left(\ln(\delta_w^+)/K+C^+\right)\right]u$ $n\cdot\nabla k=0$, $\varepsilon=C_\mu^{0.75}k^{1.5}/(K\delta_w)$, where $\delta_w^+=\delta_w\rho C_\mu^{0.25}k^{0.5}/\eta$

For the inlet velocity (u_{input}), rotary vane anemometry is well-known as a measurement technique with good spatial and time resolution and has been established as a reliable and versatile technique for velocity measurements in flow fields with low to moderate turbulence intensities. Fig. 3 is shown the Testo 435 rotary vane anemometer which is an accuracy of ±0.3 °C. From the measurements, all the data are collected as preliminary data to simulate airflow.

Fig. 3. Rotary vane anemometer (Testo Model 435)

C. Numerical Methodology

The CFD simulation setup provides a summary of the computational domain description used in the analysis along with the grid distribution, boundary condition settings, and numerical scheme [20], [21]. A grid sensitivity test was conducted to ensure the computational accuracy of the simulations with COMSOL™ Multiphysics. As shown in Fig. 4, a structured grid is deployed to discretize the computational domain for COMSOL simulation. Two-dimensional structured mesh along with the finite element method were utilized to discretize the computational domain and to describe the mass and momentum transport for each cell. There are 167,728 elements in the calculation domain.

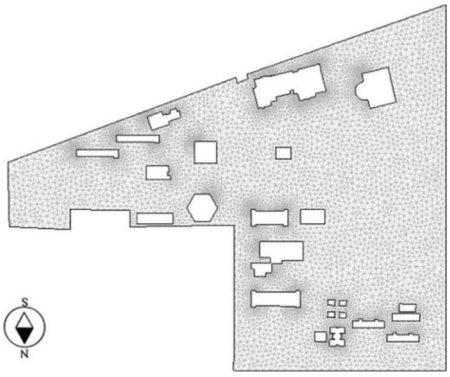

Fig. 4. Mesh generation

Fig.5 Shows the process of CFD simulation.

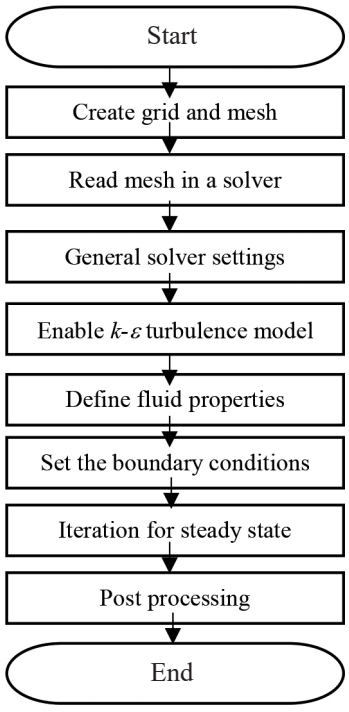

Fig. 5. Solution procedure for CFD model

III. Result and Discussion

The effects of inlet wind velocity and inlet wind direction on airflow patterns around the building in the Rajamangala University of Technology Rattanakosin (Salaya campus) are investigated using Computational Fluid Dynamics techniques. Fig.6 is shown the position and name of the building in the area.

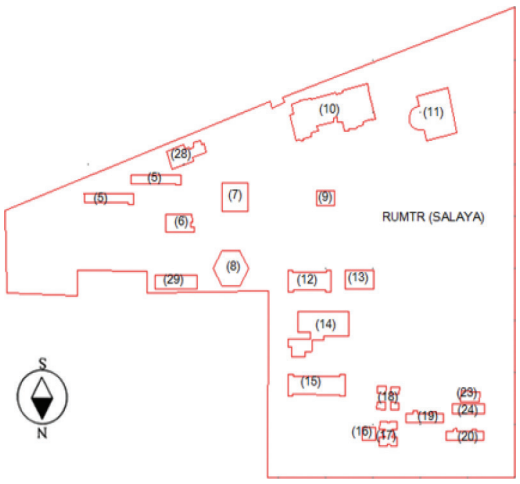

Fig. 6. The building location and name in the area of the Rajamangala University of Technology Rattanakosin (Salaya campus)

Where the buildings name according to Fig. 6 are as following:
(5) Building 1 and Building 2, Academic Promotion and Registration Office
(6) Faculty of Business Administration Building
(7) Office of the President
(8) Canteen
(9) Office of Service Science and Information Technology
(10) Sirindhorn Building
(11) Building for the 6th anniversary of the Royal Patronage
(12) Meeting room 1,500 seats
(13) Physical Education Building
(14) Faculty of Engineering Building
(15) Product design work building
(16) Office of training dormitory
(17) Training dormitory
(18) Directorate of Director General, 4 buildings
(19) Government Residential Building 1 (4 floors)
(20) Government Residential Building 2 (4 floors)
(23) House, building, location
(24) Operating Building, Premises

A. Model 1: Inlet Wind Velocity of 0.5 m/s and 1.5 m/s, Inlet Wind Direction in the West.

Fig.7 is shown the simulated air velocity pattern of model 1. The air inlet is from west (behind at university) to east (in front of the university) horizontal flow at speeds of 0.5 and 1.5 m/s respectively. Both cases (velocity 0.5 and 1.5 m/s) are based on the same airflow profiles around the buildings. The results show that when the airflow through and/or hits buildings, it affects the speed and pattern of the velocity. However, the rate of change increases with increasing inlet wind speed. From Fig. 7, the area in front of the canteen is the magnitude of velocity maximum. This is because the venturi effect causes the airflow to speed up. The high air speed is causing dust dispersion.

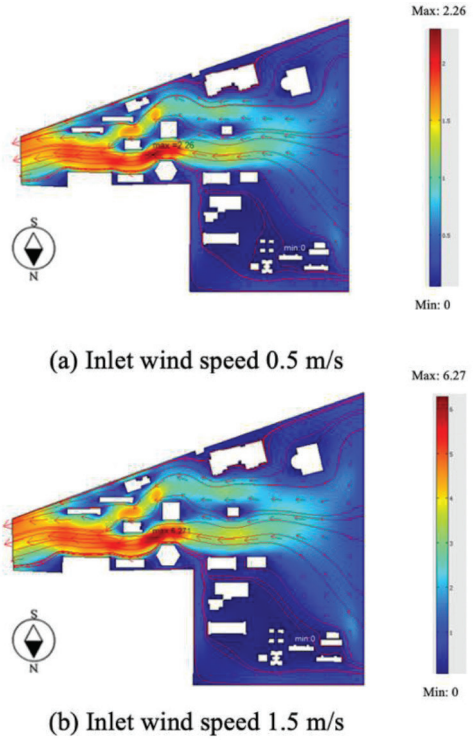

Fig. 7. The velocity profile around the building, the wind direction in the west

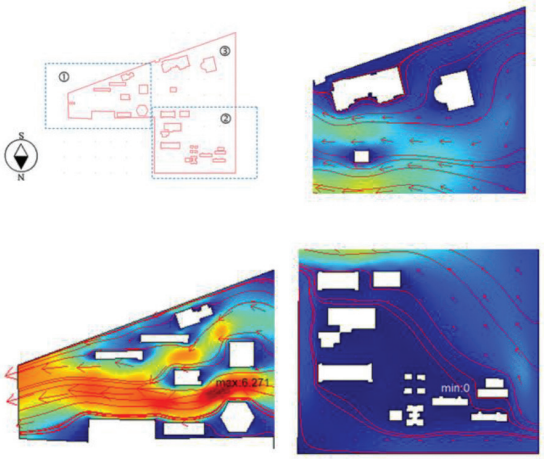

Fig. 8. The velocity profile around the building in each section, at an inlet wind speed of 1.5 m/s from west to east

Fig. 8 is shown the velocity profile in each section at a wind speed of 1.5 m/s from west to east. It is found that the comfort area (velocity about 1.0-2.0 m/s) occurs at the Office of Service Science and Information Technology. While airflow around the Government Residential Building 1 (No. 19) is the

low velocity (occurring negative pressure) because there are many buildings in the area. The air velocity is less than 0.25 m/s.

B. Model 2: Inlet Wind Velocity of 1.5 m/s, Inlet Wind Direction in the South.

Based on the results of the CFD simulation, Fig. 9 is shown the velocity profile around the building, wind speed of 1.5 m/s, and the wind direction from south to north. It is found that the magnitude of velocity occurs between 1.5-2.0 m/s. The location of buildings No. 20, 23, and 24 with a wind speed of about 2.0-2.5 m/s, and air velocity is quite suitable to designate as a rest area. It is observed that the velocity of the air increases as it flows through the openings between the buildings.

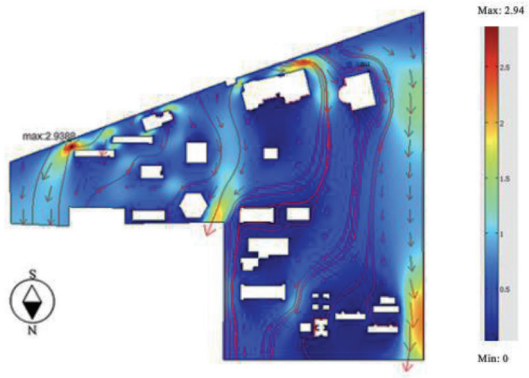

Fig. 9 The velocity profile around the building, the wind direction in the south

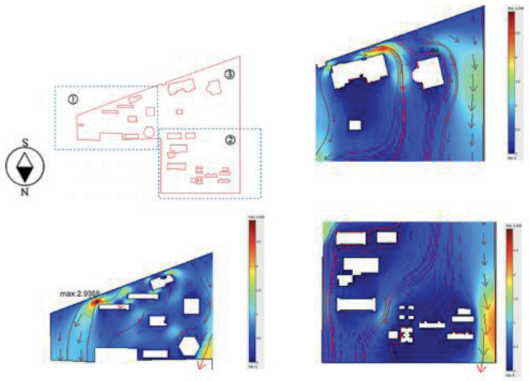

Fig.10. The velocity profile around the building in each section, at an inlet wind speed of 1.5 m/s from south to north

Fig. 10 is shown the velocity profile in each section at a wind speed of 1.5 m/s from south to north. It was found that the air velocity was about 2.9 m/s in the area behind Building 1 and Building 2 (No.5), which are the Academic Promotion and Registration Office, respectively. This is because of air hitting the buildings. While the negative pressure area occurs at the back of the 6th cycle of the King's Birthday (No. 11).

IV. Conclusions

This research was to study a numerical study of airflow around the building area of Rajamangala University of Technology Rattanakosin (Salaya) to increase the knowledge and understanding of the behavior of airflow around the building where the airflow enters in different directions.

The research begins with studying the basic knowledge of airflow, such as turbulent flow by using computational fluid dynamics. Then, a combination of the knowledge of numerical methodology including knowledge of airflow through various shapes and information on the fluid properties are used in the calculation. Finally, the nature of the airflow, when the wind blows in different directions and changes the speed is studied. The results of the research are shown for two models. For model 1, the comfort zone occurs around the Bureau of Science, Service, and Information Technology building (No. 9) with wind speeds of 1-2 m/s from west to east. For model 2, the comfort zone occurs around the Residential Building (No.20, 23, 24) These results are to obtain basic information about airflow and is the basis for the development of future mathematical models. This research is used as a tool for decision-making in building layout design within the area of Rajamangala University of Technology Rattanakosin (Salaya campus) in terms of energy saving.

V. Suggestion and Recommendation

For the next research, the models should analyze heat transfer and consider it three-dimensional to get results that are closer to the real phenomena.

The comparison magnitude of velocity between the simulation and experimental results should be carried out.

Acknowledgment

This research was conducted with the support of Rajamangala University of Technology Rattanakosin and research funding from the Thai national budget (A11/2560).

References

[1] E. Trepci, P. Maghelal, and E. Azar, "Urban Built Context as a Passive Cooling Strategy for Buildings in a Hot Climate," *Energy and Buildings*, vol. 231, p. 110606, Jan. 2021.

[2] N. Ba Chien, N. Viet Dung, T. Quoc Dung et al., "CFD Simulation of Multi-Outdoor Unit Configuration Design for a Building," *IOP Conference Series: Earth and Environmental Science*, vol. 505, no. 1, p. 12007, Jul. 2020.

[3] A. Izadi, M. Rudd, and V. M. Patrick, "The Way the Wind Blows: Direction of Airflow Energizes Consumers and Fuels Creative Engagement," *Journal of Retailing*, vol. 95, pp. 143-157, Sep. 2019.

[4] Q. Yi, M. Konig, D. Jank et al., "Wind Tunnel Investigations of Sidewall Opening Effects on Indoor Airflows of a Cross-Ventilated Dairy Building," *Energy and Buildings*, vol. 175, pp. 163-172, Jul. 2018.

[5] X. Zhang, A. U. Weerasuriya, and K. T. Tse, "CFD Simulation of Natural Ventilation of a Generic Building in Various Incident Wind Directions: Comparison of Turbulence Modeling, Evaluation Methods, and Ventilation Mechanisms," *Energy and Buildings*, vol. 229, p. 110516, Dec. 2020.
[6] G. K. Ntinas, X. Shen, Y. Wang et al., "Evaluation of CFD Turbulence Models for Simulating External Airflow Around Varied Building Roof with Wind Tunnel Experiment," *Building Simulation*, vol. 11, no. 1, pp. 115-123, Apr. 2018.
[7] W. Zuo and Q. Chen, "Real-Time or Faster-Than-Real-Time Simulation of Airflow in Buildings," *Indoor Air*, vol. 19, no. 1, pp. 33-44, Feb. 2009.
[8] F. Ascione, R. F. de Masi, M. Mastellone et al., "The Design of Safe Classrooms of Educational Buildings for Facing Contagions and Transmission of Diseases: A Novel Approach Combining Audits, Calibrated Energy Models, Building Performance (BPS) and Computational Fluid Dynamic (CFD) Simulations," *Energy and Buildings*, vol. 230, p. 110533, Jan. 2021.
[9] J. K. Calautit, D. O'Connor, P. W. Tien et al., "Development of a Natural Ventilation Windcatcher with Passive Heat Recovery Wheel for Mild-Cold Climates: CFD and Experimental Analysis," *Renewable Energy*, vol. 160, pp. 465-482, Nov. 2020.
[10] M. M. Hefny and R. Ooka, "Influence of Cell Geometry and Mesh Resolution on Large Eddy Simulation Predictions of Flow Around a Single Building," *Building Simulation*, vol. 1, no. 3, pp. 251-260, Sep. 2008.
[11] R. Ramponi and B. Blocken, "CFD Simulation of Cross-Ventilation for a Generic Isolated Building: Impact of Computational Parameters," *Building and Environment*, vol. 53, pp. 34-48, Jul. 2012.
[12] K. H. Cheong, Y. H. Teo, J. M. Koh et al., "A Simulation-Aided Approach in Improving Thermal-Visual Comfort and Power Efficiency in Buildings," *Journal of Building Engineering*, vol. 27, p. 100936, Jan. 2020.
[13] X. Tong, S. W. Hong, and L. Zhao, "CFD Modeling of Airflow, Thermal Environment, and Ammonia Concentration Distribution in a Commercial Manure-Belt Layer House with Mixed Ventilation Systems," *Computers and Electronics in Agriculture*, vol. 162, pp. 281-299, Jul. 2019.
[14] M. F. Yassin, "Numerical Study of Flow and Gas Diffusion in the Near-Wake Behind an Isolated Building," *Advances in Atmospheric Sciences*, vol. 26, no. 6, pp. 1241-1252, Nov. 2009.
[15] M. Ning, S. Mengjie, C. Mingyin et al., "Computational Fluid Dynamics (CFD) Modelling of Air Flow Field, Mean Age of Air and CO_2 Distributions Inside a Bedroom with Different Heights of Conditioned Air Supply Outlet," *Applied Energy*, vol. 164, pp. 906-915, Feb. 2016.
[16] M. S. Al-Homoud, "Computer-Aided Building Energy Analysis Techniques," *Building and Environment*, vol. 36, no. 4, pp. 421-433, May. 2001.
[17] Q. Cheng, H. Li, L. Rong et al., "Using CFD to Assess the Influence of Ceiling Deflector Design on Airflow Distribution In the Hen House with Tunnel Ventilation," *Computers and Electronics in Agriculture*, vol. 151, pp. 165-174, Aug. 2018.
[18] C. Porras-Amores, F. R. Mazarrón, I. Cañas et al., "Natural Ventilation Analysis in an Underground Construction: CFD Simulation and Experimental Validation," *Tunnelling and Underground Space Technology*, vol. 90, pp. 162-173, Aug. 2019.
[19] B. E. Launder and D. B. Spalding, "The Numerical Computation of Turbulent Flows," *Computer Methods in Applied Mechanics and Engineering*, vol. 3, no. 2, pp. 269-289, Mar. 1974.
[20] S. J. G. Shoba and A. B. Therese, "Detection of Glaucoma Disease in Fundus Images Based on Morphological Operation and Finite Element Method," *Biomedical Signal Processing and Control*, vol. 62, p. 101986, Sep. 2020.
[21] N. Mao, M. Song, D. Pan et al., "Computational Fluid Dynamics Analysis of Convective Heat Transfer Coefficients for a Sleeping Human Body," *Applied Thermal Engineering*, vol. 117, pp. 385-396, May. 2017.

Jirapol Klinbun was born in Lopburi Province, in 1973. He received the B.S. degree in mechanical engineering from Rajamangala University of Technology Thanyaburi, Pathumthani, Thailand in 1994. The M.S. and Ph.D. degree in mechanical engineering from Chiang Mai University, Thailand, in 2000 and 2008. From 2006 to 2008, he was a Research Assistant with the Heat Pipe Laboratory.

Since 2021, he has been an Associate Professor with the Mechanical Engineering Department, at Rajamangala University of Technology Rattanakosin. His research interests include Thermo-Fluid, Heat transfer in a heat pipe, Energy saving, Automotive technology, and Hydraulics-Pneumatics system.

Tipapon Khamdaeng received a B.Eng. degree in food engineering from Maejo University and a Ph.D. degree in mechanical engineering from Chiang Mai University, in 2006 and 2012. Since 2016, she has been an Assistant Professor with the Mechanical Engineering, Faculty of Engineering and Agro-Industry, Maejo University. Her main research interests include the computational modeling and simulation of solid and fluid mechanics and heat transfer characteristics of biomaterials

Numpon Panyoyai received a B.E. degree in mechanical engineering from Rajamangala University of Technology Lanna, Chiang Mai, Thailand, in 2000. He received an M.E. and D.E. degree in mechanical engineering from Chiang Mai University, Thailand, in 2005 and 2013.

Since 2012, he has been an Assistant Professor with the Mechanical Engineering, Faculty of Engineering and Agro-Industry, Maejo University. His research interest includes Mechanical and machinery design, biomass and biochar technology, thermal systems, and heat exchangers.

Sentiment Analysis on Thai Social Media Using Convolutional Neural Networks and Long Short-Term Memory

Chalisa Jitboonyapinit[1], Paralee Maneerat[2], and Nivet Chirawichitchai[3]

[1,2]School of Information Technology, Sripatum University, Bangkok, Thailand
[3]Faculty of Engineering and Technology, Panyapiwat Institute of Management, Nonthaburi, Thailand
E-mail: chalisajitboon@gmail.com, paralee.ma@spu.ac.th, nivetchi@pim.ac.th

Received: June 23, 2022/ Revised: July 5, 2022/ Accepted: July 21, 2022

***Abstract*—The objective of this research purposes a sentiment analysis of Thai social media using deep learning techniques consisting of a convolutional neural network, long short-term memory, and a gated recurrent unit. This research was used to test the algorithm with a wongnai product and service dataset and measured performance with accuracy. The experiment of this research found convolutional neural networks with long short-term memory outperform convolutional neural networks, long short-term memory, and gated recurrent units in classification accuracy, with an accuracy of 85.0%, followed by long short-term memory accuracy of 83.7%, convolutional neural network accuracy of 77.0% and finally gated recurrent unit an accuracy of 65.4% respectively. Therefore, the hybrid working model of a Convolutional Neural Network with long short-term memory is most suitable and effective for Thai sentiment analysis.**

***Index Terms*— Convolutional Neural Network, Gated Recurrent Unit, Long Short-Term Memory**

I. Introduction

Sentiment analysis is the process of analyzing customer opinion utilizing natural language processing, text analysis, and statistics. The finest companies are aware of their consumers' feelings—what they're saying, how they're telling it, and what they mean. Tweets, comments, reviews, and other sites where people mention your brand might reveal customer sentiment. Sentiment Analysis is the domain of using software to analyze these feelings, and it's a must-know for developers and business executives in today's workplace. Advances in deep learning, like many other domains, have pushed sentiment analysis to the front of cutting-edge algorithms. To extract and categorize the sentiment of words into positive, negative, or neutral categories, we now use natural language processing, statistics, and text analysis. For brand monitoring, sentiment analysis is used. One of the most well-known applications of sentiment analysis is to obtain a complete 360-degree perspective of how your brand, product, or company is perceived by customers and stakeholders. Product reviews and social media, for example, are widely available media that can give crucial insights into what your organization is doing properly or poorly. Sentiment analysis can also be used to assess the impact of a new product, ad campaign, or a consumer's reaction to recent company news on social media. Customer service agents frequently use a sentiment or intent analysis to automatically categorize incoming user emails into "urgent" or "not urgent" categories depending on the email's sentiment, proactively detecting unhappy users. The agent then prioritizes fixing the users with the most pressing issues first. Understanding the sentiment and intent of a specific case becomes increasingly critical as customer care becomes increasingly automated through machine learning. Sentiment analysis is used in market research and business intelligence to identify the subjective reasons why customers respond or do not respond to something (for example, why do consumers buy a product?). What are their thoughts on the user interface? Did the level of customer service fulfill their expectations?). Sentiment analysis can be used to examine trends, ideological bias, and opinions, assess reactions, and more in the fields of political science, sociology, and psychology. Sentiment analysis (also known as opinion mining) is a natural language processing (NLP) technique for determining the positive, negative, or neutral of data. Sentiment analysis is frequently used on textual data to assist organizations in tracking brand and product sentiment in consumer feedback and better understanding customer demands [1]-[3]. For the reasons mentioned above, the objective of this research was to create a research study to develop a sentiment analysis model on Thai social media using deep learning techniques to make an automatic model for classifying positive and negative customer opinions. We used a variety of preprocessing methods

in conjunction with various deep-learning algorithms to construct a model for evaluation purposes. We compare the models' classification accuracy as well as the amount of time they need for training and building the model. The rest of the paper is organized as follows. Section II describes the literature review. Section III describes the research framework. Section IV describes the research methods. Section V describes the experiments and results. Finally, Section VI conclusions.

II. Literature Review

We discovered that most researchers constructed their analysis models based on data from the internet, particularly from an online platform, after doing a literature study in a specific area of sentiment analysis over comments submitted in the product review system. The majority of recent sentiment analysis model development efforts have focused on evaluating text data from online business platforms such as Amazon product reviews, Twitter, IMDB movie reviews, and Yelp trip suggestions. These data are continuously generated by users, and the quantity of the data is rapidly growing as a result of the enormous number of users that provide feedback and comments via the internet on a daily basis. These data are collected by platform owners and used to assess insight information in order to better support new product design or improve the product quality that mostly fits their customers in positive ways. Because the data is in a text format that the computer cannot understand, the analyst must first preprocess the data before proceeding to the major steps of the analysis process. The most common preprocessing technique used by analyzers is a bag of words. The analyzer then uses the preprocess data to create a machine learning-based text classification model [4]-[8].

Deep learning is a popular technique for generating models right now since it produces high-accuracy classification models without the requirement for feature selection. The use of word embedding to preprocess data and then developing a model based on a convolutional neural network (CNN), the application of transfer learning strategy based on the pre-train CNN to reduce additional model training time, and the use of word embedding to preprocess data and then applying sequence analysis algorithm including recurrent neural network (RNN) and long short-term memory (LSTM) for sentiment analysis [9],[10].

From the high accuracy of the deep learning method applied for sentiment analysis as reported in the literature, we are thus interested in empirically studying the performance of deep learning. We use several machine learning techniques as a benchmark to compare against deep learning performance. The framework of our comparative study is presented in the next section.

III. Research Framework

Our processes, as illustrated in Fig. 1, are a framework for a comparative investigation of preprocessing and learning strategies that produce the best results for sentiment analysis of product comments and reviews. To begin, we gather data for text cleaning and preprocessing, which includes converting texts to lowercase, removing stop words and punctuation, and removing prefix-suffix from terms, among other natural language processing stages. Then, applying text transformation and deep learning approaches, we analyze and construct models based on a bag of words and word embedding. Finally, we evaluate the results in terms of model accuracy, precision-recall, and F1 score.

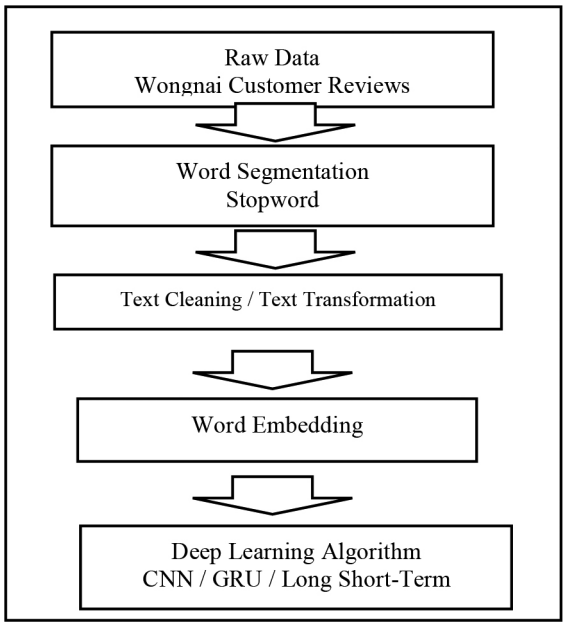

Fig. 1. Research framework

IV. Research Methods

A. Text Preprocessing

The first step in text classification is to transform documents, which typically are strings of characters, into a representation suitable for the learning algorithm and the classification task. For the Thai language, the main task of text processing is the segmentation of texts into word tokens. Thai texts are naturally unsegmented, i.e., words are written continuously without the use of word delimiters. Due to this distinct characteristic, preparing a feature set for Thai text categorization is more challenging than in Latin-based languages such as English, French, and Spanish. In Latin-based languages, a text string can easily be tokenized into terms by observing the word delimiting characters such as spaces, semicolons, commas, quotes, and periods. To prepare a feature set for the Thai social media corpus, we must first apply a word segmentation algorithm to tokenize text strings into

a series of terms. Once a set of extracted words are obtained from the training news corpus, the removal of HTML tags, removal of stop-words, and then word stemming. The stop-words are frequent words that carry no information (i.e. pronouns, prepositions, conjunctions, etc.). By word stemming we mean the process of suffix removal to generate word stems. This is done to group words that have the same conceptual meaning, such as walk, walker, walked, and walking [1]-[3].

B. Word Embedding

The word embedding techniques are used to represent words mathematically. One Hot Encoding, GloVe, Word2Vec, and FastText, are frequently used word embedding methods. One of these techniques (in some cases several) is TM because of less parameter and more simple preferred and used according to the status, size, and purpose of processing the data. Word embedding is a pre-processing strategy for converting written content into a format that the deep learning system can understand. This approach turns words into vectors for the convenience of calculation when determining word similarity. Fig. 2 shows an example of vectors. Because it can evaluate sequence data, this word embedding method is ideal for usage with recurrent neural network (RNN) algorithms including Long Short-Term Memory and Gated Recurrent Units [9],[10].

Word2Vec is a state-of-the-art algorithm to generate a fixed-length distributed vector representation of all the words in the huge corpus. The effectiveness of Word2Vec is due to two reasons — One is the use of fixed-size vectors which means the vector size does not depend on the number of unique words in the corpus. Second, incorporates semantic information in the vector representations. Word2Vec vectors are highly efficient at grouping similar words together. The algorithm can make strong estimates based on the position of the word in the corpus. For example, “Kid” and “Child” are similar and hence their vector representation will be very similar [11].

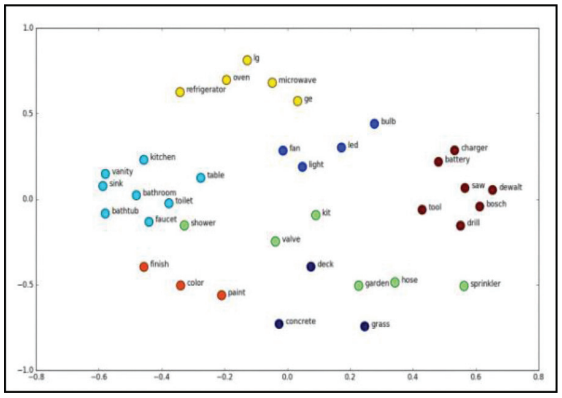

Fig. 2. Word2Vec

C. Gated Recurrent Unit

Gated Recurrent Units (GRUs) [12] are a gating mechanism in recurrent neural networks. GRU is a deep learning algorithm that reduces the complexity of LSTM networks by lowering the number of gates in each cell. As a result of the reduction, the number of parameters that must be computed in the network is reduced. Hence, the speed-up of computation time. GRU cell contains input, output, update, and reset gates. The update gate is for controlling change in the hidden state, while the reset gate is for resetting the value of the hidden state, as shown in Fig. 7. This cell structure makes GRU work faster than the LS structure.

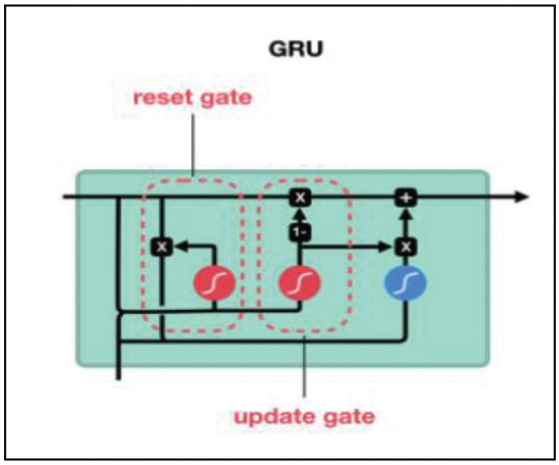

Fig. 3. Gated Recurrent Unit

D. Long Short-Term Memory

Long Short-Term Memory (LSTM) [13],[14],[17] is an artificial neural network used in the fields of artificial intelligence and deep learning. LSTM is the deep learning algorithm that has been developed from RNN for solving the gradient-descent variants problem and searching for long-term dependencies in the dataset. LSTM contains a cell as a subunit with a fundamental structure shown in Fig. 6. The cell contains a subsystem called an input gate to get input data, forget gate for weighing the significance of the memory cell state from the previously computed state, memory-cell state gate to compute a new memory cell state, and output gate for computing a new hidden state.

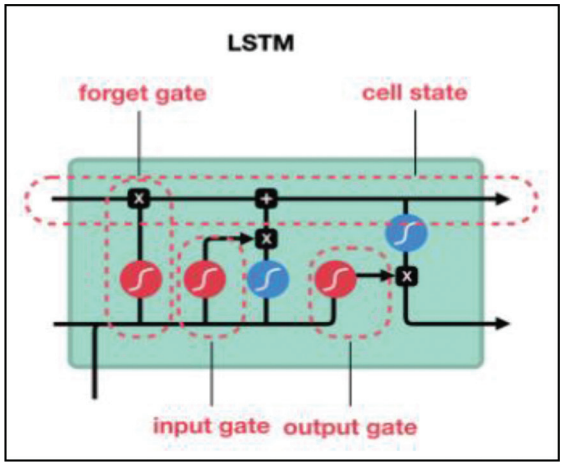

Fig. 4. Long Short-Term Memory

E. Convolutional Neural Network

A Convolutional Neural Network [10] (CNN) is a Deep Learning algorithm that can take in an input image, give importance (learnable weights and biases) to distinct aspects/objects in the image, and differentiate one from the other. CNN requires substantially less pre-processing than other classification techniques. While crude approach filters are hand-engineered, CNN can learn these filters with enough training.

Convolutional neural networks are a sort of feed-forward neural network that was first used in computer vision, recommender systems, and natural language processing. It is a deep neural network design made up of convolutional and pooling or subsampling layers that feed input to a fully-connected classification layer. Convolution layers extract features by filtering their inputs; the outputs of many filters can be merged. Pooling or subsampling layers reduce feature resolution, which can improve CNN robustness to noise and distortion. Fully connected layers perform classification tasks. An example of a CNN architecture can be seen in Fig. 5. The input data was preprocessed to reshape it for the embedding matrix. The figure shows an input embedding matrix processed by four convolution layers and two max pooling layers.

The first two convolution layers have 64 and 32 filters, which are used to train different features; these are followed by a max pooling layer, which is used to reduce the complexity of the output and prevent the overfitting of the data. The third and fourth convolution layers have 16 and 8 filters, respectively, which are also followed by a max pooling layer. The final layer is a fully connected layer that will reduce the vector of height 8 to an output vector of one, given that there are two classes to be predicted (Positive, Negative).

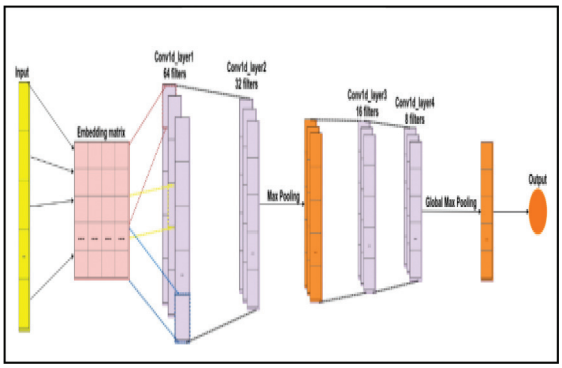

Fig. 5. Convolutional Neural Network

F. Dataset

In the research, we analyze and develop the models, we use product review data from the website wongnai.com. This dataset contains review texts in Thai as shown in some examples in Table I. This dataset has 5,000 records and 2 groups of reviews that contain 2,500 positive reviews that are labeled as positive and 2,500 negative reviews that are labeled as negative as shown on the rating column. We split data into two subsets as follows: 80% of them are the training set and the remaining 20% are the test set.

Fig. 6. Wongnai dataset

V. Experiments and Results

We performed experiments using a collection of product reviews obtained from the wongnai website. There are two categories: positive and negative. A total of 5,000 comments were selected and trained. We used TensorFlow - Keras and a deep learning tool, to perform the experiments. For deep learning methods, we use Gensim as a pre-trained model for word embedding to use with LSTM and GRU. The vector in the word embedding step has 128 dimensions

and the sequence contains 1,818 values. The architectures of LSTM are Bidirectional-LSTM = 256, activation = relu, fixed Dense = 128-64, optimizers = Adam EPOCHS = 50, Batchsize = 256, Learning Rate = 0.001 Dense output = 2, The architectures of GRU are GRU = 256, activation = relu, fixed Dense = 128-64, optimizers = Adam EPOCHS = 50, Batchsize = 256, Learning Rate = 0.001 Dense output = 2, The architectures of CNN are Conv1D filters = 32, kernel_size = 8, activation = relu, Dropout = 0.5, MaxPooling1D pool_size = 2, fixed Dense = 128, optimizers = Adam, Batchsize = 256, Learning Rate = 0.001, LSTM GRU and CNN are the same in that each having 1 layer. Each layer has 1,818 units with a dropout layer to prevent overfitting by defining a 0.2 dropout rate. Finally, we define a fully connected or dense layer as the last layer of deep learning architecture to perform the classification task by containing 1 node of the softmax function as an activation function. In the training process, this network has been configured for 50 epochs.

Classification effectiveness is usually measured using precision and recall. Precision is the proportion of true positive examples labeled positive by the system that was truly positive and recall is the proportion of true positive examples that were labeled positive by the system. The F-measure function which combines precision and recall is computed as [15]

$$F-measure=\frac{2\times Precision\times Recall}{Precision+Recall}$$

We tested all algorithms using the validation test set of 20%. The results in terms of precision, recall, and F-measure is the averaged values calculated across all cross-validation experiments. The experimental results of this word embedding scheme with respect to accuracy precision-recall and F-measure on the Thai product review corpus in combination with four deep learning are reported in Table I and Fig. 7 to Fig. 10.

TABLE I
ALGORITHM PERFORMANCE COMPARISONS

List	Accuracy	Precision	Recall	F-Measure
CNN	0.770	0.772	0.768	0.770
GRU	0.654	0.658	0.654	0.653
LSTM	0.837	0.839	0.837	0.837
CNN+LSTM	**0.850**	**0.852**	**0.848**	**0.850**

The experiment of this research found that convolutional neural networks with long short-term memory provided the most effective overall methods, with a classification accuracy of 85.0%, precision of 85.2%, recall 84.8%, and F-measure 85.0%, followed by Long Short-Term Memory an accuracy of 83.7%, precision 83.9%, recall 83.7%, and F-measure 83.7%, Convolutional Neural Network an accuracy of 77.0%, precision 77.2%, recall 76.8%, and F-measure 77.0%, Finally Gated Recurrent Unit an accuracy of 65.4%, precision 77.2%, recall 76.8%, and F-measure 77.0% respectively. The results obtained from the experiments in this research are consistent with the research of S. N. Murthy et al. [16], experiments with the IMDB movie review dataset and the Amazon product review dataset, found that CNN and LSTM were suitable and effective for sentiment analysis. This research is also consistent with the research of Kurniasari's [14] experiments with social media data in the Indonesian language found that the CNN and LSTM algorithm gives the same results of the model evaluation with good accuracy and good performance.

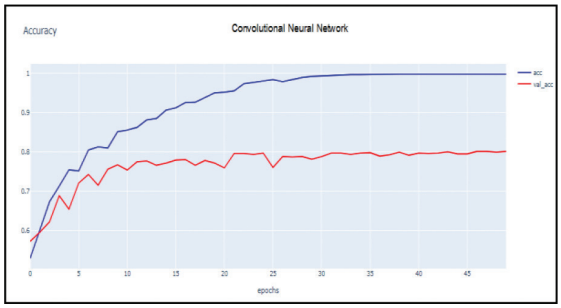

Fig. 7. Results of accuracy testing on Convolutional Neural Network algorithm

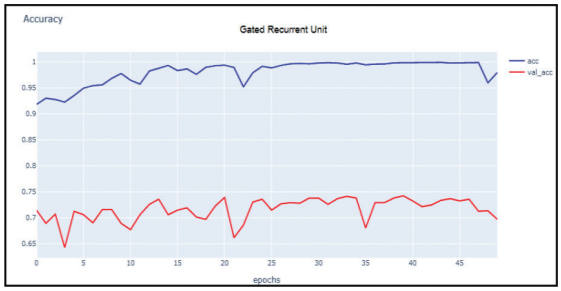

Fig. 8. Results of accuracy testing on Gated Recurrent Unit algorithm

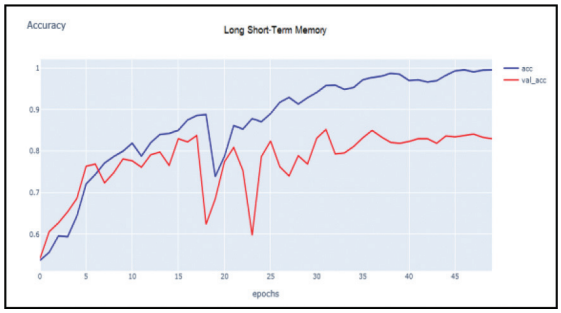

Fig. 9. Results of accuracy testing on the Long Short-Term Memory algorithm

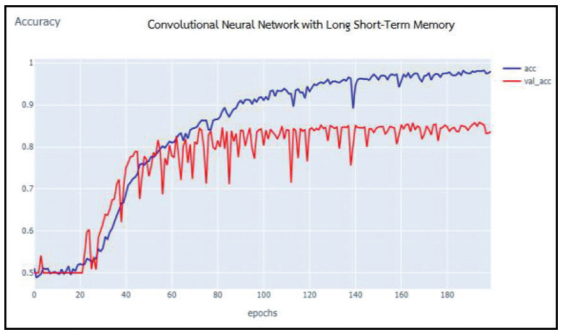

Fig. 10. Results of accuracy testing on Convolutional Neural Network with Long Short-Term Memory algorithm

VI. Conclusion

The experimental of this research purposes sentiment analysis on Thai social media using deep learning techniques consisting of the convolutional neural network, long short-term memory, and gated recurrent unit. This research was used to test the algorithm with the wongnai product and service dataset and measured performance with accuracy. This experiment of this research found convolutional neural networks with long short-term memory outperform convolutional neural networks, long short-term memory, and gated recurrent units in classification accuracy, with an accuracy of 85.0%, followed by long short-term memory accuracy of 83.7%, convolutional neural network accuracy of 77.0% and finally gated recurrent unit an accuracy of 65.4% respectively. Therefore, the hybrid model working with are convolutional neural network with long short-term memory is most suitable and effective for Thai sentiment analysis.

References

[1] D. Sharma, "Sentiment Analysis Techniques for Social Media Data: A Review," in *Proc. ICTSCI.*, 2019, pp.75-90.

[2] R. Ahmad and Y. Shaikh, "Opinion Mining and Sentiment Analysis for Classification of Opinions on Social Networking Sites Using Machine Learning Algorithms: Systematic Literature Review," *International Journal of Advanced Research in Computer and Communication Engineering*, vol.10, no. 5, May. 2011.

[3] B. Pang, L. Lee, and S. Vaithyanathan, "Thumbs Up? Sentiment Classification Using Machine Learning Techniques," in *Proc. Conf. Empirical Methods in Natural Language Processing*, 2002.

[4] K. Floyd, R. Freling, S. Alhoqail et al., "How Online Product Reviews Affect Retail Sales: A Meta-Analysis," *Journal of Retailing*, vol. 90, no. 2, pp. 217-232, Jun. 2014.

[5] S. Poria, E. Cambria, D. Hazarika et al., "A Deeper Look into Sarcastic Tweets Using Deep Convolutional Neural Networks," in *Proc. Int. Conf. 26th on Computational Linguistics*, 2016, pp. 1601-1610.

[6] R. Taemung and N. Chirawichitchai. "Thai Sentiment Analysis of Product Review Online Using Support Vector Machine," *Journal of Engineering Siam University*, vol. 18, no 34, pp. 1-12, Jun. 2017.

[7] N. Chirawichitchai. "Developing Term Weighting Scheme Based on Term Occurrence Ratio for Sentiment Analysis," *Information Science and Applications*, vol. 339, pp. 737-744, Feb. 2015.

[8] N. Chirawichitchai, "Emotion Classification of Thai Text-Based Using Term Weighting and Machine Learning Techniques," in *Proc. Conf. 11th JCSSE.*, 2014, pp. 91-96.

[9] V. Q. Nguyen. "Real-Time Event Detection Using Recurrent Neural Network in Social Sensors," *International Journal of Distributed Sensor Networks*, vol. 15, no. 6, pp. 1-15, Jun. 2019.

[10] N. Kalchbrenner, E. Grefenstette, and P. Blunsom. "A Convolutional Neural Network for Modelling Sentences," in *Proc. ACL.,* 2014, pp. 655-665.

[11] S. Li and B. Gong. "Word Embedding and Text Lassification Based on Deep Learning Methods," in *Proc. CSCNS2020,* 2021, pp.1-5.

[12] J. Chung, C. Gulcehre, K. Cho et al., "Empirical Evaluation of Gated Recurrent Neural Networks on Sequence Modeling," in *Proc. Int. Conf. NeurIPS.,* 2014. pp. 1-9.

[13] P. Srivastava. (2019, Dec. 31). *Essentials of Deep Learning: Introduction to Long Short-Term Memory*. [Online]. Available: https://www.analyticsvidhya.com/blog/2017/12/fundamentals-of-deep-learning-introduction-to-lstm

[14] L. Kurniasari, "Sentiment Analysis Using Recurrent Neural Network-LSTM in Bahasa Indonesia," *Journal of Engineering Science and Technology*, vol. 15, no. 5, pp. 3242-3256, Oct. 2020.

[15] N. Chirawichitchai, "Sentiment Classification by a Hybrid Method of Greedy Search and Multinomial Naïve Bayes Algorithm," in *Proc. ICT&KE.,* 2013, pp. 1-4.

[16] S. N. Murthy, S. R. Allu, B. Andhavarapu et al. "Text-Based Sentiment Analysis Using LSTM," *International Journal of Engineering Research & Technology*, vol. 9, no. 5, pp. 299-303, May. 2020.

[17] X. Shi, Z. Chen, H. Wang et al., "Convolutional LSTM Network: A Machine Learning Approach for Precipitation Nowcasting," in *Proc. Int. Conf. NeurIPS.,* 2015, pp. 802-810.

Chalisa Jitboonyapinit received her B.Sc. and M.Sc. in Information Technology, Dhurakij Pundit University, Thailand. Currently, she is a Ph.D. candidate in the Doctor of Philosophy Program in Information Technology at Sripatum University.

Paralee Maneerat received her B.Sc in Computer Science from Rangsit University, M.Sc. in Information Technology, Mongkut's Institute of Technology Ladkrabang, Thailand, and Ph.D. degree in Technopreneurship and Innovation Management from Chulalongkorn University. She currently has the rank of director, of the Master of Information Technology Program, Faculty of Information Technology, Sripatum University.

Nivet Chirawichitchai received his B.B.A. in Industrial Management and B.A. in Mass Communication from Ramkham haeng University, M.Sc. in Information Technology, and Ph.D. degree in Information Technology from King Mongkut's Institute of Technology North Bangkok, Thailand. He currently has the rank of director, Master of Engineering Program in Engineering and Technology, Faculty of Engineering and Technology, Panyapiwat Institute of Management, Thailand.

PAPER FORMAT (IEEE Style)

I. Format

- Your paper must use a paper size corresponding to A 4 which is 210 mm (8.27 inch) Wide and 297 mm (11.69 inch)
- Your paper must be in two column format
- Articles not more than 15 pages in length, single-sided A4 paper, margins (top, bottom, left, right) are 1 inch (2.54 cm)
- Abstract and References and content set to double columns,
- English font is Times New Roman, as follows:

TABLE I
Font Sizes for Papers

Content	Font Size	Labelling
Title (Single column)	18 (CT)	bold
Authors (Single column)	11 (CT)	bold
Authors Information (Single column)	10 (CT)	regular
Abstract	10 (LRJ)	bold
Index Terms (Keywords)	10 (LRJ)	bold
Content	10 (LRJ))	regular
Heading1	10 (CT)	bold (Capitalization)
Heading 2	10 (LJ)	regular
Table Title (Place above the Table)	8 (CT)	regular
Table content	8 (CT)	regular
Figure caption (Place below the figure)	8 (LJ)	regular
Reference Head	10 (CT)	regular (Capitalization)
Reference	8 (LJ)	regular
Author Profiles	10 (LRJ)	bold author name/ profile regular

CT=Centre Text, LJ=Left Justified, RJ=Right Justified, LRJ=Left & Right Justified

II. Composition of the Article

A. Article title

B. Authors information, Write (all) the author's name, affiliation, department, city, country and E-mail (set to Single Column) all.

C. Abstract, Must be under 200 words and not include subheadings or citations. Define all symbols used in the abstract. Do not delete the blank line immediately above the abstract.

D. Index Terms, Enter key words or phrases in alphabetical order, separated by commas.

E. Content

1) Academic article, should include: Introduction, Content, and Conclusion.

2) Research article, should include: introduction, literature review, Materials methods, Results, Discussion, and conclusion.

Clearly summarize the important findings of the paper. It should contain such as objectives, methods and major results.

F. Introduction

The Introduction section of reference text expands on the background of the work (some overlap with the Abstract is acceptable). The introduction should not include subheadings.

G. Pictures, table, etc., Must be use in numerical order in the article, provided the source correctly, cannot use other people' copyright.

Chart should be colored contrastingly or in black and white.

H. Reference

1) Cited in the main text. Indicate the number in the [ ] mark at the end of the text or the name of the referring person. Let the numbers be in the same line of content as [1].

2) Cited after the article. Put all bibliographical reference after articles, and order according to the author's name, please refer IEEE format. The footer reference format is as follows.

III. Rererences

References in research articles and scholarly articles. For academic and research journals, INTERNATIONAL SCIENTIFIC JOURNAL OF ENGINEERING AND TECHNOLOGY (ISJET). The technology defines referrals according to the IEEE format. All references should be listed at the end of the paper using the following.

Basic format for books:

J. K. Author, "Title of chapter in the book," in *Title of His Published Book,* xth ed. City of Publisher, Country if not USA: Abbrev. of Publisher, year, ch. x, sec. x, pp. xxx–xxx.

Examples:

[1] G. O. Young, "Synthetic structure of industrial plastics," in *Plastics,* 2nd ed., vol. 3, J. Peters, Ed. New York: McGraw-Hill, 1964, pp. 15-64.

[2] W.-K. Chen, *Linear Networks and Systems.* Belmont, CA: Wadsworth, 1993, pp. 123-135.

Basic format for periodicals:

J. K. Author, "Name of paper," *Abbrev. Title of Periodical*, vol. x, no. x, pp. xxx-xxx, Abbrev. Month. year.

Examples:

[3] J. U. Duncombe, "Infrared navigation—Part I: An assessment of feasibility," *IEEE Trans. Electron Devices*, vol. ED-11, no. 1, pp. 34-39, Jan. 1959.

[4] E. P. Wigner, "Theory of traveling-wave optical laser," *Phys. Rev*., vol. 134, pp. A635-A646, Dec. 1965.

[5] E. H. Miller, "A note on reflector arrays," *IEEE Trans. Antennas Propagat*., to be published.

Basic format for reports:

J. K. Author, "Title of report," Abbrev. Name of Co., City of Co., Abbrev. State, Rep. xxx, year.

Examples:

[6] E. E. Reber, R. L. Michell, and C. J. Carter, "Oxygen absorption in the earth's atmosphere," Aerospace Corp., Los Angeles, CA, Tech. Rep. TR-0200 (4230-46)-3, Nov. 1988.

[7] J. H. Davis and J. R. Cogdell, "Calibration program for the 16-foot antenna," Elect. Eng. Res. Lab., Univ. Texas, Austin, Tech. Memo. NGL-006-69-3, Nov. 15, 1987.

Basic format for handbooks:

Name of Manual/Handbook, x ed., Abbrev. Name of Co., City of Co., Abbrev. State, year, pp. xxx-xxx.

Examples:

[8] *Transmission Systems for Communications*, 3rd ed., Western Electric Co., Winston-Salem, NC, 1985, pp. 44-60.

[9] *Motorola Semiconductor Data Manual*, Motorola Semiconductor Products Inc., Phoenix, AZ, 1989.

Basic format for books (when available online):

Author. (year, month day). *Title.* (edition) [Type of medium]. *volume (issue).* Available: site/path/file

Example:

[10] J. Jones. (1991, May 10). *Networks.* (2nd ed.) [Online]. Available: http://www.atm.com

Basic format for journals (when available online):

Author. (year, month). Title. *Journal.* [Type of medium]. *volume (issue),* pages. Available: site/path/file

Example:

[11] R. J. Vidmar. (1992, Aug.). On the use of atmospheric plasmas as electromagnetic reflectors. *IEEE Trans. Plasma Sci.* [Online]. *21(3),* pp. 876-880. Available: http://www.halcyon.com/pub/journals/21ps03-vidmar

Basic format for papers presented at conferences (when available online):

Author. (year, month). Title. Presented at Conference title. [Type of Medium]. Available: site/path/file

Example:

[12] PROCESS Corp., MA. Intranets: Internet technologies deployed behind the firewall for corporate productivity. Presented at INET96 Annual Meeting. [Online]. Available: http://home.process.com/Intranets/wp2.htp

Basic format for reports and handbooks (when available online):

Author. (year, month). Title. Comp any . City, State or Country. [Type of Medium]. Available: site/path/file

Example:

[13] S. L. Talleen. (1996, Apr.). The Intranet Archi-tecture: M anaging information in the new paradigm. Amdahl Corp., CA. [Online]. Available:http://www.amdahl.com/doc/products/bsg/intra/infra/html

Basic format for computer programs and electronic documents (when available online):

ISO recommends that capitalization follow the accepted practice for the language or script in which the information is given.

Example:

[14] A. Harriman. (1993, June). Compendium of genealogical software. *Humanist.* [Online]. Available e-mail: HUMANIST @NYVM.ORG Message: get GENEALOGY REPORT

Basic format for patents (when available online):

Name of the invention, by inventor's name. (year, month day). *Patent Number* [Type of medium]. Available: site/path/file

Example:

[15] Musical toothbrush with adjustable neck and mirror, by L.M.R. Brooks. (1992, May 19). *Patent D 326 189* [Online]. Available: NEXIS Library: LEXPAT File: DESIGN

Basic format for conference proceedings (published):

J. K. Author, "Title of paper," in *Abbreviated Name of Conf.*, City of Conf., Abbrev. State (if given), year, pp. xxxxxx.

Example:

[16] D. B. Payne and J. R. Stern, "Wavelength-switched pas- sively coupled single-mode optical network," in *Proc. IOOC-ECOC,* 1985, pp. 585-590.

Example for papers presented at conferences (unpublished):

[17] D. Ebehard and E. Voges, "Digital single sideband detection for interferometric sensors," presented at the 2nd Int. Conf. Optical Fiber Sensors, Stuttgart, Germany, Jan. 2-5, 1984.

Basic format for patents:

J. K. Author, "Title of patent," U.S. Patent x xxx xxx, Abbrev. Month. day, year.

Example:

[18] G. Brandli and M. Dick, "Alternating current fed power supply," U.S. Patent 4 084 217, Nov. 4, 1978.

Basic format for theses (M.S.) and dissertations (Ph.D.):

J. K. Author, "Title of thesis," M.S. thesis, Abbrev. Dept., Abbrev. Univ., City of Univ., Abbrev. State, year.

J. K. Author, "Title of dissertation," Ph.D. dissertation, Abbrev. Dept., Abbrev. Univ., City of Univ., Abbrev. State, year.

Examples:

[19] J. O. Williams, "Narrow-band analyzer," Ph.D. dissertation, Dept. Elect. Eng., Harvard Univ., Cambridge, MA, 1993.

[20] N. Kawasaki, "Parametric study of thermal and chemical nonequilibrium nozzle flow," M.S. thesis, Dept. Electron. Eng., Osaka Univ., Osaka, Japan, 1993.

Basic format for the most common types of unpublished references:

J. K. Author, private communication, Abbrev. Month, year.

J. K. Author, "Title of paper," unpublished.

J. K. Author, "Title of paper," to be published.

Examples:

[21] A. Harrison, private communication, May 1995.

[22] B. Smith, "An approach to graphs of linear forms," unpublished.

[23] A. Brahms, "Representation error for real numbers in binary computer arithmetic," IEEE Computer Group Repository, Paper R-67-85.

Basic format for standards:

Title of Standard, Standard number, date.

Examples:

[24] IEEE Criteria for Class IE Electric Systems, IEEE Standard 308, 1969.

[25] Letter Symbols for Quantities, ANSI Standard Y10.5-1968.

First A. Author and the other authors may include biographies at the end of regular papers. Biographies are often not included in conference related papers. The first paragraph may contain a place and/or date of birth (list place, then date). Next, the author's educational background is listed. The degrees should be listed with type of degree in what field, which institution, city, state, and country, and year the degree was earned. The author's major field of study should be lower-cased.

The second paragraph uses the pronoun of the person (he or she) and not the author's last name. It lists military and work experience, including summer and fellowship jobs. Job titles are capitalized. The current job must have a location; previous positions may be listed without one. Information concerning previous publications may be included. Try not to list more than three books or published articles. The format for listing publishers of a book within the biography is: title of book (city, state: publisher name, year) similar to a reference. Current and previous research interests end the paragraph.

The third paragraph begins with the author's title and last name (e.g., Dr. Smith, Prof. Jones, Mr. Kajor, Ms. Hunter). List any memberships in professional societies. Finally, list any awards and work for committees and publications. If a photograph is provided, the biography will be indented around it. The photograph is placed at the top left of the biography, and should be of good quality, professional-looking, and black and white (see above example). Personal hobbies will be deleted from the biography. Following are two examples of an author's biography.

Second B. Author was born in Greenwich Village, New York City, in 1977. He received the B.S. and M.S. degrees in aerospace engineering from the University of Virginia, Charlottesville, in 2001 and the Ph.D. degree in mechanical engineering from Drexel University, Philadelphia, PA, in 2008. From 2001 to 2004, he was a Research Assistant with the Princeton Plasma Physics Laboratory. Since 2009, he has been an Assistant Professor with the Mechanical Engineering Department, Texas A&M University, College Station. He is the author of three books, more than 150 articles, and more than 70 inventions. His research interests include high-pressure and high-density nonthermal plasma discharge processes and applications, microscale plasma discharges, discharges in liquids, spectroscopic diagnostics, plasma propulsion, and innovation plasma applications. He is an Associate Editor of the journal *Earth*, *Moon*, *Planets*, and holds two patents.

Mr. Author was a recipient of the International Association of Geomagnetism and Aeronomy Young Scientist Award for Excellence in 2008, the IEEE Electromagnetic Compatibility Society Best Symposium Paper Award in 2011, and the American Geophysical Union Outstanding Student Paper Award in Fall 2005.

Third C. Author received the B.S. degree in mechanical engineering from National Chung Cheng University, Chiayi, Taiwan, in 2004 and the M.S. degree in mechanical engineering from National Tsing Hua University, Hsinchu, Taiwan, in 2006. He is currently pursuing the Ph.D. degree in mechanical engineering at Texas A&M University, College Station.

From 2008 to 2009, he was a Research Assistant with the Institute of Physics, Academia Sinica, Tapei, Taiwan. His research interest includes the development of surface processing and biological/ medical treatment techniques using nonthermal atmospheric pressure plasmas, fundamental study of plasma sources, and fabrication of micro- or nanostructured surfaces.

Mr. Author's awards and honors include the Frew Fellowship (Australian Academy of Science), the I. I. Rabi Prize (APS), the European Frequency and Time Forum Award, the Carl Zeiss Research Award, the William F. Meggers Award and the Adolph Lomb Medal (OSA).

Remark: More detail information, Pleases read Preparation of Papers for INTERNATIONAL SCIENTIFIC JOURNAL OF ENGINEERING AND TECHNOLOGY (ISJET), https://ph02.tci-thaijo.org/index.php/isjet/index

Panyapiwat Institute of Management (PIM)
85/1 Moo 2, Chaengwattana Rd,
Bang Talat, Pakkred, Nonthaburi 11120, Thailand
Tel. +66 2855 1560
https://www.tci-thaijo.org/index.php/isjet/index
https://isjet.pim.ac.th
E-mail: isjet@pim.ac.th